Distribution Agreement

In presenting this thesis or dissertation as a partial fulfillment of the requirements for an advanced degree from Emory University, I hereby grant to Emory University and its agents the non-exclusive license to archive, make accessible, and display my thesis or dissertation in whole or in part in all forms of media, now or hereafter known, including display on the world wide web. I understand that I may select some access restrictions as part of the online submission of this thesis or dissertation. I retain all ownership rights to the copyright of the thesis or dissertation. I also retain the right to use in future works (such as articles or books) all or part of this thesis or dissertation.

Signature:

_____ _____

Rachel Tillage Date

The role of noradrenergic-derived galanin in stress-related behavior

By

Rachel P. Tillage
Doctor of Philosophy

Graduate Division of Biological and Biomedical Science
Neuroscience

_____
David Weinshenker
Advisor

_____
Brian Dias
Committee Member

_____
Shannon Gourley
Committee Member

_____
Philip Holmes
Committee Member

_____
Jay Weiss
Committee Member

Accepted:

_____
Lisa A. Tedesco, Ph.D.
Dean of the James T. Laney School of Graduate Studies

_____
Date

The role of noradrenergic-derived galanin in stress-related behavior

By

Rachel P. Tillage

B.S., University of Richmond, 2015

Advisor: David Weinshenker, Ph.D.

An abstract of

A dissertation submitted to the Faculty of the

James T. Laney School of Graduate Studies of Emory University

in partial fulfillment of the requirements for the degree of

Doctor of Philosophy in Neuroscience

2020

Abstract

The role of noradrenergic-derived galanin in stress-related behavior

By Rachel P. Tillage

Stress is a primary risk factor for many neuropsychiatric disorders, including affective and anxiety disorders. Although these conditions are highly prevalent and are a leading cause of disability worldwide, the current therapeutic treatments available are often ineffective for many people and carry adverse side effects. Furthermore, the neurobiological mechanisms underlying stress-related neuropsychiatric disorders are not well understood. The neuropeptide galanin has been implicated in the pathophysiology of affective and anxiety disorders in both human and animal studies. Galanin is abundantly expressed in the main noradrenergic nucleus, the locus coeruleus, which is an important node in the stress response and is dysregulated in stress-related neuropsychiatric disorders. However, we currently lack a comprehensive understanding of the specific role noradrenergic-derived galanin plays in regulating stress-related behaviors. Here, we addressed this knowledge gap by using genetic and environmental manipulations of the galanin system to improve our understanding of how galanin from the locus coeruleus modulates stress-induced behaviors. We examined how chronic lack of galanin in noradrenergic neurons affects both neurochemistry and behavior using mice that lack galanin expression specifically in noradrenergic neurons. We found that noradrenergic neurons are a significant source of galanin to the hippocampus and prefrontal cortex, and that noradrenergic-derived galanin regulates behavioral coping responses. Next, we attempted to disentangle the roles of noradrenergic-derived galanin and norepinephrine in regulating behavioral responses to stress using mice that lack either norepinephrine or noradrenergic-derived galanin. Our data suggest that norepinephrine is important for acute stress-induced anxiety-like behavior, while both norepinephrine and noradrenergic-derived galanin participate in prolonged behavioral changes after a stressor. Finally, we examined how chronic elevation of noradrenergic galanin affects stress resilience. We found that chronic wheel running increased galanin expression in the locus coeruleus of mice and conferred resilience to a stressor, and galanin abundance predicted the degree of stress resilience. The beneficial effects of exercise were phenocopied by transgenic overexpression of galanin in noradrenergic neurons. Together, these studies provide new information about the complex role of noradrenergic-derived galanin in regulating stress-related behaviors and indicate the importance of continuing this line of research for developing new therapeutics to treat affective and anxiety disorders.

The role of noradrenergic-derived galanin in stress-related behavior

By

Rachel P. Tillage

B.S., University of Richmond, 2015

Advisor: David Weinshenker, Ph.D.

A dissertation submitted to the Faculty of the

James T. Laney School of Graduate Studies of Emory University

in partial fulfillment of the requirements for the degree of

Doctor of Philosophy in Neuroscience

2020

Acknowledgements

I am incredibly grateful to my advisor, David Weinshenker, for his support, encouragement, and advice throughout my time in graduate school. I feel so lucky to have been able to be in the Weinshenker lab and learn from David. His curiosity, optimism, and level-headed guidance allowed me to keep pushing forward when experiments failed and helped me become a better scientist. I would also like to thank my undergraduate mentors at University of Richmond, John Warrick and Omar Quintero, who helped me discover my love for research and gave me the confidence that I could succeed in graduate school.

I owe thanks to my wonderful thesis committee members, Brian Dias, Shannon Gourley, Phil Holmes, and Jay Weiss, for their time and guidance through the progression of my dissertation research. I am fortunate to have been able to learn from them and benefit from their knowledge and perspectives. I greatly appreciate all of their advice and encouragement throughout the years.

I've received lots of help and learned so much from my fellow Weinshenker lab members, both past and present. First, I want to acknowledge Canaan Jerome for his tireless management of our mouse colony. I want to give a huge thanks to my fellow galanin teammate, Stephanie Foster, who has been in the lab with me since the beginning and was a wonderful source of empathy and advice through the years, and to my other labmates, Danny Lustberg, Alexa Iannitelli, and Michael Kelberman, for being truly amazing lab members and making lab fun. I also want to thank the previous Weinshenker lab postdocs and graduate students, who taught me so much and helped me get my project off the ground: Dan Manvich, Kirsten Porter-Stransky, Jacki Rorabaugh, Claire Galloway, Karl Schmidt, Natty Chalermpalanupap, and Sydney Rowson.

Finally, I would like to thank my family for their unwavering support through my very long educational journey. I would not have been able to achieve what I have without the help and encouragement I received from my parents, Cindy and English Pearcy, my sister, Hannah, and my wonderful husband, Tyler. My parents recognized and fostered my love for science from a young age and have always encouraged me to follow my interests. Tyler has been an incredible and supportive partner throughout both my undergraduate and graduate education, keeping me grounded through stressful times and celebrating my achievements. Without this supportive environment around me, I would not be where I am today.

TABLE OF CONTENTS

FIGURES

ABBREVIATIONS

ANOVA	analysis of variance
ARs	adrenergic receptors
CNS	central nervous system
ChR2	channelrhodopsin-2
DBH	dopamine β-hydroxylase
ELISA	enzyme-linked immunosorbent assay
EPM	elevated plus maze
EZM	elevated zero maze
FST	forced swim test
GalR	galanin receptor
GPCRs	G-protein coupled receptors
HPLC	high performance liquid chromatography
i.p.	intraperitoneal
KPBS	potassium phosphate-buffered saline
LC	locus coeruleus
LPS	lipopolysaccharide
L-DOPA	L-dihydroxyphenylalanine
MHPG	3-methoxy-4-hydroxyphenylglycol
mg/kg	milligrams per kilogram
NE	norepinephrine
NET	norepinephrine transporter
OF	open field
PFA	paraformaldehyde
PBS	phosphate buffered saline
SEM	standard error of mean
SNP	single nucleotide polymorphism
SubC	subcoeruleus
TH	tyrosine hydroxylase
TST	tail suspension test
WT	wild type

CHAPTER 1:

Introduction

1.1 Stress-related neuropsychiatric disorders

1.1.1 Epidemiology

The stress response is a complex set of coordinated physiological, endocrine, and behavioral changes that allow us to respond adaptively to threatening situations. Under normal conditions, these changes are tightly regulated to promote optimal responding, but when these systems become dysregulated, they can aid in the development of devastating neuropsychiatric disorders. Understanding the underlying neurobiological mechanisms that regulate how organisms respond to stress and how these mechanisms relate to psychopathology is necessary for the discovery of new, effective treatments for people suffering from stress-related neuropsychiatric disorders.

Stress is a primary risk factor for many neuropsychiatric disorders, including affective and anxiety disorders. These disorders are highly prevalent worldwide, with both major depressive disorder (MDD) and all anxiety disorders (including generalized anxiety disorder (GAD), panic disorder, and various phobias) having a lifetime prevalence rate of approximately 30% (Nestler et al., 2002; Kessler et al., 2005; Kruijshaar et al., 2005; U.S. Department of Health and Human Services, 2019). The harmful impacts of these disorders extend beyond the affected individual, often bringing adverse effects for family, co-workers, and friends, as well as huge economic burdens for society. Depression and anxiety disorders are estimated to cost the global economy $1 trillion in lost productivity annually (Chisholm et al., 2016). MDD, GAD, and panic disorder are leading causes of disability worldwide because the debilitating symptoms often lead the affected person to function poorly in their daily life (Kessler et al., 2005; James et al., 2018). Furthermore, these disorders are closely linked to suicide and so can be deadly. Suicide was the tenth leading cause of death in the United States in 2017, and the second leading cause of death among people between ages 10 and 34, according to the Centers for Disease Control and

Prevention's Web-based Injury Statistics Query and Reporting System Leading Causes of Death Report.

There are numerous ways to classify affective and anxiety disorders based on symptoms, susceptibility to treatment, or endophenotypes, but broadly they can all be thought of as disorders of stress coping (Bale et al., 2019). The etiology of these disorders is thought to consist of an interaction between stressful psychosocial factors, such as childhood adversity or trauma, and genetic vulnerability, resulting in maladaptive or dysregulated stress coping and pathological symptoms, such as excessive worry, negative mood, or anhedonia (Selye, 1995; Bandelow et al., 2017). For people with MDD, GAD, or panic disorder, the onset of a relapsing episode is often triggered by an adverse event, and stressful experiences during childhood or adolescence, such as physical or emotional abuse and parental neglect, are vulnerability factors for developing MDD (Kendler, 2012; Bandelow et al., 2017). Post-traumatic stress disorder (PTSD), which was originally classified as an anxiety disorder, has now been categorized as a "trauma or stressor-related disorder" in the Diagnostic and Statistical Manual of Mental Disorders, Fifth Edition (DSM-5) and explicitly requires exposure to a traumatic experience as a diagnostic criterion (American Psychological Association, 2013). Not everyone who experiences traumatic events goes on to develop PTSD, however, indicating that stress resilience and coping mechanisms differ between individuals causing only a subset of people to be susceptible. While the symptoms and etiologies of these disorders are varied, their connection to stressful experiences and stress resilience is a common theme pointing to the importance of achieving a better understanding of stress neurobiology in order to shed light on the pathophysiology of these disorders.

1.1.2 Current treatments

Without having a full understanding of the neurobiological mechanisms underlying stress-related neuropsychiatric disorders, it is not surprising that the current treatments available are ineffective for many people and often carry adverse side effects, making drug compliance a significant problem. For example, pharmacological treatments for anxiety and depression are estimated to help only 50% of patients achieve complete remission and between one- and two-thirds of patients will not respond to the first drug prescribed (Nestler et al., 2002; Carek et al., 2011). Approximately 15% to 33% of patients show resistance to multiple pharmacological interventions, and even among those individuals who respond well to initial treatments, some continue to experience residual symptoms and have an increased risk of future relapse (Carek et al., 2011; Jorm et al., 2017; Ashdown-Franks et al., 2020). Individuals often have highly varied responses to specific drugs, potentially due to individual genetic differences leading to altered drug efficacy or side effects, causing a difficult pattern of trial and error where patients must try multiple different compounds and doses until they find something that might work for them (Lenze et al., 2010). This issue could be addressed in the near future by pharmacogenetics, a relatively new area of research that aims to predict whether a patient will benefit from a medication based on their unique genetic sequences, therefore allowing a personalized treatment plan that is tailored to the individual. While implementation of pharmacogenetics in psychiatry is still in its infancy, it is a promising tool that could help improve future treatment for many patients (Bousman et al., 2019).

There is high co-morbidity between anxiety and affective disorders, and because of our current lack of knowledge about the specific etiologies of these illnesses, there is often a ‘one size fits all’ approach to treating symptoms. The most common drugs used for stress-related

disorders today are benzodiazepines, which allosterically activate $GABA_A$ receptors to increase inhibition when GABA is present, and monoamine reuptake inhibitors, specifically selective serotonin reuptake inhibitors (SSRIs) and serotonin and norepinephrine reuptake inhibitors (SNRIs), which increase the extracellular concentrations of these neurotransmitters (Cryan and Sweeney, 2011; Nestler et al., 2015). Benzodiazepines have limited efficacy in depression but can be a very effective intervention for anxiety disorders because of their potent anxiolytic effect. However, benzodiazepines also have negative side effects which prevent them from being long-term options for people, such as dependence liability, fatigue, dizziness, and impaired cognitive function (Cryan and Sweeney, 2011; Bandelow et al., 2017). In contrast, monoamine reuptake inhibitors tend to have fewer side effects and can be helpful in many types of disorders including MDD, anxiety disorders, PTSD, obsessive-compulsive disorder, and chronic pain disorders (Nestler et al., 2002). Due to their low risk and potential benefits, SSRIs and SNRIs are the current first-line treatments for anxiety and affective disorders over benzodiazepines (Bandelow et al., 2017). However, although SSRIs and SNRIs increase monoaminergic transmission almost immediately, the mood-elevating effect of these drugs is quite delayed, occurring only after administration for several weeks, and so must be caused by more complex mechanisms that are not fully understood yet. Furthermore, while monoamine reuptake inhibitors lack abuse liability and have fewer side effects than older antidepressant drugs, they can still cause aversive effects for some people, such as nausea, sleep disturbance, weight change, and sexual dysfunction (Nestler et al., 2002).

There are also non-pharmacological therapeutic treatments for individuals suffering from affective and anxiety disorders, such as cognitive-behavioral therapy, which can be equally as effective as pharmacotherapies (Roshanaei-Moghaddam et al., 2011; Bandelow et al., 2017).

Increased physical activity is a particularly promising, non-pharmacological treatment option for stress-related disorders. Aerobic exercise is strongly linked to improvements in neuropsychiatric disorder risk factors and has comparable efficacy to many standard pharmacological treatments, suggesting increased exercise may be a beneficial way to combat these disorders (Petruzzello et al., 1991; Herring et al., 2010; Carek et al., 2011; Cooney et al., 2013; Ashdown-Franks et al., 2020). Individuals who regularly exercise are less likely to be diagnosed with stress-related disorders, including depression, anxiety, and PTSD (Whitworth and Ciccolo, 2016; Chekroud et al., 2018; Harvey et al., 2018). Exercise also carries low risk for most patients and conveys many beneficial side effects for cardiovascular and general physical health. Conversely, physical inactivity is associated with increased development of stress-related disorders (Carek et al., 2011). The mechanisms underlying the psychological benefits of increased physical activity are not well understood yet. Research investigating these mechanisms could lead to novel pharmacotherapies to help treat stress-related disorders in individuals who may be unable to engage in aerobic exercise.

1.1.3 Animal models of stress

There is a long history of using stress protocols in rodents to better understand neuropsychiatric disorders in humans. While different models have been used to study the neurobiological mechanisms of specific disorders, no individual paradigm can truly model a single disorder because animal models can never fully reproduce the psychopathology that occurs in humans. However, rodent models do allow us to dissect molecular and circuit level mechanisms underlying both normal and dysregulated stress processes at a level that of detail that is not currently possible in humans (Nestler and Hyman, 2010).

Historically, the most common way mice and rats have been used to study behaviors related to neuropsychiatric disorders is through testing in simple behavioral assays for anxiety-like and depressive-like behaviors. Canonical tests for anxiety-like behavior include the open field, elevated plus maze, and light-dark box. These approach-avoidance tasks rely on rodents' innate fear of novel environments or open spaces and use the quantification of avoidance behavior to measure anxiety-like responses to the environment. There are also non-canonical tests for anxiety-like behavior, such as shock probe defensive burying, marble burying, and novelty-suppressed feeding, which are tasks that rely on an active response (e.g. digging or feeding) as the quantitative measure, and may elicit increased levels of stress compared to approach-avoidance tasks (Cryan and Sweeney, 2011). Canonical assays for depression-like behavior involve tests for "anhedonia" (e.g. sucrose preference) or measuring differences in "passive" or "active" behaviors in acutely stressful situations (forced swim and tail suspension tests). These tests can be controversial because there are numerous ways to interpret the behavioral results beyond how they have traditionally been understood (de Kloet and Molendijk, 2016; Anyan and Amir, 2018). Furthermore, the mechanisms of action leading to "antidepressant" behavioral changes in these tasks are likely different than the mechanisms leading to antidepressant effects in humans because antidepressant drugs acutely impact rodent behavior in these tasks, but take weeks to provide relief for humans.

In order to assess stress resilience using animal models, more complex behavioral paradigms that involve prior exposure to a stressor before testing are employed, which are thought to model stress-related disorders more closely than testing naïve animals (Sciolino and Holmes, 2012; Weinshenker and Holmes, 2016). There are numerous such paradigms that can involve acute or chronic stressors and various stressor modalities, such as physical or

psychosocial stress. Some of the most common paradigms for studying stress-related behavioral changes include uncontrollable stress, chronic unpredictable stress, learned helplessness, and social defeat stress. These paradigms have varying levels of validity for modeling specific behavioral features of affective or anxiety disorders. For example, chronic stress paradigms, which typically involve subjecting rodents to repeated physical stressors (e.g., restraint, swim stress, exposure to cold temperatures) for a number of weeks or months, are often used to model MDD. Over this period of stress, animals are reported to develop depressive-like behaviors, such as anhedonia (reduced sucrose preference), indicating face validity, and this can be reversed by chronic, but not acute, administration of antidepressant medications, showing good predictive validity (Nestler and Hyman, 2010). Recent research has also shown that some mouse models, including chronic variable stress, adult social isolation, and chronic social defeat stress, can reproduce some of the same transcriptional changes seen in humans with MDD, indicating that mouse chronic stress models can recapitulate aspects of the molecular pathology of human MDD (Scarpa et al., 2020). Some drawbacks of these paradigms are the lack of reliability between different mouse strains, such as the resilient C57BL/6 compared to the more susceptible BALB/c strains, and difficulty in reproducing stress effects across labs (Willner, 2017; Muir et al., 2019). These drawbacks point to the importance of developing and validating a reliable paradigm to appropriately test the question being asked.

1.2 The noradrenergic system

1.2.1 Norepinephrine synthesis, signaling, and function

Norepinephrine (NE) is an important neurotransmitter for regulating how an animal responds to a stressor. In the brain, noradrenergic transmission is associated with a wide range of functions,

including stress, arousal, attention, memory, and pain. NE is synthesized from the amino acid tyrosine, which is converted to L-dihydroxyphenylalanine (L-DOPA) by the enzyme tyrosine hydroxylase (TH). This enzyme is the rate-limiting step in NE synthesis and is commonly used as a marker for noradrenergic and dopaminergic neurons. L-DOPA is then converted by aromatic amino-acid decarboxylase to form dopamine, which is packaged into synaptic vesicles by the vesicular monoamine transporter 2. The enzyme dopamine β-hydroxylase (DBH), which is localized inside the synaptic vesicles, then converts dopamine to NE (**Fig. 1.1a**). After NE is released via exocytosis during neuronal activation, it can be taken back up into the presynaptic neuron by the NE transporter (NET). NE is degraded by monoamine oxidase A or catechol-O-methyltransferase enzymes into various metabolites including vanillylmandelic acid and 3-methoxy-4-hydroxyphenylglycol (MHPG) (Kandel et al., 2013). NE is the synthetic precursor to epinephrine, which is present at very low levels in the brain (Mefford, 1988).

NE signals are transduced by adrenergic receptors (ARs), which have a range of intracellular effects and impacts on neuronal excitability, depending on the receptor type and localization. There are three families of adrenergic receptors (α1ARs, α2ARs, and βARs), all of which are metabotropic G-protein coupled receptors (GPCRs). Each family of ARs signals through different pathways and therefore has different effects on neuronal physiology.

α1ARs (subtypes α_{1A}, α_{1B}, α_{1D}) are generally excitatory, signaling mainly through $G_{q/11}$ proteins which activate phospholipase C (PLC) to cleave phosphatidylinositol 4,5-biphosphate (PIP2), resulting in inositol trisphosphate (IP3) and diacylglycerol (DAG), leading to increased intracellular calcium and the subsequent activation of protein kinase C (PKC) (Kandel et al., 2013; Schmidt and Weinshenker, 2014). α1ARs are heteroreceptors expressed throughout the

brain and are associated with many functions including arousal, pain perception, memory, and motor activation (Gilsbach and Hein, 2008).

In contrast, α2ARs (subtypes α_{2A}, α_{2B}, α_{2C}) are primarily inhibitory, signaling through $G_{i/o}$ proteins which inhibit adenylate cyclase to reduce production of cyclic-adenosine monophosphate (cAMP) and therefore reduce activities of ion channels and protein kinase A (PKA). α2ARs function as inhibitory autoreceptors on noradrenergic neurons, as well as heteroreceptors on target cells. α2 autoreceptors on LC neurons are crucial for the negative feedback mechanisms that regulate LC activity (Nestler et al., 2015).

Signaling through βARs (subtypes β_1, β_2, β_3) leads to neuronal activation by acting through G_s proteins, which increase cAMP and PKA signaling. Activation of βARs and the resulting signaling cascade are important for the protein synthesis that underlies synaptic plasticity and long-term potentiation in the hippocampus essential for learning and memory. Recent studies have shown that βAR signaling in the amygdala induces anxiety-like behavior in rodent models (Daviu et al., 2019).

1.2.2 Locus coeruleus anatomy and physiology

The locus coeruleus (LC) is the main source of NE in the brain. The name of this brain region comes from the Latin word for "blue spot" due to the dark neuromelanin pigmentation naturally marking LC neurons in primates, which is absent in rodents (Maeda, 2000). The neurons in the LC are arranged into a tightly packed nucleus with extraordinarily long, highly ramified axonal projections that innervate almost every brain region, including stress-sensitive regions such as the amygdala, ventral tegmental area, prefrontal cortex, and hippocampus (Schwarz and Luo, 2015; Bari et al., 2020) (**Fig. 1.2**). These thin, largely unmyelinated axons have many varicosities

along them that were originally thought to be non-synaptic, indicating that NE transmission occurs primarily through volume transmission instead of direct synaptic transmission. Later research, however, showed that there are more synaptic contacts between NE terminals and targets than originally reported, indicating that NE transmission likely occurs via through both synaptic and non-synaptic mechanisms (Aston-Jones and Waterhouse, 2016; Waterhouse and Chandler, 2016). While the LC, also known as A6, is the main source of NE in the brain, there are other noradrenergic neurons in the brain outside of the LC. These anatomically defined nuclei (A1, A2, A4, A5, and A7) are located in the brainstem and pons, but are more dispersed and have fewer projections that LC neurons (Waterhouse and Chandler, 2016).

The LC receives inputs from a wide range of structures including the cortex, hypothalamus, amygdala, spinal cord, and cerebellum. Rabies viral tracing has indicated that each individual LC neuron receives inputs from around 9 to 15 other regions (Schwarz and Luo, 2015). This structural organization allows the LC to integrate incoming sensory and physiological information and broadcast signals out to the rest of the brain, thereby coordinating downstream effects across multiple regions and networks. LC neuron activity occurs in tonic and phasic modes, which are thought to regulate the behavioral state of the animal. Low tonic firing (~1-2 Hz) is associated with a quiet waking state, while high tonic activity (~3-10 Hz) occurs during periods of increased arousal and stress (Berridge and Waterhouse, 2003; Valentino and Van Bockstaele, 2008). High frequency phasic bursts of LC activity (10-20 Hz) occur in response to salient sensory stimuli and are associated with sustained attention (Aston-Jones and Waterhouse, 2016). Phasic activity occurs most frequently during moderate tonic activity and decreases either when tonic activity is very low, such as during drowsiness or non-REM sleep, or

when tonic activity increases beyond a moderate level, such as during stress (Valentino and Van Bockstaele, 2008).

The LC was originally thought the be a largely homogenous nucleus due to observations of its anatomy and synchronous physiology. However, recent research has revealed that there is both molecular and projection-specific heterogeneity within the LC. The majority of neurons in the central and dorsal portions of the LC project to the forebrain, while the more ventral portions project to the spinal cord and cerebellum (Berridge and Waterhouse, 2003; Schwarz and Luo, 2015). New studies have found that there are heterogenous populations of LC neurons with distinct projection patterns and coding properties that control modulation of opposing behavioral states and allow for behavioral flexibility (Uematsu et al., 2015; Chandler, 2016; Kebschull et al., 2016; Hirschberg et al., 2017; Uematsu et al., 2017). Molecularly, while all neurons in the LC contain NE, a subset of cells also co-express neuropeptides. The most abundant neuropeptide in the LC is galanin, which is expressed in at least 80% of LC neurons. Cells that co-express NE and galanin are found throughout the LC but are localized most densely in the central and dorsal LC regions (Holets et al., 1988; Schwarz and Luo, 2015).

1.2.3 The role of the LC-NE system in the stress response

LC neurons are consistently activated by a variety of stressful stimuli, including physical stress, immune challenges, predator stress, and social stress (Valentino and Van Bockstaele, 2008). During stress, LC neurons exhibit high tonic activity, which is thought to facilitate a short-term adaptive behavioral state characterized by increased vigilance and arousal that increases the likelihood of survival in a threatening situation. A main driver of LC activation during stress is corticotropin-releasing factor (CRF). The LC receives CRF projections from several regions,

including the central nucleus of the amygdala (CeA) and the periventricular nucleus of the hypothalamus (PVN), and both *in vitro* and *in vivo* studies have shown that CRF causes elevated LC activity (Valentino and Foote, 1988; Curtis et al., 1997; Jedema and Grace, 2004; Valentino and Van Bockstaele, 2008). Recent work has further demonstrated that specific optogenetic activation of CRF+ terminals from the central amygdala in the LC increases LC activity and drives anxiety-like behaviors through activation of CRF receptor 1 expressed in LC neurons (McCall et al., 2015).

Current evidence indicates that activation of the LC is necessary and sufficient to drive anxiety-like behavior. Recent studies using direct optogenetic manipulation of LC neurons have shown that increasing high tonic, but not phasic, firing of the LC leads to aversion and anxiety-like behavior in mice, and that inhibiting LC activity using chemogenetics blocks stress-induced anxiety-like behavior (McCall et al., 2015; Li et al., 2018). Furthermore, βAR signaling specifically in the BLA via LC projections has been found to induce anxiety-like behavior and regulate pain-induced anxiety-like behavior, adding support to the theory that increased NE release from the LC can induce anxiety (McCall et al., 2017; Llorca-Torralba et al., 2019). However, there is some evidence to the contrary. For example, several studies have suggested that lesioning the LC leads to decreased anxiety-like behavior (Nassif et al., 1983; Britton et al., 1984; Koob et al., 1984). More specifically, a previous study pharmacologically activated the LC via local infusion of the selective α2AR antagonist idazoxan, and found that this manipulation led to decreased anxiety-like behavior in an open field drinking test in rats (Weiss et al., 1994). Additionally, electrical stimulation of the LC using intracranial self-stimulation in rats has produced mixed results, with some studies reporting a reinforcing effect of direct LC stimulation and others refuting that effect (Crow et al., 1972; Ritter and Stein, 1973; Amaral and

Routtenberg, 1975; Simon et al., 1975). It is likely that pharmacological and optogenetic manipulations of the LC result in different patterns of LC activation, and so this difference in effects may be due to different patterns of LC activation being elicited. It is possible that only manipulations that increase tonic firing to ~5 Hz and above result in anxiogenic effects. If a stimulus preferentially increases phasic activity instead of high tonic activity, then anxiety may not manifest, and reward-like properties could emerge. It is also important to take LC circuitry into consideration. Recent studies have suggested that activation of distinct, projection-specific subsets of LC neurons can lead to different, even opposing, effects on behavior (Uematsu et al., 2015; Chandler, 2016; Hirschberg et al., 2017). For example, activation of LC neurons that project to the amygdala promotes aversive learning, while activation of a separate, mPFC-projecting group of LC neurons extinguishes aversive responses (Uematsu et al., 2017). Therefore, it is possible that the LC may indeed be able to differentially modulate anxiety, depending on the exact pattern of LC activity elicited and which subpopulations of LC neurons are recruited.

Activation of the LC is an important mediator of a host of downstream effects that coordinate responses to stress. A major player is the sympathetic nervous system, which regulates the peripheral fight-or-flight response and leads to changes in autonomic activities that promote survival in a stressful situation, such as increased blood pressure, heart rate, and decreased metabolism. NE from the LC, as well as other NE nuclei, increases sympathetic activity via projections to the spinal cord, leading to the activation of excitatory α1ARs on preganglionic sympathetic neurons and reducing parasympathetic activity via the activation of inhibitory α2ARs on preganglionic parasympathetic neurons (Samuels and Szabadi, 2008). LC activation also induces a cognitive response to stress through its projections to the basolateral

amygdala (BLA), medial prefrontal cortex (mPFC), and hippocampus, where NE signaling is important for regulating the emotional response to stress and forming the memory of a stressful experience (Wyrofsky et al., 2019).

LC activity and NE release are tightly regulated through autoinhibitory feedback from the α2ARs receptors expressed on LC soma, dendrites, and axon terminals. This negative feedback is crucial for the LC to maintain its normal physiology. Disruption in this autoinhibition could lead to unchecked LC hyperactivity following activation, such as during stress, which is hypothesized to contribute to a variety of diseases including epilepsy, sleep disorders, anxiety, PTSD, depression, opiate withdrawal, and neurodegenerative diseases (Valentino and Van Bockstaele, 2008; Morris et al., 2020). Drugs that increase LC-NE transmission, such as the α2AR antagonist yohimbine, are acutely anxiogenic in both humans and rodents (Charney et al., 1983; Holmes et al., 2002; Kuehl et al., 2020), although there are conflicting results on this effect (Gower and Tricklebank, 1988). Clinical studies have indicated that aberrant LC activity occurs in people with stress-related neuropsychiatric disorders, such as depression and PTSD. To date, fewer studies have focused on determining the role of the LC in anxiety disorders in humans; however, excessive worry in GAD has been associated with increased connectivity between the LC and amygdala (Meeten et al., 2016). Postmortem analysis of antidepressant-free brains from people with MDD showed increased levels of NE and its metabolites in cerebrospinal fluid, as well as increased expression of TH in the LC compared to non-depressed control brains, indicating an increase in LC activity (Roy et al., 1988; Ordway et al., 1994; Zhu et al., 1999; Ehnvall et al., 2003). Depressed individuals also showed elevated levels of CRF and NMDA receptor subunits in the LC, indicating altered excitatory regulation of LC activity (Bissette et al., 2003; Bernard et al., 2011; Chandley et al., 2014). Functional magnetic resonance imaging

studies have shown that PTSD patients display higher LC blood-oxygen-level-dependent (BOLD) responses to fearful stimuli, and elevated LC activity in response to loud sounds compared to controls (Morey et al., 2015; Naegeli et al., 2018). This research indicates that LC activity is dysregulated in people with stress-related disorders, but due to the limited nature of human studies, a direct causal relationship has been challenging to establish.

1.3 Galanin

1.3.1 Galanin synthesis and expression patterns

The neuropeptide galanin was first discovered in the early 1980s in porcine gut by researchers at the Karolinska Institute (Tatemoto, 1983). The name was conceived from the amino acids at the beginning and end of the sequence, an N-terminal glycine and C-terminal alanine. Galanin is made up of 30 amino acids in humans (29 amino acids in other species) and is encoded by the *GAL* gene. After translation, the preprogalanin form of the peptide is cleaved in to the mature galanin peptide and galanin message associated protein (GMAP). No *in vivo* functions for GMAP have been reported in mammals and there are currently no known receptors. Beyond galanin and GMAP, there are two other peptides considered to be in the galanin family: galanin-like peptide (GALP) and alarin, which are encoded by the *GALP* gene. GALP is the only other peptide in galanin family known to be active at galanin receptors due to the high sequence similarity between GALP and the N-terminal region of galanin. There is 85% homology between rat, mouse, porcine, bovine, and human galanin sequences, with the N-terminal sequence highly conserved across all species, suggesting that this part of the peptide is crucial for its receptor binding and functional activity (Lang et al. 2015).

Although the expression patterns of galanin vary in many brain regions between species, galanin is consistently highly expressed in the LC of mice, rats, non-human primates, and humans, suggesting a conserved and important evolutionary purpose for this source of galanin in the brain (Skofitsch, 1985; Melander, 1986; Holets et al., 1988; Chan-Palay et al., 1990; Cheung et al., 2001; Perez et al., 2001; Le Maitre et al., 2013). Lesion studies have suggested that the majority of galanin in the hippocampus and PFC in rodents comes from the LC (Melander, 1986; Hökfelt et al., 1998; Weiss et al., 1998; Xu et al., 1998). Galanin is expressed in other brain regions that contain noradrenergic neurons, such as the nucleus of the solitary tract (NTS), but very few neurons in this region appear to co-express both NE and galanin in mice. The hypothalamus also shows consistently high galanin expression across species, specifically the preoptic, periventricular, and dorsomedial hypothalamic nuclei. Other brain regions, such as the serotonergic dorsal raphe, show varied galanin expression across species. In rats, approximately 50% of dorsal raphe neurons express galanin, but in mice there is little to no galanin expression in the cell bodies of this region (Kordower et al., 1992; Cheung et al., 2001; Perez et al., 2001). Outside of the central nervous system (CNS), galanin is expressed in many peripheral tissues, including the gut, adrenal medulla, skin, and cardiovascular tissue (Lang et al., 2015).

Galanin expression is highly plastic and sensitive to pharmacological and environmental manipulations. Studies have shown that galanin expression is upregulated by nerve damage, inflammation, and seizures (Hobson et al., 2008; Lerner et al., 2008). In the LC, galanin expression is increased after chronic stress, and diminished after chronic antidepressant administration (Holmes et al., 1995; Rovin et al., 2012). However, other studies have found that a variety of manipulations which can be effective in treating MDD, such as chronic administration of different classes of antidepressants, electroconvulsive therapy, chronic

exercise, and sleep deprivation cause elevated galanin gene expression in the LC (Van Hoomissen et al., 2004; Lu et al., 2005; Holmes et al., 2006; Christiansen, 2011; Sciolino et al., 2012; Epps et al., 2013; Ogbonmwan et al., 2015; Sciolino et al., 2015). There is also evidence that chronic opiate exposure and withdrawal, which are closely associated with stress, increase galanin expression in the LC (Zachariou et al., 2000; McClung et al., 2005; Holmes et al., 2012).

1.3.2 Galanin signaling and functions

Galanin, like other neuropeptides, is stored in large dense core vesicles (LDCV) after being synthesized. These LDCVs contain chromogranin glycoproteins, which play crucial roles in the formation and sorting of proteins into the vesicles. Neuropeptides are almost always co-packaged with small molecule neurotransmitters in these vesicles, including NE (Ross et al., 2019). LDCVs can be released from axon terminals or from cell bodies and dendrites, but fusion to the cell membrane only occurs under conditions of high intracellular calcium, such as during high frequency or burst firing (**Fig. 1.1b**) (Lang et al., 2015). Unlike classic neurotransmitters, there is no reuptake mechanism for neuropeptides to be reused by cells. Neuropeptides are degraded in the extracellular space by peptidases, meaning that new neuropeptide must be synthesized *de novo.* Together, these differences cause contrasting dynamics for neuropeptides like galanin compared to classic neurotransmitters, such as NE. Neuropeptide signaling is generally considered to be longer lasting and less temporally confined than signaling from small molecule neurotransmitters.

Galanin transmission is mediated by three G-protein coupled receptors (GalR1, GalR2, and GalR3), and can result in both acute neuromodulatory effects and slower neurotrophic effects (Weinshenker and Holmes, 2016). All three receptors can signal through $G_{i/o}$ proteins,

which inhibit adenylate cyclase to reduce production of cAMP and lead to the opening of G protein-coupled inwardly rectifying potassium (GIRK) channels, thereby causing an inhibitory effect (Wang et al., 1998; Hobson et al., 2008). GalR2, however, can also couple to $G_{q/11}$ proteins to activate PLC and PKC, as well as mediate inhibition of both Rho and Cdc42 GTPases. Inhibition of these GTPases leads to an increase in the activation of the actin-binding protein cofilin, which in turn promotes neurite growth (Hobson et al., 2008; Hobson et al., 2013). Therefore, GalR2 signaling is thought to be the main mediator for galanin's neurotrophic properties, whereas GalR1 and GalR3 are thought to be primarily important for inhibitory neuromodulation by galanin.

GalR1 mRNA is widely expressed in the CNS, with dense localization in the olfactory regions, amygdala, thalamus, hypothalamus, pons, medulla, and spinal cord in mice and rats. GalR2 is also broadly expressed in the CNS, with high levels in the hippocampus and hypothalamus of rodents (Lang et al., 2015). Less is known about GalR3, but it appears to be more abundant in peripheral tissues than in the CNS in rats, with mRNA expression found in limited regions of the hypothalamus, bed nucleus of the stria terminalis, periaqueductal gray, and the LC (Mennicken et al., 2002). Little is known about galanin receptor expression patterns in humans; however, post-mortem human tissue studies have shown that there are high levels of GalR3 expression in the human LC compared to GalR1 or GalR2 (Le Maitre et al., 2013).

Slice electrophysiology studies have shown that galanin has an inhibitory effect on LC neuron activity; both galanin and GalR1 agonists potently hyperpolarize LC neurons, suppress spontaneous firing, and enhance α2AR negative feedback via GalR1 (Seutin et al., 1989; Pieribone et al., 1995; Ma et al., 2001; Xu et al., 2001). Furthermore, amperometric studies have shown that LDCVs are released from the soma of LC-NE neurons during high activation, and

high resolution *in situ* hybridization imaging in combination with tannic acid application has indicated that galanin is both synthesized and released from LDCVs in the dendrites of LC neurons (Huang et al., 2007; Vila-Porcile et al., 2009). Together, these results suggest that galanin can be released somatodentritically from LC-NE neurons and produce an autoinhibitory effect on LC neuron activity, although this hypothesis has yet to be directly tested.

1.3.3 Galanin in neuropsychiatric disorders

There is ample evidence from human studies that the galanin system is involved in the etiology of stress-related neuropsychiatric disorders, indicating that galanin may be an important target for future therapeutic development (Kuteeva et al., 2008a). Several genome-wide association studies have revealed that genetic variants in coding and non-coding regions of the *GAL* and galanin receptor genes confer increased risk of depression and anxiety in humans (Wray et al., 2012; da Conceicao Machado et al., 2018; Keszler et al., 2019). This association was found to be especially strong for several variants when researchers took environmental stress exposures into account, confirming a role for gene x environment interactions (Juhasz et al., 2014; Gonda et al., 2018). Galanin has also been implicated in addiction, which is heavily influenced by stress, and variants in the human *GAL* gene are associated with heroin dependence (Levran et al., 2008). The functional effects of these genetic variants on galanin transmission are still largely unknown. Interestingly, a recent study identified an interaction between allelic variation in a highly conserved *GAL* enhancer sequence and increased alcohol intake and anxiety in men, then used CRISPR genome editing to disrupt the same enhancer sequence in mice, which led to reduced galanin expression in the amygdala and hypothalamus and a corresponding reduction in ethanol intake and anxiety-like behavior in male mice, mirroring the patterns seen in humans (McEwan

et al., 2020). Postmortem analyses of brain tissue from individuals with MDD have also uncovered evidence of alterations in the galanin system, including increased galanin mRNA expression and decreased DNA methylation at the *GAL* gene in the LC, suggesting dysregulation of galanin specifically in the LC (Barde et al., 2016). Despite this strong evidence indicating a role for galanin in stress-related disorders, the specific mechanisms involved are still unclear due to the inherent limitations of human studies.

1.3.4 Galanin and stress resilience

Research using animal models is necessary to elucidate the basic mechanisms underlying the role of galanin in stress-related disorders. Previous studies using rodents to examine the effects of galanin have relied primarily on global knockouts or intracerebroventricular infusion of galanin receptor agonists or antagonists. These experimental strategies lack regional specificity and have often generated conflicting results. For example, galanin receptor agonists administered intracerebroventricularly have been reported to elicit an anxiolytic effect in some tests (e.g. conflict test and elevated zero maze), and no effect in other anxiety assays (elevated plus maze, light-dark exploration, and open field) (Bing et al., 1993; Karlsson et al., 2005; Karlsson and Holmes, 2006; Rajarao et al., 2007). Galanin receptor agonists also produce mixed effects on behavior in the antidepressant-sensitive forced swim and tail suspension tests (Bartfai et al., 2004; Holmes et al., 2005; Lu et al., 2005; Kuteeva et al., 2008a; Kuteeva et al., 2008b). Similarly, the transgenic mouse lines generated to study the role of galanin have generally been global manipulations and have shown little to no effects in canonical tests for anxiety and depression-like behavior (Karlsson and Holmes, 2006; Lang et al., 2015). These results suggest that galanin's effects are specific to the cell type, brain region, circuit, and/or receptor(s) being

engaged. Thus, strategies to manipulate galanin in a cell type- and brain region-specific manner will help unravel its distinct functional roles in physiological processes and disease states. Furthermore, because galanin can act through both acute neuromodulatory mechanisms as well as chronic neurotrophic mechanisms, the timescale of the manipulation (short-term pharmacological effects vs. lifelong genetic effects) may lead to different outcomes.

Studies designed to examine resilience or susceptibility to a stressor to complement baseline behavioral testing have provided some clarity on the role of galanin. As discussed previously, neuropeptides are preferentially released when neurons fire at high frequencies, suggesting that galanin from the LC may modulate behavioral states induced by high levels of noradrenergic activation, such as during stress, but may not play a role under less challenging conditions (Bartfai et al., 1988; Karlsson et al., 2005; Sciolino and Holmes, 2012). For example, although transgenic mice overexpressing galanin in noradrenergic neurons do not have a baseline phenotype in anxiety-like behavioral tests, they are insensitive to the anxiogenic effects of the α2AR antagonist yohimbine in a light-dark exploration assay (Holmes et al., 2002). Similarly, experimentally-naïve GalR2 knockout mice have little to no phenotype in behavioral assays such as the elevated plus maze, light/dark box, forced swim, or tail suspension tests, but they show increased susceptibility to a learned helplessness paradigm, which measures the impact of uncontrollable stress exposure on subsequent responding to stressors (Lu et al., 2008). These findings suggest that the effects of galanin are more prominent under conditions that strongly activate the LC.

1.4 Summary and thesis aims

In summary, both the galaninergic and noradrenergic systems are involved in stress-related neuropsychiatric disorders, but the specific mechanisms in play are not well understood. Rodent studies have suggested a role for galanin from the LC in regulating behavioral responses to stress. However, there are still many gaps in our knowledge about exactly how and when noradrenergic-derived galanin may function to influence stress-induced behavior. The experiments described in the following chapters assess the role of noradrenergic-derived galanin in regulating stress-related behavior in a variety of ways. Broadly, we tested transgenic mice that either lack or overexpress galanin specifically in noradrenergic neurons to assess the effects of these manipulations at baseline and after stress exposure. We chose to employ a single, uncontrollable foot shock stressor because it is an easily implemented and quantitatively consistent approach that led to reliable anxiogenic behavioral changes in control mice. In our stress paradigm, we assessed immediate fear to the foot shock itself by measuring freezing behavior during the foot shock. We then exposed the animals to an anxiogenic novel environment either immediately following the foot shock or 24 h later to measure adaptive stress-induced anxiety-like behavior. The studies focused on the following questions: (1) How does chronic removal of galanin from noradrenergic neurons affect neurochemistry and baseline behavior?; (2) What are the distinct roles of noradrenergic-derived galanin compared to NE in regulating stress resilience?; and (3) How does chronic environmental or genetic elevation of galanin affect stress resilience? Together, these studies provide valuable information about the complex role of noradrenergic-derived galanin in regulating stress-related behaviors.

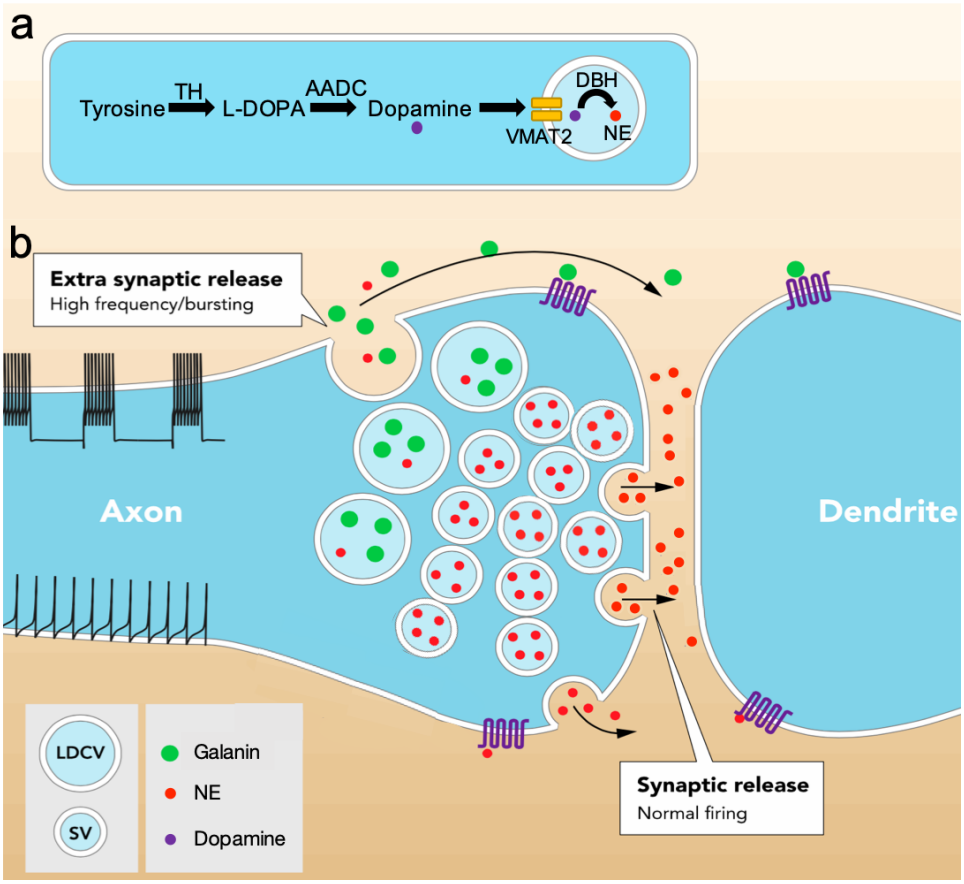

Figure 1.1. Synthesis, storage, and release of NE and neuropeptides. (a) NE is synthesized from tyrosine, which is converted to L-dihydroxyphenylalanine (L-DOPA) by tyrosine hydroxylase (TH). L-DOPA is converted by aromatic amino-acid decarboxylase (AADC) to dopamine, which is packaged into synaptic vesicles by the vesicular monoamine transporter 2 (VMAT2). The enzyme dopamine β-hydroxylase (DBH) then converts dopamine to norepinephrine (NE). (b) Galanin is stored in large, dense core vesicles (LDCV) along with other co-transmitters. These vesicles require higher frequency activity to induce exocytosis from the neuron. SV, synaptic vesicle. Source: *Modified from Lang et al. 2015*

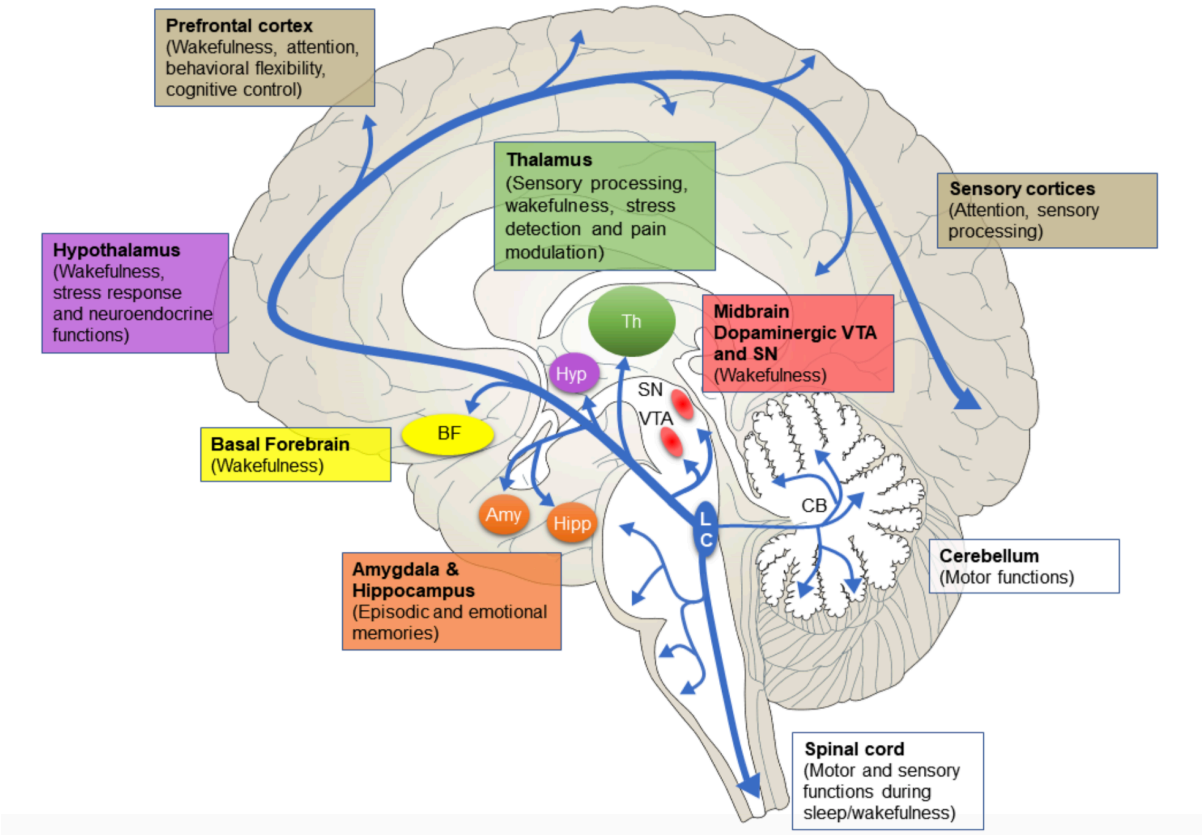

Figure 1.2 Major LC projections and functions. The LC has broad projects throughout the brain that allow regulation of many processes, including stress responses, wakefulness, attention, memory, and cognition. *Modified from Bari et al. 2020*

CHAPTER 2:

Elimination of galanin synthesis in noradrenergic neurons reduces galanin in select brain areas and promotes active coping behaviors

Adapted from:

R.P. Tillage*, N.R. Sciolino*, N.W. Plummer, D. Lustberg, L.C. Liles, M. Hsiang, J.M. Powell, K.G. Smith, P. Jensen, D. Weinshenker. *Co-first authors

Elimination of galanin synthesis in noradrenergic neurons reduces galanin in select brain areas and promotes active coping behaviors

Brain Structure and Function
March 2020; 225(2):785-803

2.1 Abstract

Accumulating evidence indicates that disruption of galanin signaling is associated with neuropsychiatric disease, but the precise functions of this neuropeptide remain largely unresolved due to lack of tools for experimentally disrupting its transmission in a cell type-specific manner. To examine the function of galanin in the noradrenergic system, we generated and crossed two novel knock-in mouse lines to create animals lacking galanin specifically in noradrenergic neurons ($Gal^{cKO\text{-}Dbh}$). We observed reduced levels of galanin peptide in pons, hippocampus, and prefrontal cortex of $Gal^{cKO\text{-}Dbh}$ mice, indicating that noradrenergic neurons are a significant source of galanin to those brain regions, while midbrain and hypothalamic galanin levels were comparable to littermate controls. In these same brain regions, we observed no change in levels of norepinephrine or its major metabolite at baseline or after an acute stressor, suggesting that loss of galanin does not affect noradrenergic synthesis or turnover. $Gal^{cKO\text{-}Dbh}$ mice had normal performance in tests of depression, learning, and motor-related behavior, but had an altered response in some anxiety-related tasks. Specifically, $Gal^{cKO\text{-}Dbh}$ mice showed increased marble and shock probe burying and had a reduced latency to eat in a novel environment, indicative of a more proactive coping strategy. Together, these findings indicate that noradrenergic neurons provide a significant source of galanin to discrete brain areas, and noradrenergic-specific galanin opposes adaptive coping responses.

2.2 Introduction

The neuropeptide galanin was first discovered in the early 1980s in porcine gut. Subsequent studies revealed that galanin is expressed throughout the brain and body of both humans and rodents (Tatemoto et al., 1983; Kofler et al., 2004; Fang et al., 2015; Lang et al., 2015) and modulates a variety of physiological processes including feeding, nociception, seizures, stress responses, cognition, and mood (Mitsukawa et al., 2008; Lang et al., 2015). Given this broad range of functions, it is not surprising that genome-wide association studies have implicated variants in genes encoding galanin and its receptors in conferring increased risk of depression and anxiety in humans (Wray et al., 2012; Juhasz et al., 2014; da Conceicao Machado et al., 2018). The exact role of galanin in these complex disorders, however, has yet to be determined.

Preclinical studies examining the effects of galanin have relied heavily on global knockouts or intracerebroventricular infusion of galanin agonists or antagonists. These experimental strategies lack regional specificity and often generate conflicting results. For example, galanin agonists administered into the rodent brain have been reported to elicit an anxiolytic effect in some tests (e.g. conflict test and elevated zero maze), and no effect in other anxiety assays (elevated plus maze, light-dark exploration, and open field) (Bing et al., 1993; Karlsson et al., 2005; Karlsson and Holmes, 2006; Rajarao et al., 2007). Likewise, galanin agonists also produce mixed effects on behavior in the forced swim and tail suspension tests (Bartfai et al., 2004; Holmes et al., 2005; Lu et al., 2005; Kuteeva et al., 2008a; Kuteeva et al., 2008b). Furthermore, global galanin knockout mice exhibit a wide variety of phenotypes, including endocrine, neurological, and behavioral deficits (Wynick et al., 1998; Holmes et al., 2000; Wynick and Bacon, 2002; Zachariou et al., 2003; Ahren et al., 2004; Adams et al., 2008). These findings suggest that galanin's effects are specific to the cell type, brain region, circuit,

and/or receptor(s) being engaged. Thus, strategies to manipulate galanin in a cell type-specific manner will help unravel its distinct functional roles in diverse physiological processes and disease states.

Galanin is expressed abundantly in a subset of noradrenergic neurons located in the locus coeruleus (LC) and subcoeruleus (SubC) in both rodents and humans (Skofitsch and Jacobowitz, 1985; Melander, 1986; Holets et al., 1988; Chan-Palay et al., 1990; Perez et al., 2001; Le Maitre et al., 2013). Intriguingly, transgenic mice overexpressing galanin in all noradrenergic neurons exhibit seizure resistance, mild cognitive deficits, and resilience against yohimbine-induced anxiety-like behavior (Mazarati et al., 2000; Steiner et al., 2001; Holmes et al., 2002). Because the transgene is expressed in all neurons that produce norepinephrine (NE) and epinephrine, and ectopically in some non-NE neurons (e.g. piriform cortex, entorhinal cortex) (Steiner et al., 2001), it is difficult to ascribe phenotypes to the subset of NE neurons that endogenously express galanin. The role of noradrenergic-derived galanin in normal and impaired brain function therefore remains unclear (for reviews see (Sciolino and Holmes, 2012; Lang et al., 2015; Weinshenker and Holmes, 2016; Hokfelt et al., 2018).

To begin to address this important question, we combined two new mouse alleles - a conditional knockout allele of *Gal* and a knock-in cre driver allele under control of the noradrenergic-specific *Dbh* promoter - to generate a mouse model in which galanin is selectively disrupted in noradrenergic neurons. Using this model, we measured the proportion of noradrenergic neuron-derived galanin in discrete brain regions and determined the consequences of its loss on behaviors relevant to anxiety, depression, cognition, and gross motor function. Our biochemical findings reveal that noradrenergic neurons provide a significant source of galanin to the cortex and hippocampus, and that loss of galanin has no effect on NE levels or turnover.

Furthermore, we demonstrate that noradrenergic neuron-specific galanin signaling plays a role in the regulation of defensive coping behaviors in the context of anxiogenic environmental manipulations.

2.3 Methods

Animals

All procedures related to the use of animals were approved by the Animal Care and Use Committee of the National Institute of Environmental Health Sciences and Emory University and were in accordance with the National Institutes of Health guidelines for the care and use of laboratory animals. Mice were maintained on a 12/12 h light-dark cycle with access to food and water *ad libitum* unless stated otherwise.

Generation of mouse lines

To generate the Gal^{cKO} allele ($Gal^{tm1a(KOMP)Pjen}$), we obtained a targeting vector (Project ID: CSD82928) containing loxP-flanked *Gal* exon 3 and FRT-flanked *LacZ* and *Neo* cassettes from the KOMP Repository (https://www.komp.org). Linearized vector was electroporated into G4 embryonic stem cell (George et al., 2007), and homologous recombinants were identified by Southern blotting with a *Neo* probe and long range PCR. Recombinant cells were injected into B6(Cg)-Tyr^{c-2J}/J blastocysts to produce chimeric mice. Heterozygous offspring of the chimeras were crossed to B6.Cg-*Tg(ACTFlpe)9205Dym*/J mice (Rodriguez et al., 2000; Jackson Lab stock no. 005703) to excise the FRT-flanked *LacZ* and *Neo* cassettes and generate the conditional allele. The Gal^{cKO} mice were thereafter maintained by backcrossing to C57BL/6J mice. *Cre*-mediated recombination of this allele deletes exon 3 and introduces a frameshift if exon 2 is

spliced to exon 4, thus eliminating expression of both galanin and galanin message associated protein (GMAP), which are encoded by the same mRNA.

To generate the *Dbh*^{cre} allele, we employed homologous recombination in G4 embryonic stem cells to insert a rox-flanked transcriptional stop cassette, *cre* cDNA, rabbit β-globin polyadenylation cassette, and attB/attP-flanked neomycin resistance cassette into the *Dbh* locus, immediately following the start codon. A recombinant clone was transiently transfected with pPGKPhiC31obpa (Raymond and Soriano, 2007) to excise the neomycin resistance cassette before cells were injected into B6(Cg)-*Tyr*$^{c-2J}$ blastocysts to produce chimeric mice. Following germline transmission, we crossed heterozygotes with B6;129-*Tg(CAG-dre)1Afst* mice to permanently excise the rox-flanked stop cassette and generate the *Dbh*^{cre} mouse line. The *Dbh*^{cre} mice were thereafter maintained by backcrossing to C57BL/6J.

Dbh^{cre}*; RC::LTG* mice were generated by crossing heterozygous *Dbh*^{cre} to homozygous *RC::LTG* mice (Plummer et al., 2017). *Gal*$^{cKO\text{-}Dbh}$ mutants were created by crossing *Dbh*$^{cre/+}$;*Gal*$^{cKO/+}$ double heterozygotes or *Dbh*$^{cre/+}$;*Gal*^{cKO} homozygotes to *Gal*^{cKO} homozygotes (**Fig. 1a**). *Gal*$^{cKO\text{-}Nestin}$ mutants were created by crossing *Nestin*$^{cre/+}$;*Gal*^{cKO} homozygotes to *Gal*^{cKO} homozygotes (*Nestin*$^{cre/+}$ breeders were obtained from The Jackson Laboratory, Bar Harbor, ME, Stock No. 003771). *Gal*^{NULL} mutants were generated by crossing *Gal*^{cKO} heterozygotes to a FVB/N-Tg(ACTB-cre)2Mrt (*hßactin-cre)* heterozygotes (Lewandoski et al., 1997) (*hßactin-cre* breeders were obtained from The Jackson Laboratory, Stock No. 003376). The *Gal*^{cKO} and *Dbh*^{cre} strains are both available at The Jackson Laboratory as Stock No. 034319 and 033951, respectively. For long-range PCR to identify homologous recombinants for *Gal*^{cKO} allele generation, the primer pairs were 5'-GAAGTCCGACAGCTGGTCCATCTGAG and 5'-CACAACGGGTTCTTCTGTTAGTCC for the upstream junction, and 5'-

CACACCTCCCCCTGAACCTGAAAC and 5'-GCTAGAAGGATGCTGTATAGAGTAGGCTTC for the downstream junction.

Stereotaxic delivery of colchicine

Colchicine, a disrupter of microtubule polymerization, was used to amplify galanin peptide signal for experiments requiring immunofluorescent cell body detection, as previously described (Skofitsch and Jacobowitz, 1985; Perez et al., 2001). Mice received intracerebroventricular injections of colchicine (10 μg in 0.5 μl sterile saline, 100 nL/min delivery rate) using the following stereotaxic coordinates: 0.48 posterior to bregma, 1.0 mm lateral to midline, and 2.8 mm ventral to skull surface. To treat colchicine-induce sickness, mice were administered acetaminophen (1.6 mg/ml) in the drinking water for 1-2 days before and after surgery. Mice were euthanized for tissue collection approximately 48-h following colchicine injection.

Tissue collection

Adult male and female mice were deeply anesthetized with sodium pentobarbital (0.1 mL of 50 mg/mL i.p.) and perfused transcardially with PBS followed by 4% PFA in PBS. Brains were postfixed overnight by immersion in 4% PFA at 4°C. Following rinse in PBS, tissue was cryoprotected in 30% sucrose in PBS and embedded in Tissue Freezing Medium (General Data Healthcare, Cincinnati, OH). For immunohistochemistry, 40-μm free-floating tissue cryosections were collected on a Leica CM3050-S cryostat (Leica Biosystems, Buffalo Grove, IL). Tissue for *in situ* hybridization was cryosectioned at 14-μm and collected onto Superfrost Plus slides, air dried and stored at -80°C.

To assess c-fos activation in the LC, mice were subjected to 1 h of acute restraint stress. Ninety min after the start of the stress, mice were anesthetized with isoflurane and transcardially perfused with potassium phosphate-buffered saline (KPBS) followed by 4% PFA in PBS. Brains were postfixed overnight by immersion in 4% PFA at 4°C, and then transferred to 30% sucrose in KPBS for 48 h at 4°C. Brains were flash frozen in isopentane on dry ice and embedded in Tissue Freezing medium. Tissue for immunohistochemistry was cryosectioned at 40-µm.

Half of the mice used for HPLC were subjected to foot shock stress for 20 min (nineteen 1 mA shocks lasting 0.5 ms with a random intershock interval of 30, 60 or 90 s), and brains were collected 15 min after the end of the foot shock exposure. For galanin ELISA and HPLC, mice were deeply anesthetized with isoflurane and rapidly decapitated for brain extraction. Hypothalamus, PFC, dorsal and ventral hippocampus, pons, and midbrain (ELISA) or PFC, pons, and whole hippocampus (HPLC) were rapidly dissected and snap-frozen in isopentane on dry ice. The samples were weighed and stored at -80°C until processing.

Immunohistochemistry

Immunohistochemistry was performed as previously described (Robertson et al., 2013; Sciolino et al., 2016). For immunofluorescent staining, noradrenergic cell bodies were labeled with Rabbit anti- TH (1:1000) and Goat anti-rabbit 488 secondary antibody (1:1000) or Goat anti-rabbit 633 (1:1000). Galanin fibers were labeled using rabbit anti-galanin (1:2000) and goat anti-rabbit 488 secondary antibody (1:1000). EGFP-expressing neurons and axons were detected using Chicken anti-GFP primary antibody (1:10,000) and Goat anti-chicken Alexa Fluor 488 secondary antibody (1:1000). For immunoperoxidase staining, we used Chicken anti-GFP primary antibody and biotinylated Goat anti-chicken secondary antibody (1:500), together with

Vectastain Elite ABC kit (PK6100), and DAB (SK4100) (all Vector Laboratories). Coverslips were applied using Vectashield hard-set mounting medium with or without DAPI (H-1500 or H-1400, Vector Labs, Burlingame, CA) or Prolong Diamond Anti-Fade mounting medium (P36970, Invitrogen).

Activated neurons were detected with rabbit anti c-fos primary antibody (1:5,000) and goat anti-rabbit 488 secondary (1:600). TH-expressing cells were detected using chicken anti-TH (1:1000) and goat anti-chicken 568 secondary (1:600). After staining, sections were mounted on slides and cover slipped with Fluoromount plus DAPI (Southern Biotech, Birmingham, AL). Antibodies are summarized in **Table 1**.

In situ hybridization

In situ hybridization was performed using BaseScope™ Probe BA-Mm-Gal-E3-1ZZ-st (Catalog #712941, Lot #18067A; Advanced Cell Diagnostics, Newark CA), which targets nucleotides 228-266 of mouse *Gal* (exon 3). Tissue was labeled according to the manufacturer's instructions and then processed for immunohistochemistry as described above.

Image acquisition

Images of fluorescently-labeled cell bodies were collected on a Zeiss LSM 710 or 880 confocal microscope (Carl Zeiss Microscopy, Thorwood NY) at 10 and 40x. Images of c-fos immunofluorescent-labeled sections were collected on a Leica DM6000B epifluorescent upright microscope at 20x. Images of immunoperoxidase-labeled cell bodies were collected on a Leica epifluorescent Zeiss Observer Z1 microscope at 40x. Anatomical location was confirmed by reference to a mouse brain atlas (Paxinos and Franklin, 2013).

Images of fluorescently labeled fibers were collected at 20x on a Zeiss LSM 880 confocal microscope. Three matched sections (425 x 425 □m) were acquired from each subject within the following defined regions relative to bregma: cingulate regions of the PFC A25 and A24a (1.98 to 1.42 mm), hippocampal dentate gyrus (DG) (-1.06 to -1.94), hypothalamic PVN and LHA (-0.58 to -1.22 mm), and midbrain VTA (-2.80 to -3.16) with reference to a mouse brain atlas. In a few cases (<5% of the total samples), two sections instead of three were obtained due to tissue damage or loss.

Image processing and quantification

For images of immunoperoxidase-labeled GFP-positive cell bodies, 8-μm Z-stacks were converted to a single image using the extended focus feature of Zen 2012 Blue Software (Carl Zeiss). For images of immunofluorescent-labeled galanin-positive cell bodies, a colocalization mask was created in the MIP image. Mask thresholds were empirically determined and applied equally to the control and mutant groups using NIH Image J (https://imagej.nih.gov/ij/). Using an 'AND' operation for co-expression between galanin and TH, the masks represented pixels with no expression (black) and co-expression (white). To optimize the full dynamic range of the fluorescence signal, only brightness and contrast adjustments were applied.

For quantification of c-fos immunofluorescence, three LC sections from each mouse were analyzed and averaged together to determine group means. All image analysis was performed with ImageJ software for background subtraction, threshold application (Otsu method) and quantification based on size and shape criteria for c-fos positive nuclei (30–70 mm^2, circularity 0.7–1.0). TH immunoreactivity was used to define LC area and only neurons within that area

were used for c-fos quantification. Experimenter was blind to genotype during image collection and analysis.

For quantification of galanin fibers, we first removed fluorescent artifacts from our 425 x 425 μm^2 image using the DEFiNE macro (https://figshare.com/s/1be5a1e77c4d4431769a) 'Clean Images' function with default settings to subtract artifacts, both large and small, that were morphologically distinct from fibers, as previously described (Powell et al., 2018). To remove blood vessels from the maximum intensity projection (MIP) images, we then performed two subtractions to remove particles larger than 65 μm^2 by converting the images to binary format at a threshold of 1 standard deviation above average pixel intensity. Large artifacts were identified using FIJI's 'Analyze Particle' function and were removed from the grayscale MIP using FIJI's 'Image Calculator – AND' function.

An experimenter blind to treatment group used DEFiNE's 'Quantify Fiber' function to set background-sensitive thresholds for the single-channel z-stack image. FIJI's 'Skeletonize' function was then applied to the resulting binary images to normalize variability in axon circumference. The number of μm^2 pixels in each binary image was measured for the galanin channel. For each subject, the number of pixels in the images from each region was averaged. Representative images were matched for anatomy and were converted to grayscale to enhance visibility of the fibers.

Galanin ELISA

Samples were put in buffer (2.5% aprotinin in 0.5M acetic acid), homogenized, heated (100°C for 10 min), and centrifuged (30 min at 4°C, 3000 rpm). Supernatant was collected, evaporated in a vacuum-sealed concentrator (10 h at 60°C and 20,000mm Hg; Labconco

Centrivap) and then stored at -20°C. Samples were reconstituted in 250 µL EIA buffer (Peninsula Laboratories, San Carlos, CA), and processed according to the manufacturer's instructions (Galanin Rat and Mouse ELISA kit, S1208, Peninsula Laboratories, San Carlos, CA). Wells were read at 450 nm, averaged across duplicates, and a curve of best fit was used to calibrate to standards.

HPLC

Tissue was thawed on ice and sonicated at 4°C in 0.1 N perchloric acid (10 µl/mg tissue) for 12 sec of 0.5 sec pulses. Sonicated samples were centrifuged (16100 rcf) for 30 min at 4°C, and the supernatant was then centrifuged through 0.45 µm filters at 4000 rcf for 10 min at 4°C. For HPLC, an ESA 5600A CoulArray detection system, equipped with an ESA Model 584 pump and an ESA 542 refrigerated autosampler was used. Separations were performed at 23ºC using an MD-150 × 3.2 mm C18 column. The mobile phase consisted of 90 mM sodium acetate, 37 mM citric acid, 0.2 mM EDTA, 0.4 mM 1-octanesulfonic acid sodium, 0.025% triethylamine, and 4.5% methanol at pH 4.4. A 25 µl of sample was injected. The samples were eluted isocratically at 0.4 mL/min and detected using a 6210 electrochemical cell (ESA, Bedford, MA) equipped with 5020 guard cell. Guard cell potential was set at 600 mV, while analytical cell potentials were −175, 150 and 400 mV. NE and its primary metabolite MHPG were measured with electrochemical detection. Analytes were identified by matching criteria of retention time and sensor ratio measures to known standards (Sigma-Aldrich, St. Louis, MO). Compounds were quantified by comparing peak areas to those of standards on the dominant sensor.

Behavior

Adult male and female mice were tested between 3 and 8 months of age, and sexes were balanced for all tests. Mice were group-housed for the duration of behavioral testing, unless stated otherwise. Tests were separated by at least 4 days.

Diurnal locomotor activity

Mice were placed in automated locomotor recording chambers (transparent Plexiglas cages on a rack; San Diego Instruments, La Jolla, CA), and ambulation (consecutive photobeam breaks) were recorded for 23 h in 30 min time bins.

Fear conditioning

Fear conditioning training, contextual fear testing, and cued fear testing were conducted over 3 consecutive days. The chamber (Coulbourn Instruments, Holliston, MA) was equipped with a house light, ceiling-mounted camera, speaker and an electric grid shock floor that could be replaced with a non-shock wire mesh floor. Chambers were cleaned in between animals with Virkon. The acquisition trial on day 1 lasted 6 min, followed by 3 tone-shock pairings during which the tone was present for 20 s and was co-terminated with a 3 s, 0.5 mA foot shock. Mouse behavior was recorded for 60 s following tone-shock presentation before the next round. Contextual fear testing on day 2 was performed in the same chamber as day 1 and lasted 7 min without any presentation of tone or shock. Cued fear testing on day 3 was conducted in a different chamber than days 1 and 2, with a non-shock mesh floor instead of the previous shock grid floor. The cued fear testing trial lasted 8 min, with the tone starting after 3 min and continuing until the end of the trial. Trials were programmed and run using the FreezeFrame software (Coulbourn) to automatically record freezing behavior during each trial.

Forced swim test

Mice were placed in a 3.5 L beaker with 3 L of water (25°C) and behavior was videotaped for 6 min. Behavior in the last 4 min of the test was scored by an observer blind to genotype with immobility defined as lack of any movements besides those which are required for balance and to keep the animal's head above water.

Tail suspension test

Climbstoppers (1.5 in long, clear flexible tubing) were placed over the base of each animal's tail to prevent tail climbing (Can et al., 2012). A piece of medical tape was placed around the tail, halfway between the base and the tip, and the mouse was suspended from a ring stand 16-18" from the counter. Behavior was videotaped for 6 min and the entire test was later scored by an observer blind to genotype, with immobility defined as a lack of all movement.

Sucrose preference

Mice were individually housed at least 1 week prior to the start of sucrose preference testing. Two small water bottles (modified 15mL conical tubes), one filled with 1% sucrose water and the other with tap water, were placed in the home cage. Bottles were weighed every 24 h, refilled as necessary, and the location of the bottles was switched every 24 h to control for side bias. The amount of water consumed from the bottles during each 24-h period was calculated by subtracting the weight from the previous measurement. Percent sucrose preference was then calculated as (sucrose water consumed) ÷ (normal + sucrose water consumed) × 100.

Open field

Mice were placed in the open field arena (36" x 36" x 36") for 5 min under dim light. An overhead camera and TopScan software were used to automatically detect the time spent in the center of the square, total distance travel, and ambulation velocity.

EZM

Mice were placed in the zero maze (2” wide track, 20” diameter) for 5 min under dim light. An overhead camera and TopScan software (Clever Sys Inc., Reston, VA) were used to automatically detect the time spent in open arms.

EPM

Mice were placed in the plus maze (25” by 25” arms, 2.5” track width) for 5 min under dim light. An overhead camera and TopScan software were used automatically detect the time spent in open arms.

Novelty-suppressed feeding

Following 24-h food deprivation, mice were placed in the corner of a novel arena (36” x 36” x 36”) that was illuminated by red light and contained a regular chow pellet in the center of the arena. Each food pellet was weighed before the start of the experiment. Mice were observed for up to 10 min while the latency to initiate feeding behavior (biting the food) was recorded. If the mouse did not bite the pellet after 10 min elapsed, the experiment ended, and a value of 600 s was assigned. To control for appetite, each animal was moved individually to a new home cage that contained the food pellet from the previous arena, and food intake was measured for 1 h. The arena was cleaned with Virkon between animals.

Marble burying

Twenty black glass marbles were arranged in a grid pattern on top of bedding (2” deep) in a cage (10” x 18” x 10”) with no lid. The mouse was placed in the center of the cage and left undisturbed for 30 min under bright light. At the end of the test period, images of each cage were taken from the same distance and angle. The number of marbles buried was determined by an experimenter blind to genotype by counting the number of marbles that remained unburied and

subtracting that count from 20. Marbles were considered buried when at least 2/3 of the marble could not be seen.

Shock probe defensive burying

The test cage (13" x 7" x 6") was filled with approximately 3 cm of clean bedding, and a shock probe was located on one wall of a chamber (14 cm long and 0.5 cm in diameter). The probe extended 10 cm into the cage and was wrapped with 2 alternating copper wires that were connected to a shock generator (Coulbourne). For testing, mice were placed in the cage at the opposite side from the probe. When the animal touched the probe, they received a 0.5 mA shock, and behavior was videotaped for 15 min from the time of the first shock (Degroot and Nomikos, 2004). The probe remained electrified throughout the test. Videos were later scored by an observer blind to genotype. Measured behaviors included number of probe touches, time spent digging, freezing, grooming, and number of rearing events.

Nestlet shredding

Mice were individually placed in novel cages (13" x 7" x 6") with 1 cm of clean bedding and a cotton fiber nestlet (5 cm x 5 cm, 0.5 cm thick, ~2.5 g) placed on top of the bedding. Each nestlet was weighed prior to the start of testing. Mice were left undisturbed for 2 h, after which the weight of the remaining untorn nestlet was recorded and the percent shredded by each mouse was calculated.

Statistical Analysis

Data were found to be normally distributed using the D'Agostino-Pearson test. Data were analyzed via unpaired t-test, one-way or two-way ANOVA with *post hoc* Tukey's test for multiple comparisons when appropriate. Significance was set at $p<0.05$ and two-tailed variants

of tests were used throughout. Data are presented as mean ± SEM. Calculations were performed and figures created using Prism Version 7 and 8 (GraphPad Software, San Diego, CA).

2.4 Results

$Gal^{cKO\text{-}Dbh}$ mice lack galanin mRNA and protein in noradrenergic neurons

To characterize the role of galanin in noradrenergic neurons, we first generated a knock-in allele that expresses cre recombinase under control of the noradrenergic-specific dopamine β-hydroxylase promoter (*Dbh^{cre}*). To evaluate the expression pattern and activity of *Dbh^{cre}*, we crossed it to the cre-responsive reporter *RC::LTG* (Plummer et al., 2017) which drives EGFP expression upon *cre* recombination. We observed EGFP expression in tyrosine hydroxylase+ (TH) noradrenergic neurons in the peripheral and central nervous system of *Dbh^{cre}; RC::LTG* double heterozygotes (**Fig. 2.1a** and data not shown). Similar to some *Dbh-cre* transgenic alleles (Matsushita et al., 2004; Gerfen et al., 2013), we also observed scattered EGFP+ cells in the adult cortex that likely reflect early transient expression of *Dbh* (**Fig. 2.1**). Importantly for the present study, the EGFP+ cortical neurons were negative for *Gal* mRNA expression (**Fig. 2.1**).

We next generated a conditional knockout allele of *Gal* (*Gal^{cKO}*) and crossed it with *Dbh^{cre}* to create the experimental mice referred to as *$Gal^{cKO\text{-}Dbh}$* mutants (**Fig. 2.2**). To confirm that mutants lack galanin expression selectively in noradrenergic neurons, we used *in situ* hybridization to detect *Gal* mRNA in adult brains of *$Gal^{cKO\text{-}Dbh}$* mutant and littermate control mice. *Gal* mRNA was abundant in LC and SubC noradrenergic neurons of control mice, but completely absent in these nuclei in *$Gal^{cKO\text{-}Dbh}$* mutants (**Fig. 2.2**). Importantly, *Gal* mRNA expression remained intact in TH-negative neurons in C2/A2 and other non-noradrenergic brain

regions, including the bed nucleus of the stria terminalis (BNST), lateral preoptic area, lateral hypothalamus and inferior olive (**Fig. 2.2 and 2.3**).

Next, we examined galanin protein expression by immunohistochemistry. To induce accumulation of the peptide in neuronal somata and thus improve its visualization, we injected the axonal transport blocker colchicine (10 μg) into the lateral ventricle of adult *Gal*$^{cKO\text{-}Dbh}$ mutant and littermate control mice. Like the pattern of mRNA expression, galanin was evident in TH+ neurons of the LC and SubC of littermate controls but abolished in almost all noradrenergic neurons in *Gal*$^{cKO\text{-}Dbh}$ mutants (**Fig. 2.4** and data not shown). In both *Gal*$^{cKO\text{-}Dbh}$ mutant and littermate control mice, we observed galanin immunoreactivity in non-noradrenergic populations, including the inferior olive (**Fig. 2.4** and data not shown). Interestingly, galaninergic fibers persisted in the LC region of *Gal*$^{cKO\text{-}Dbh}$ animals (**Fig. 2.4**), revealing that LC cells are innervated by galanin-containing neurons from non-noradrenergic sources. Combined, these findings indicate that *Gal*$^{cKO\text{-}Dbh}$ mice have a selective disruption of galanin synthesis in noradrenergic neurons.

Noradrenergic neurons provide a significant proportion of galanin to select brain regions

To assess the proportion of galanin in the brain that comes from noradrenergic neurons, we measured galanin protein levels in dissected tissue from the prefrontal cortex (PFC), dorsal and ventral hippocampus, hypothalamus, midbrain, and pons by ELISA. As a negative control and for comparison, we also generated and tested mice lacking galanin throughout the brain (*Gal*$^{cKO\text{-}nestin}$). *Gal*$^{cKO\text{-}Dbh}$ mice had significantly decreased galanin in the PFC (t_8=3.069, p=0.0154), pons (t_9=2.823, p=0.020), dorsal hippocampus (t_8=6.593, p=0.0002), and ventral hippocampus (t_8=2.314, p=0.0494) compared to littermate controls, but no difference in the midbrain

(t_7=0.5440, p=0.6033) or hypothalamus (t_{10}=0.4800, p=0.6415) (**Fig. 2.5**). These findings suggest that noradrenergic neurons provide a significant source of galanin to the cortex and hippocampus.

To provide finer neuroanatomical resolution, we quantified the density of galanin-positive fibers in the cingulate cortex (A25 and A24a), hippocampal dentate gyrus (DG), lateral and paraventricular nuclei of the hypothalamus (LHA and PVN) and midbrain ventral tegmental area (VTA) of $Gal^{cKO\text{-}Dbh}$, littermate control, and galanin null mice (Gal^{NULL}). We observed a significant reduction in galanin fiber expression in the A25 (t_{13}=2.276, p=0.0404), A24a (t_{13}=2.283, p=0.0399) and DG (t_{17}=2.536, p=0.0213) brain areas of $Gal^{cKO\text{-}Dbh}$ mice (**Fig. 2.6**), revealing these discrete regions within the prefrontal cortex and hippocampus are innervated by noradrenergic-derived galanin neurons. By contrast, $Gal^{cKO\text{-}Dbh}$ and littermate controls exhibited similar levels of galanin fiber expression in the midbrain VTA (t_{16}=0.7647, p=0.4556) as well as the hypothalamic PVN (t_{17}=0.7152, p=0.4842) and LHA (t_{17}=0.7952, p=0.4375) (**Fig. 2.6**), demonstrating that these areas do not receive significant innervation by noradrenergic-derived galanin neurons.

Normal NE abundance and turnover in $Gal^{cKO\text{-}Dbh}$ mutants

To determine whether loss of noradrenergic-derived galanin affects NE metabolic activity, we measured concentrations of NE, its major metabolite MHPG (3-Methoxy-4-hydroxyphenylglycol), and turnover ratio of MHPG:NE in dissected tissue from the PFC, pons, and whole hippocampus by HPLC at baseline and immediately after foot shock stress (**Fig. 2.7**). A two-way ANOVA showed that stress caused a significant decrease in NE in the pons ($F_{1,20}$=7.282, p=0.014) and hippocampus ($F_{1,20}$=5.653, p=0.028), but not PFC ($F_{1,20}$=0.255,

p=0.619), and a significant increase in MHPG in all three regions (pons, $F_{1,20}$=37.27, p<0.0001; hippocampus, $F_{1,20}$=27.4, p<0.0001; PFC, $F_{1,20}$=11.26, p<0.01). This resulted in an overall increase in NE turnover, as measured by the MHPG:NE ratio in the pons ($F_{1,20}$=698.9, p<0.0001), hippocampus ($F_{1,20}$=195.8, p<0.0001), and PFC ($F_{1,20}$=23.4, p<0.001). No genotype differences were observed (**Fig. 2.7a-c**).

Given that somatodendritic release of galanin is thought to inhibit LC activity (Pieribone et al., 1995; Xu et al., 2001; Vila-Porcile et al., 2009), we next wanted to determine if LC activity is influenced by the absence of noradrenergic-derived galanin. To do this, we measured c-fos, an immediate early gene used as a proxy for neuronal activation, at baseline and after a mild stressor, acute restraint. A two-way ANOVA comparing *Gal*$^{cKO\text{-}Dbh}$ mutants and controls at baseline and after stress showed that, as expected, stress increased c-fos expression in the LC ($F_{1,6}$=119.7, p<0.0001). However, there was no genotype effect ($F_{1,6}$=0.065, p=0.806), indicating that c-fos expression was comparable between *Gal*$^{cKO\text{-}Dbh}$ mutants and littermate controls (**Fig. 2.7d**). Together, these findings suggest that NE transmission remains intact when galanin is absent from noradrenergic neurons. It is important to keep in mind, however, that these measures are indirect and lack the sensitivity to detect subtle alterations in noradrenergic system function.

Gal$^{cKO\text{-}Dbh}$ *mice display a more proactive coping strategy in anxiogenic tasks measuring active defensive behaviors*

Next, we assessed the behavior of adult *Gal*$^{cKO\text{-}Dbh}$ mutants and littermate control mice in a battery of anxiety-, depression-, learning-, and motor-related tests. We observed no differences between *Gal*$^{cKO\text{-}Dbh}$ and littermate control mice in canonical tests of anxiety-like behavior (elevated plus maze, t_{22}=0.9379, p=0.3585; zero maze, t_{24}=0.0951, p=0.925; open field,

t_{36}=0.1769, p=0.8606) (**Fig. 2.8a-c**) or depressive-like behavior (tail suspension test, t_{23}=1.366, p=0.1853; forced swim test, t_{23}=1.55, p=0.1347; sucrose preference, $F_{1,16}$=0.004, p=0.9479) (**Fig. 2.8d-f**). In addition, $Gal^{cKO\text{-}Dbh}$ exhibited normal cognitive responses in contextual ($F_{1,20}$=0.1053, p=0.7489) and cued fear conditioning ($F_{1,20}$=2.778, p=0.1111) (**Fig. 2.8g**), as well as circadian locomotor activity ($F_{1,22}$=0.5295, p=0.4745) (**Fig. 2.8h**).

Having established that $Gal^{cKO\text{-}Dbh}$ mutants preform normally in standard tests of anxiety and depression that are reliant on *passive* behavioral responses (e.g. immobility, avoidance of open spaces, freezing), we next examined non-canonical anxiety tasks that assess *active* coping behaviors (e.g. digging). Using the marble burying assay, we observed that $Gal^{cKO\text{-}Dbh}$ mice buried significantly more marbles than littermate control mice (t_{36}=3.85, p<0.001) (**Fig. 2.9a**), indicating an enhancement of proactive defensive behavior. Mutants showed no difference in repetitive/compulsive behavior during the nestlet shredding task (t_{18}=0.4845, p=0.634) (**Fig. 2.9b**). Similarly to the marble burying results, in the shock probe defensive burying assay, $Gal^{cKO\text{-}Dbh}$ mice showed increased time spent in active digging (t_{15}=2.191, p=0.0447) (**Fig. 2.9c**), and a trend towards a decrease in passive freezing (t_{15}=1.601, p=0.1303) (**Fig. 2.9d**). Additional analysis of concurrent exploratory behaviors revealed $Gal^{cKO\text{-}Dbh}$ mice and littermate controls exhibited similar time spent grooming (WT = 47.57 ± 13.95, $Gal^{cKO\text{-}Dbh}$ = 61.44 ± 16.75; t_{15}=0.6271, p=0.54) and number of rearing events (WT = 35.75 ± 4.515, $Gal^{cKO\text{-}Dbh}$ = 36.78 ± 5.444; t_{15}=0.1431, p=0.8881) (data not shown). There was no difference in the number of times the mice were shocked by the probe (WT = 2.375 ± 0.5957, $Gal^{cKO\text{-}Dbh}$ = 2.444 ± 0.3379; t_{15}=0.1044, p=0.9182) (data not shown), indicating that alterations in behavior were not caused by differences in higher numbers of shocks to one group. We next examined performance in the novelty-suppressed feeding task, a conflict test that pits a mouse's innate fear of an unfamiliar

environment against a desire to feed. $Gal^{cKO\text{-}Dbh}$ mice were quicker to start eating (t_{34}=2.348, p=0.0248) (**Fig. 2.9e**), but ate a similar overall amount (t_{20}=1.331, p=0.1983) (**Fig. 2.9f**), suggesting the $Gal^{cKO\text{-}Dbh}$ phenotype was not driven by increased appetite. Taken together, these data indicate that selective galanin gene inactivation from noradrenergic neurons shifts defensive behavior to an active coping strategy under anxiogenic conditions.

2.5 Discussion

We have generated the first cell type-specific galanin knockout mouse by selectively deleting the *Gal* gene in noradrenergic neurons, leading to a loss of Gal mRNA and protein in these cells. Our results indicate that a large proportion of the galanin in the hippocampal DG and PFC, as well as about half the galanin in the brainstem, is derived from noradrenergic neurons, whereas alternate sources are responsible for the majority of hypothalamic and midbrain galanin. Measurement of tissue NE and MHPG levels in LC projection regions and c-fos expression in the LC suggest that the noradrenergic system is largely functioning normally in $Gal^{cKO\text{-}Dbh}$ mice, at least under baseline conditions and following an acute stressor. Finally, we found that $Gal^{cKO\text{-}Dbh}$ mice display a more active coping strategy in three independent tasks measuring active defensive behaviors in an anxiogenic context (marble burying, shock probe defensive burying, novelty-suppressed feeding), but their performance in other tests relevant to anxiety, depression, gross motor function, and cognition are indistinguishable from littermate controls.

Prior studies using slice electrophysiology show that galanin has an inhibitory effect on LC neuron activity (Xu et al., 2005; Hokfelt et al., 2018). Additionally, it has been suggested that galanin can be released somatodentritically from large dense core vesicles in LC-NE neurons and thereby produce an autoinhibitory effect on LC neuron activity, although this hypothesis has yet

to be tested directly (Huang et al., 2007; Vila-Porcile et al., 2009). While the lack of NE-LC system deficits in the *Gal*$^{cKO\text{-}Dbh}$ mice may seem surprising, it is important to keep in mind that the measures for noradrenergic system function used in the present study were indirect and may have lacked the sensitivity to detect subtle changes. Although steady-state tissue levels of NE and MHPG have been used to estimate NE turnover, *in vivo* microdialysis is a more direct measure of NE overflow and transmission. Likewise, while c-fos is a validated proxy for neuronal activity, it is a binary response that lacks the temporal resolution and sensitivity of electrophysiology. Despite these methodological considerations, our data indicate that the noradrenergic system is not grossly altered in the *Gal*$^{cKO\text{-}Dbh}$ mice, and that their behavioral phenotypes are caused by galanin depletion rather than alterations in NE signaling. Because *Gal*$^{cKO\text{-}Dbh}$ mice lack galanin expression in the LC throughout development, it is possible there may be compensatory mechanisms that allow LC activity regulation in the absence of autoinhibitory galanin release. Additionally, our immunohistochemical data uncovered a previously unrecognized galaninergic input to LC neurons that arises from a non-noradrenergic source(s) (**Fig. 2.4**) that persists in *Gal*$^{cKO\text{-}Dbh}$ mice and could play a role in regulating LC activity.

Previous studies using the neurotoxin 6-hydroxydopamine (6-OHDA) to lesion the LC suggested that the majority of galanin in the hippocampus and PFC comes from noradrenergic sources by examining the overlap between DBH-positive and galanin-positive fibers or measuring galanin peptide levels in brain regions innervated by the LC (Melander, 1986; Hökfelt et al., 1998; Weiss et al., 1998; Xu et al., 1998). However, these experiments had only been performed in rats, and neurotoxin lesioning is not cell type-specific, is rarely complete, can lead to axonal sprouting, and causes neuroinflammation. We overcame these caveats by using region-

specific tissue measurements and galaninergic fiber analysis to show that *Gal*$^{cKO\text{-}Dbh}$ mice have decreased levels of galanin peptide in LC projection fields, including the hippocampal DG and PFC. Our ELISA results indicated that galanin levels in the hippocampus and PFC of the *Gal*$^{cKO\text{-}Dbh}$ mutants was similar to that observed in mice lacking galanin in all neurons and glia, supporting the idea that galanin in these regions comes primarily from noradrenergic sources (**Fig. 2.5**). Similarly, fiber analysis showed a significant reduction of galanin-positive fibers in the *Gal*$^{cKO\text{-}Dbh}$ compared to littermates, although it was still above the level seen in the negative control tissue (**Fig. 2.6**). This slight divergence may be a result of differences in the sensitivity of these two techniques. Regardless, when taken together these results demonstrate that a significant portion of galanin protein found in the cortex and hippocampal DG comes from noradrenergic sources.

A previous study showed that intracerebroventricular 6-OHDA treatment in rats eliminated DBH-positive fibers in both the dorsal and ventral hippocampus, but abolished galanin-positive fibers in only the dorsal hippocampus, suggesting that galanin in the ventral hippocampus may come from non-noradrenergic neurons (Xu et al., 1998). We observed galanin depletion in both the dorsal and ventral hippocampus of *Gal*$^{cKO\text{-}Dbh}$ mice, possibly indicative of a species differences in the source of galanin in the ventral hippocampus. Further, our data suggest that, in mice, galanin in the midbrain and hypothalamus is derived from non-noradrenergic sources, consistent with the abundant expression of galanin in many hypothalamic neurons (Skofitsch and Jacobowitz, 1985; Melander, 1986). By contrast, a previous study in rats reported decreased galanin in the ventral tegmental area following LC lesion using 6-OHDA (Weiss et al., 1998). Our ELISA and fiber analysis results do not support this conclusion, as we saw no change in galanin peptide or galaninergic fibers in the midbrain as a whole or VTA specifically in

Gal$^{cKO\text{-}Dbh}$ mice compare to their littermates. This difference may be due to the improved specificity of our knockout model compared to lesion studies, or could indicate a species difference.

The performance of *Gal*$^{cKO\text{-}Dbh}$ mice was normal in all behavioral assays examined except for ethological-based anxiety tests that measure active, innate patterns of species-typical defensive behaviors. Specifically, *Gal*$^{cKO\text{-}Dbh}$ mutants buried more marbles, likely a result of increased digging (Thomas et al., 2009), and showed increased digging in the shock probe defensive burying task (**Fig. 2.9**). Increased digging is sometimes interpreted as increased anxiety-like behavior and could indicate that endogenous noradrenergic-derived galanin may have an anxiolytic effect. However, our other findings do not support this interpretation, as we did not see any differences in canonical approach-avoidance tests for anxiety-like behavior such as the open field, elevated plus maze, and zero maze (**Fig. 2.8**). These canonical tasks rely on innate, passive avoidance behavior to measure anxiety, whereas marble burying and shock probe burying are defensive tasks that rely on an active response (e.g., digging) as the measure of anxiety behavior, and may elicit increased levels of stress compared to approach-avoidance tasks (Cryan and Sweeney, 2011). Increased digging in mice has also been interpreted as a repetitive, perseverative behavior, but we did not observe any other evidence of repetitive behaviors in these mice, such as increased nestlet shredding (Thomas et al., 2009; Angoa-Perez et al., 2012; Angoa-Perez et al., 2013). Additionally, in the novelty-suppressed feeding task, we found that *Gal*$^{cKO\text{-}Dbh}$ mutants start eating sooner than controls, traditionally interpreted as decreased anxiety- or depressive-like behavior. This task is a conflict task that pits the desire for food against the fear of being in a novel environment, and therefore involves a component of motivation that the other tasks do not possess. Combined, these behavioral data indicate a role

for noradrenergic-derived galanin in regulating active coping strategies to environments that elicit immediate or potential threat. To our knowledge, the conventional galanin knockout mice have not been tested in either the canonical or noncanonical anxiety-like behavioral assays used in the present study, but these experiments would allow for an interesting comparison of the role of noradrenergic-derived galanin versus galanin from other sources.

Although the mechanism and circuitry underlying the increase in active coping in the *Gal*$^{cKO\text{-}Dbh}$ mutants is unclear, both galanin and NE signaling in the amygdala have been implicated in the regulation of stress-related behaviors. For example, intra-amygdala infusion of galanin decreased punished drinking episodes, which could be interpreted as a decrease in active coping (Moller et al., 1999) and is consistent with the enhanced active stress responses we observed in the *Gal*$^{cKO\text{-}Dbh}$ mutants. Another potential downstream target is the lateral septum, which is innervated by both galaninergic and noradrenergic fibers (Melander, 1986; Menard and Treit, 1996), and local infusion of the galanin receptor antagonist M40 decreased digging behavior in the shock probe defensive burying test in rats (Echevarria et al., 2005). This result suggests that galanin acting in the lateral septum has the opposite effect of what we report for the *Gal*$^{cKO\text{-}Dbh}$ mice, but this may be due to a species difference or an alteration in the function of the lateral septum in the *Gal*$^{cKO\text{-}Dbh}$ mutants due to the lack of galanin throughout development.

Neuropeptides, such as galanin, are preferentially released when neurons fire at high frequencies, and previous research has repeatedly suggested a role for galanin under challenging conditions that strongly activate noradrenergic neurons (Bartfai et al., 1988; Sciolino and Holmes, 2012; Lang et al., 2015). A recent study showed that selective optogenetic activation of galanin-containing LC neurons was sufficient to induce avoidance behavior (McCall et al., 2015). β-adrenergic receptor blockade prevented this effect, indicating that LC-derived NE plays

a role, but a potential contribution of galanin was not tested. It is possible that stronger behavioral phenotypes would emerge if the noradrenergic systems of *Gal*$^{cKO\text{-}Dbh}$ mutants were challenged by increasing the intensity and/or duration of stress during or prior to behavioral testing. It may also be informative to test the *Gal*$^{cKO\text{-}Dbh}$ mutants following chronic voluntary exercise, which is widely reported to increase galanin in the LC and has anxiolytic/antidepressant properties (Sciolino et al., 2012; Epps et al., 2013; Sciolino et al., 2015). Future studies using environmental manipulations, as well as optogenetic strategies for manipulating noradrenergic neuron activity, may help uncover a role for NE-derived galanin in modulating coping behaviors often associated with anxiety and depression.

Collectively, our studies using the *Gal*$^{cKO\text{-}Dbh}$ mutant model reveal that galanin plays an important role within the NE system by organizing a characteristic repertoire of defensive behaviors. This model is a useful tool to probe the many other functions hypothesized to be under the control of NE-derived galanin. Similar strategies targeting other cell type-specific galaninergic populations will help elucidate the broader neuroanatomy of the galanin system and its contribution to many physiological processes and disease states.

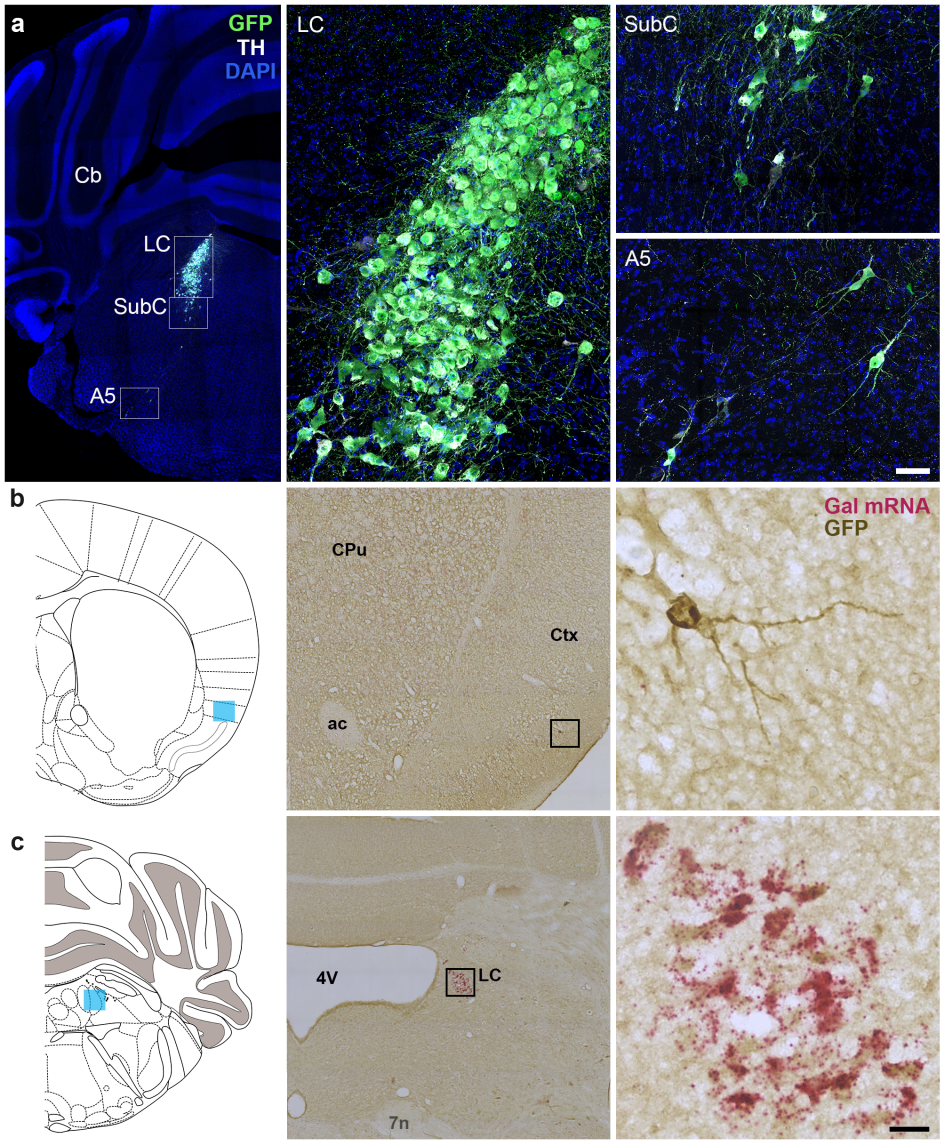

Figure 2.1. *Dbh*^{cre} drives cre recombinase expression in noradrenergic neurons and a sparse population of Gal-negative cortical neurons. (a) Representative coronal sections of *Dbh*^{cre}*;RC::LTG* brains stained for EGFP and TH-expressing neurons of the LC, SubC, and A5. Scale, 379 µm (brain), 50 µm (LC). Cb, cerebellum. LC, locus coeruleus. SubC, sub-coeruleus. (b-c) Coronal sections of *Dbh*^{cre}*; RC::LTG* brains stained for Gal (riboprobe, magenta) and EGFP (DAB antibody, brown). Scattered EGFP+, Gal-negative neurons are observed in the adult cortex (b), while EGFP+ neurons in the LC are Gal-positive (c). Coronal schematics of the adult brain (left) indicate the position of imaged neurons (blue shading). Scale, 20 µm (high magnification), 252 µm (low magnification). ac, anterior commissure. CPu, caudate putamen. Ctx, cortex. LC, locus coeruleus. 4V, fourth ventricle. 7N, facial nerve.

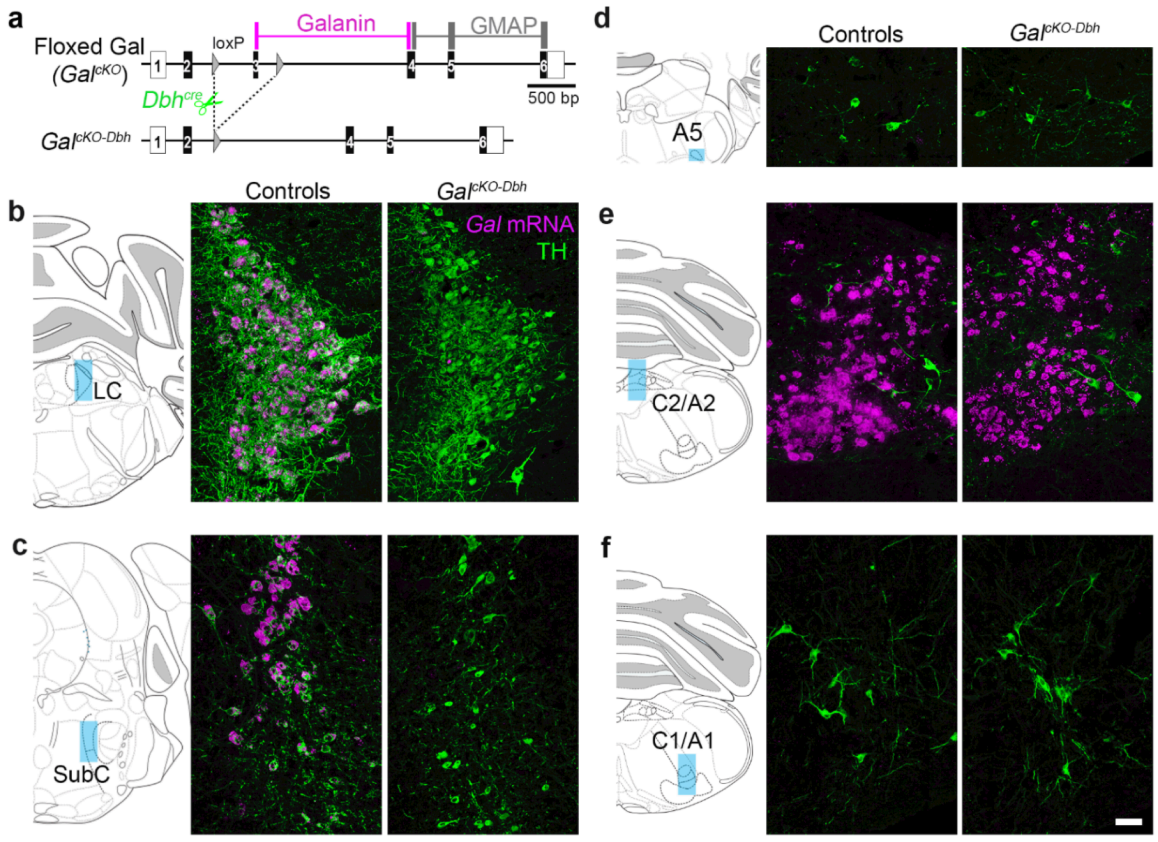

Figure 2.2. *Gal* conditional knockout allele permits selective disruption of galanin synthesis in noradrenergic neurons. (a) Schematic diagram of Gal^{cKO} allele. Recombination by Dbh^{cre} leads to disruption of galanin synthesis in NE neurons. (b-f) *Left*. Schematic illustration of coronal mouse brain showing location of images. *Right*. Representative coronal brain sections stained for *Gal* mRNA (riboprobe; magenta) and tyrosine hydroxylase (TH antibody; green). *Gal* mRNA is absent from the SubC and LC of mutant mice ($Gal^{cKO\text{-}Dbh}$). Scale bar, 50 µm. LC, locus coeruleus. SubC, sub-coeruleus.

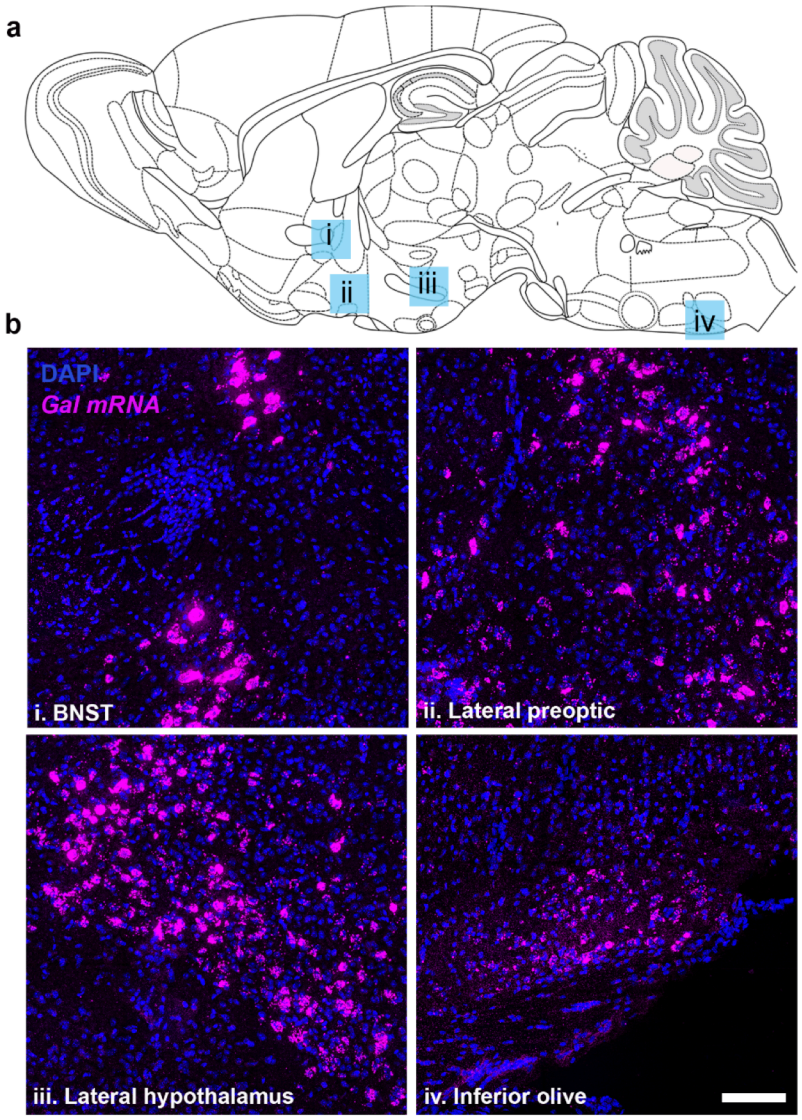

Figure 2.3. *Gal* mRNA expression persists outside the noradrenergic system of *Gal*$^{cKO\text{-}Dbh}$ mice. (a) Schematic illustration of sagittal mouse brain showing location of images. (b) Representative sagittal sections from brains of *Gal*$^{cKO\text{-}Dbh}$ mice stained for *Gal* mRNA (riboprobe; magenta) and DAPI (blue). Scale, 100 µm. BNST, bed nucleus of the stria terminalis.

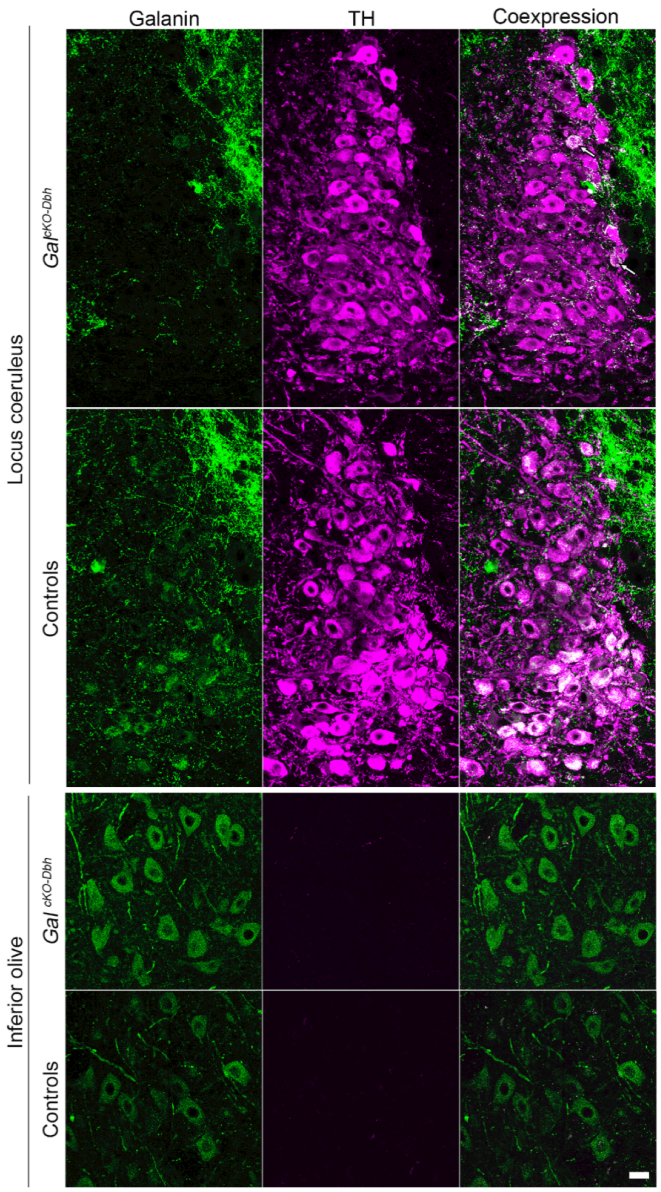

Figure 2.4. Galanin protein expression is reduced selectively in noradrenergic neurons of *Gal*$^{cKO\text{-}Dbh}$ mice. Representative coronal brain sections stained for galanin (antibody; green) and tyrosine hydroxylase (TH antibody; purple). *Top*. In littermate controls, the majority of noradrenergic locus coeruleus (LC) neurons co-express TH and galanin (white). In *Gal*$^{cKO\text{-}Dbh}$ mice, galanin (green) is absent from the majority of TH+ (purple) LC neurons. Arrows indicate an occasional TH+ neuron in in *Gal*$^{cKO\text{-}Dbh}$ mice that co-expresses galanin (white). Dense TH-negative, galanin+ fibers (green) surround and innervate the LC in *Gal*$^{cKO\text{-}Dbh}$ mice and littermate controls. *Bottom*. Galanin is expressed normally in non-noradrenergic olivary neurons of *Gal*$^{cKO\text{-}Dbh}$ mice and littermate controls. Scale, 20 µm.

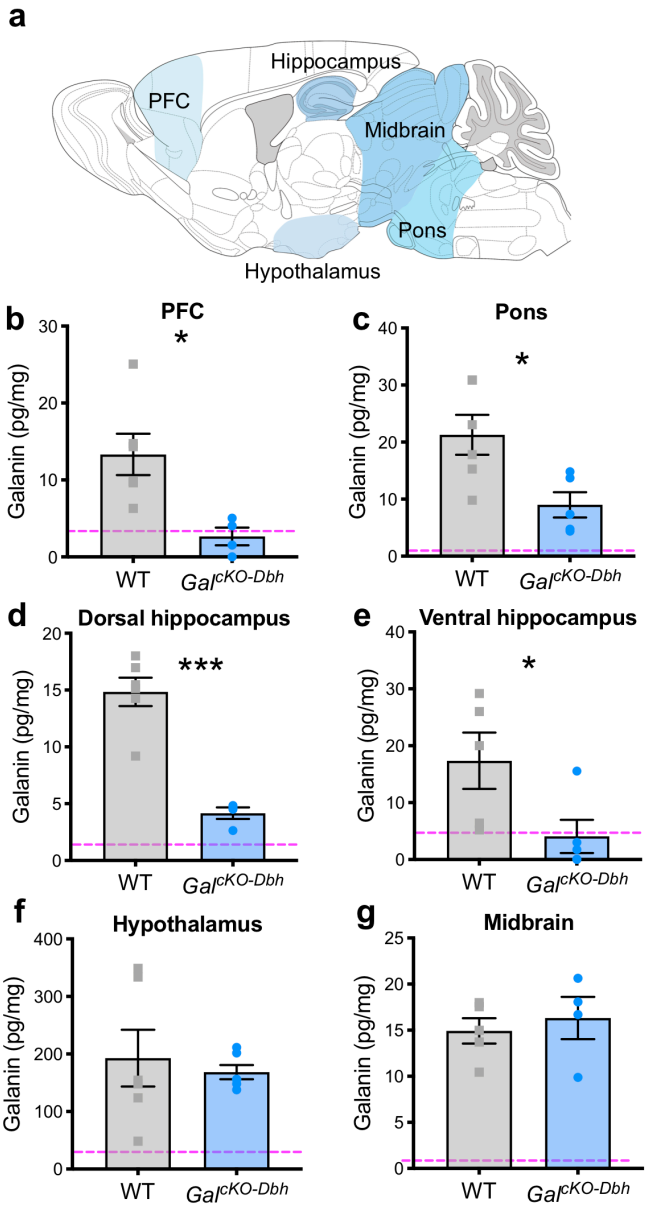

Figure 2.5. *Gal*$^{cKO\text{-}Dbh}$ mice have decreased galanin in the hippocampus, prefrontal cortex, and pons. Tissue galanin levels were measured by galanin ELISA. Tissue was collected via rapid dissection of whole regions (see methods for more detail) (a). *Gal*$^{cKO\text{-}Dbh}$ mice showed significantly decreased galanin in the PFC (b), pons (c), and dorsal and ventral hippocampus (d, e), with no differences in the hypothalamus (f) or midbrain (g) compared to littermate controls. Dashed line shows the average signal determined in each discrete brain region of negative control *Gal*$^{cKO\text{-}nestin}$ tissue. In the PFC and hippocampus, *Gal*$^{cKO\text{-}Dbh}$ galanin levels were reduced to an equivalent level as seen in the negative control samples (a, c, d). n = 4-6 mice per group. Data were analyzed by independent samples t-tests (two-tailed). Error bars show SEM. *p<0.05, ***p<0.001

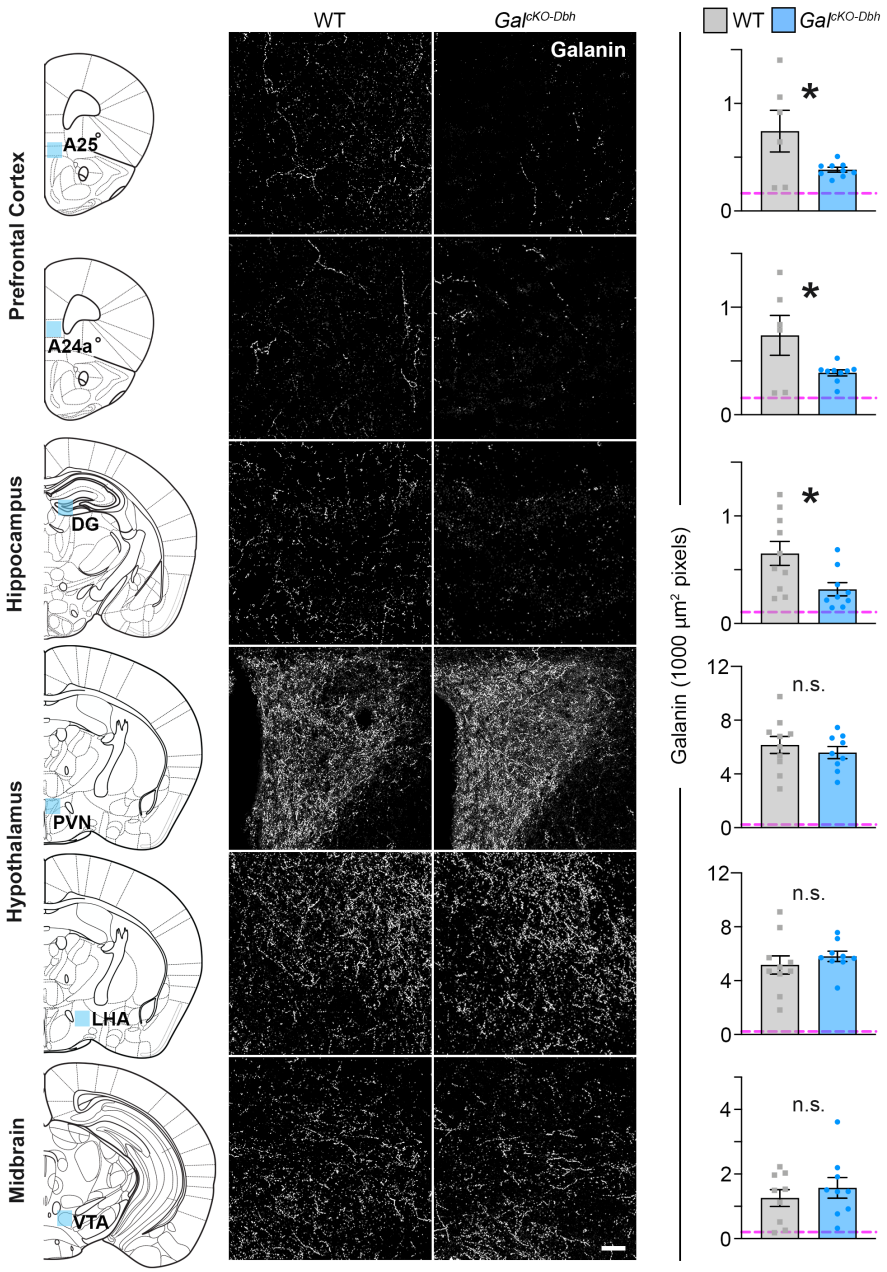

Figure 2.6. *Gal*$^{cKO\text{-}Dbh}$ mice have a reduction in galanin-positive fibers in subregions of the prefrontal cortex and hippocampal dentate gyrus. *Left*. Blue shading on schematic of coronal mouse brain shows the location of fiber quantification. *Middle*. Representative coronal brain sections immunostained for galanin (white). Scale bar, 50 µm. *Right*. Average galanin fiber density in discrete brain regions. Dashed line shows the average background signal determined in each discrete brain region of *Gal*^{NULL} tissue. *Gal*$^{cKO\text{-}Dbh}$ mice showed reduced galanin fiber expression in prefrontal cortex (A25 and A24a) and hippocampus (DG), with no differences in the hypothalamus (PVN and LHA) or midbrain (VTA) compared to littermate controls. n = 6-10 littermate controls, n = 9 *Gal*$^{cKO\text{-}Dbh}$ mutants. Data were analyzed by independent samples t-tests (two-tailed). Error bars show SEM. *p<0.05. n.s., non-significant.

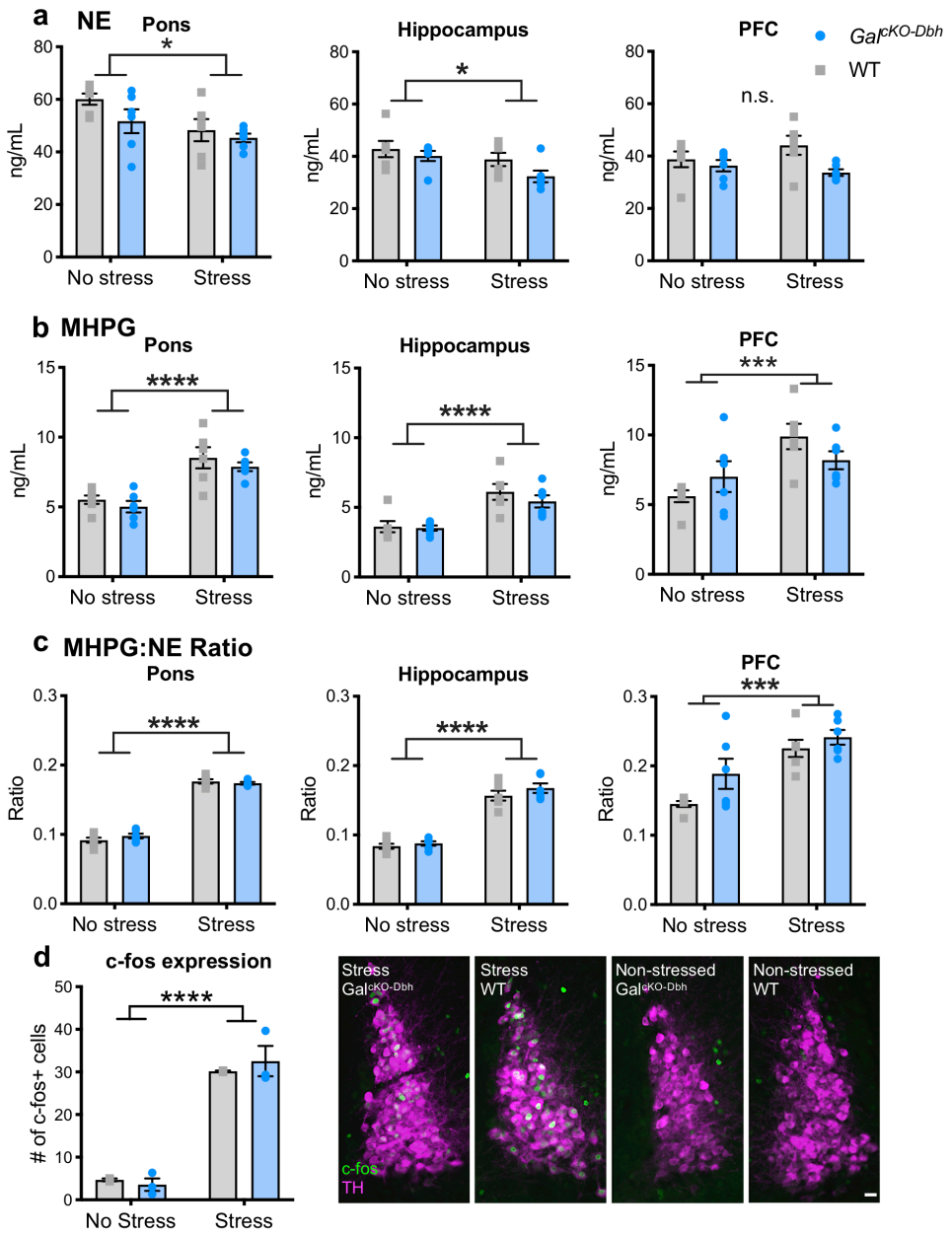

Figure 2.7. Baseline and stress-induced NE turnover and LC c-fos expression are normal in *Gal*$^{cKO\text{-}Dbh}$ mice. NE (a) and the major metabolite of NE, MHPG (b), were measured via HPLC at baseline and after acute foot shock stress in the pons, hippocampus, and PFC. Foot shock stress caused an overall decrease in NE and increase in MHPG, leading to an increase in the MHPG:NE ratio in all three brain regions. No differences were seen between genotypes in either the raw measurements or the MHPG:NE ratio. n = 6 mice per group. Fos immunohistochemistry and quantification did not show any differences between *Gal*$^{cKO\text{-}Dbh}$ mice and WT littermate control mice at baseline or after acute restraint stress (d) *Right*. Representative LC sections stained for Fos (antibody; green) and tyrosine hydroxylase (TH antibody; magenta). n = 3 slices per animal, 2-3 animals per group. Data were analyzed by two-way ANOVA. Scale bar, 20 µm. Error bars show SEM. *p<0.05, ***p<0.001, ****p<0.0001, n.s., non-significant.

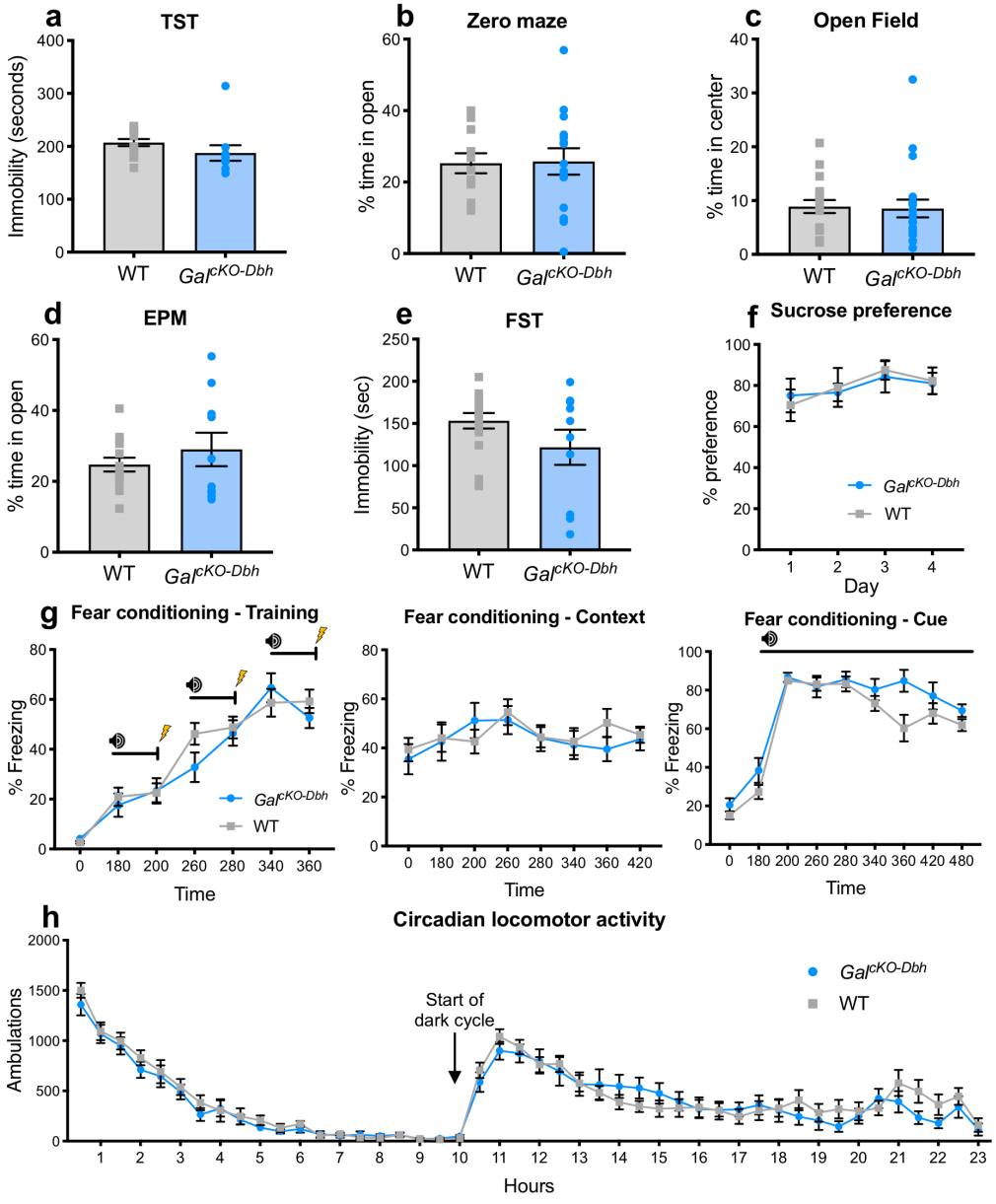

Figure 2.8. *Gal*$^{cKO\text{-}Dbh}$ display normal behavior at baseline in canonical tests for anxiety- and depression-like behavior, locomotion, and associative learning. There were no differences between *Gal*$^{cKO\text{-}Dbh}$ and WT littermate control mice in elevated plus maze (EPM) (a), zero maze (b), open field (c), tail suspension test (TST) (d), forced swim test (FST) (e), sucrose preference (f), fear conditioning (g), or locomotor activity (h). n = 10-20 per group; mixed males and females. Error bars show SEM.

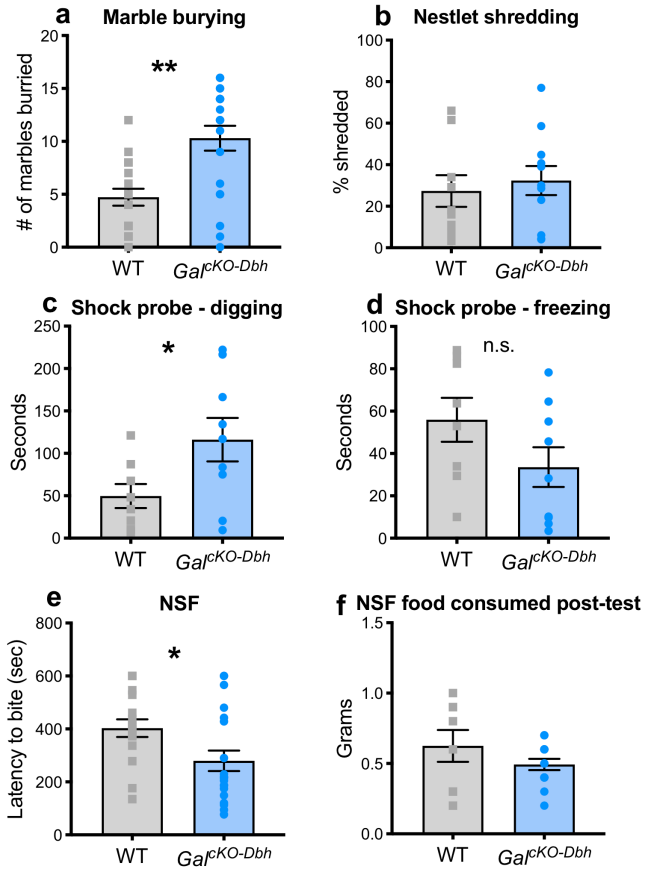

Figure 2.9. *Gal*$^{cKO\text{-}Dbh}$ display increased digging behavior in the marble burying and shock probe defensive burying tasks and decreased latency to feed in the novelty-suppressed feeding task. In the marble burying assay (a), *Gal*$^{cKO\text{-}Dbh}$ mice buried significantly more marbles than WT littermate control mice. There were no differences between *Gal*$^{cKO\text{-}Dbh}$ and WT controls in nestlet shredding behavior (b). *Gal*$^{cKO\text{-}Dbh}$ mice showed increased digging in the shock probe defensive burying task and a trend towards decreased freezing (c, d). In the novelty-suppressed feeding task (NSF), *Gal*$^{cKO\text{-}Dbh}$ mice showed a decrease in latency to feed but consumed the same amount of food as WT controls in the hour after the test (e, f). n = 10-20 per group; mixed males and females. Error bars show SEM. *p<0.05, ***p<0.001

CHAPTER 3:

Disentangling the functional roles of co-transmitters norepinephrine and galanin in stress-induced behavior

3.1 Abstract

It is now widely recognized that a single neuron can release multiple neurotransmitters and neuromodulators, increasing the complexity and flexibility of neural circuits. However, separating out the individual effects of multiple transmitters within a single cell type has been a challenge for researchers. Both the noradrenergic and galaninergic systems in the brain are dysregulated in stress-related neuropsychiatric disorders like anxiety and depression, and these two systems overlap in the locus coeruleus (LC), where a majority of noradrenergic neurons also co-express galanin across species. In this study, we aimed to disentangle the functional roles of these co-transmitters in mediating stress-induced behavioral changes by comparing anxiety-like behaviors in genetically modified male and female mice that lack either norepinephrine (NE) (*Dbh*$^{-/-}$ mice) or galanin (*Gal*$^{cKO\text{-}Dbh}$ mice) specifically in noradrenergic neurons. We found that NE-deficient mice were resistant to the acute anxiogenic effects of foot shock and optogenetic LC stimulation in the elevated zero maze, while mice lacking NE-derived galanin and wild-type controls showed similar increases in anxiety-like behavior. However, when mice were tested for behavioral changes 24 h after foot shock, we found that both *Dbh*$^{-/-}$ and *Gal*$^{cKO\text{-}Dbh}$ mice were resistant. These data indicate that NE and galanin in noradrenergic neurons play partially overlapping, but distinguishable roles in behavioral responses to aversive stimuli. Our findings suggest that NE is important for the expression of acute stress-induced anxiety, while both NE and noradrenergic-derived galanin appear to be involved in mediating more persistent behavioral changes.

3.2 Introduction

The colocalization of multiple neuroactive substances in a single neuron was first discovered in the 1970s (Bartfai et al., 1988; Hokfelt et al., 2018). Since then, many examples of co-transmission have been found throughout the nervous system, leading to a deeper understanding of the complexity of these systems. We now know that co-transmitters lead to an increase in the versatility of neural circuits through mechanisms that can have opposing or complementary effects, can be regulated independently of each other, and can show differential transmission based on the postsynaptic target (Nusbaum et al., 2017; Oh et al., 2019; Pomrenze et al., 2019; Granger et al., 2020). Although some of the complexity created by co-transmission has been dissected with the aid of modern neuroscience techniques, studying the functional effects of co-released neurotransmitters from a single cell type has remained a challenge.

Since the discovery of the neuropeptide galanin, neuroanatomical mapping studies have found consistently high galanin levels co-expressed with norepinephrine (NE) in the locus coeruleus (LC) of mice, rats, monkeys, and humans (Skofitsch, 1985; Melander, 1986; Holets et al., 1988; Chan-Palay et al., 1990; Perez et al., 2001; Le Maitre et al., 2013). The vast majority of LC research, however, has focused exclusively on NE. Less attention has been paid to LC-derived galanin and trying to disentangle the roles of these co-transmitters, despite the fact that each have been independently implicated in stress-induced behaviors in rodents and stress-related neuropsychiatric disorders in humans (Karlsson and Holmes, 2006; Weinshenker and Holmes, 2016; Borodovitsyna et al., 2018; Hokfelt et al., 2018). Stress strongly activates LC neurons, which broadly innervate the rest of the brain and play an important role in regulating the fight-or-flight response to a stressful event (Valentino and Van Bockstaele, 2008). Given that the LC is a major source of both NE and galanin to many brain regions, it is a powerful

neuroanatomical tool to study the roles of NE and galanin co-transmission in stress-induced behaviors.

Traditional pharmacological and genetic studies allow functional investigation of single or even combinations of neurotransmitters, but often lack the resolution to manipulate each one in a single cell type. On the other hand, application of newer neuroscience tools, such as optogenetics and chemogenetics, can achieve cell type-specificity but modulate neurotransmission indiscriminately, obscuring the potentially unique effects of co-released molecules. To overcome these limitations, we utilized genetically modified mouse lines that lack NE (dopamine β-hydroxylase; $Dbh^{-/-}$ mice) or galanin ($Gal^{cKO\text{-}Dbh}$) specifically in noradrenergic neurons. Importantly, $Dbh^{-/-}$ mice have normal galanin expression in the LC (unpublished data), and $Gal^{cKO\text{-}Dbh}$ mice have normal NE levels (Tillage et al., 2020). The $Dbh^{-/-}$ mice have been extensively studied since their initial creation (Thomas et al., 1995), and do not differ from controls in traditional tests for anxiety-like behavior at baseline (Marino et al., 2005; Schank et al., 2008; Lustberg et al., 2020). Likewise, $Gal^{cKO\text{-}Dbh}$ mice also show normal anxiogenic behavior at baseline in classic anxiety assays, but have increased active coping behavior in some less common paradigms, indicating a role for NE-derived galanin in mediating passive coping behaviors (Tillage et al., 2020) (see Chapter 2).

Here, we exposed these two mouse lines to either foot shock or LC-specific optogenetic activation followed by behavioral testing in order to determine the functional roles of noradrenergic neuron-derived NE and galanin in regulating stress-induced behavior.

3.3 Methods

Animals

All procedures related to the use of animals were approved by the Institutional Animal Care and Use Committee of Emory University and were in accordance with the National Institutes of Health guidelines for the care and use of laboratory animals. All mice were group housed, unless noted otherwise, and maintained on a 12/12 h light-dark cycle with access to food and water *ad libitum*. All manipulations and behavioral tests occurred during the light cycle. Adult male and female mice (3-9 months) were used for all experiments. No sex differences were observed, and data for males and females were combined.

Dbh$^{-/-}$ mice lack expression of the DBH enzyme, which is required for NE synthesis, resulting in a total depletion of NE throughout the brain and body (Thomas et al., 1998). These mice were generated and maintained on a mixed 129/SvEv and C57BL/6J background, as previously described (Thomas et al., 1995; Thomas et al., 1998). To prevent the embryonic lethality associated with the homozygous *Dbh* deficiency, pregnant *Dbh*$^{+/-}$ dams were given the adrenergic receptor agonists isoproterenol and phenylephrine (20 μg/ml each) from E9.5 to E14.5, and the synthetic precursor to NE, L-3,4-dihydroxyphenylserine (DOPS; 2 mg/ml), from E14.5 to parturition in their drinking water. *Dbh*$^{+/-}$ mice were used as controls in experiments with *Dbh*$^{-/-}$ mice because their behavior and brain catecholamine levels are indistinguishable from WT (*Dbh*$^{+/+}$) mice (Thomas et al., 1995; Thomas and Palmiter, 1997; Szot et al., 1999; Bourdelat-Parks et al., 2005; Marino et al., 2005; Gaval-Cruz et al., 2012). *Gal*$^{cKO\text{-}Dbh}$ mice were generated as described in Chapter 2 and maintained on a C57BL/6J background by crossing *Dbh*$^{cre+}$*;Gal*$^{flx/flx}$ mice to *Dbh*$^{cre-}$*;Gal*$^{flx/flx}$ mice. Because of this difference in genetic background (mixed 129/C57 vs pure C57), *Dbh*$^{-/-}$ mice could not be directly compared to *Gal*$^{cKO\text{-}Dbh}$ mice, so

all experiments were designed to compared $Dbh^{-/-}$ to their $Dbh^{+/-}$ littermates, and $Gal^{cKO\text{-}Dbh}$ mice to their $Dbh^{cre\text{-}};Gal^{flx/flx}$ littermates (referred to as WT).

Stress paradigm

The foot shock stress protocol was modified from a previously published paradigm (Lecca et al., 2016). Mice were individually exposed to 20 min of foot shock exposure consisting of 19 shocks randomly interspaced by 30, 60 or 90 s (0.5ms shocks, 1mA) in chambers equipped with a house light, a ceiling-mounted camera, and an electric grid shock floor (Coulbourn Instruments, Holliston, MA). Control animals were placed in the chamber for 20 min but were not administered shocks. Chambers were cleaned with MB-10 between animals.

Corticosterone (CORT) measurement

Mice used for CORT measurement went through the foot shock stress paradigm described above and were anesthetized with isoflurane 15 min after the end of the stress. Mice were rapidly decapitated, and trunk blood was collected in EDTA-coated tubes (Sarstedt Inc., Newton, NC) and chilled on ice. Blood was centrifuged for 20 min at 3000 rpm at 4°C, and resulting plasma was collected and stored at -80°C. CORT was measured using the Enzo Life Sciences kit (Farmingdale, NY) following the manufacturer's small volume protocol for blood plasma, including diluting samples 1:40 with a steroid displacement reagent solution.

Stereotaxic surgery

For optogenetic experiments, mice were anesthetized with isoflurane and given meloxicam (5 mg/kg, s.c.) at the start of the surgery. A lentiviral vector containing channelrhodopsin-2 (ChR2)

with an mCherry tag under control of the noradrenergic-specific PRSx8 promoter (Hwang et al., 2001) (Penn Vector Core, Philadelphia, PA) was infused unilaterally into the LC (-5.4AP; +1.2ML; -4.0DV) with a 5 µL Hamilton syringe and Stoelting Quintessential Stereotaxic Injector pump at a rate of 0.15 µL/min. Unilateral LC stimulation is sufficient to produce behavioral effects in mice that are indistinguishable from bilateral stimulation (Carter et al., 2010; McCall et al., 2015). Control mice received a lentivirus containing mCherry alone under the PRSx8 promoter (Penn Vector Core). Each animal received a 0.7 µL infusion, and the infusion needle was left in place for 5 min after infusion to allow for viral diffusion. An optic fiber ferrule (ThorLabs, Newton, NJ) was implanted 0.5 mm dorsal to the viral injection site (-5.4AP; +1.2ML; -3.5DV), and permanently attached to the skull with screws and dental acrylic. Mice were singly housed after this surgery to prevent cage mates from damaging the headcap and given at least 3 weeks to recover and allow for full viral expression before testing.

Optogenetic stimulation and elevated zero maze (EZM)

Mice were habituated to handling and connection of the optic patch cable to the implanted optic ferrule for at least one week prior to testing. The LC optogenetic stimulation was based on a previously published paradigm (McCall et al., 2015). Photostimulation was delivered to the LC for 30 min (5 Hz tonic stimulation, 10 ms light pulses, 473 nm) in 3 min on/off bins in the home cage immediately before testing in the EZM, which was conducted as previous described (Tillage et al., 2020). The EZM was used because it is a validated test for anxiety-like behavior in rodents and mouse behavior in the EZM is sensitive to LC activity manipulations (Shepherd et al., 1994; McCall et al., 2015). Furthermore, both mutants and their WT counterparts show

normal behavior at baseline in this assay, allowing us to observe stress-induced behavioral changes (Lustberg et al., 2020; Tillage et al., 2020).

Histology

In order to assess correct targeting of the LC in mice used for optogenetic experiments, all animals were exposed to 5 Hz LC photostimulation for 15 min in the home cage, then anesthetized 90 min later with isoflurane and transcardially perfused with potassium phosphate-buffered saline (KPBS), followed by 4% PFA in PBS. Brains were postfixed overnight by immersion in 4% PFA at 4°C, and then transferred to 30% sucrose in KPBS for 48 h at 4°C. Brains were flash frozen in isopentane on dry ice and embedded in Tissue Freezing Medium. Tissue was cryosectioned at 40-µm for immunohistochemistry. Viral expression and correct optic fiber targeting were assessed by immunostaining for the mCherry tag using rabbit anti-DsRed primary antibody (1:1000) and goat anti-rabbit 568 secondary (1:500). Sections were co-stained for the noradrenergic marker tyrosine hydroxylase (TH) with chicken anti-TH (1:1000) and goat anti-chicken 488 secondary (1:500). In adjacent LC sections, activated LC neurons were detected with rabbit anti c-Fos primary antibody (1:5,000) with goat anti-rabbit 488 secondary (1:500) and TH-expressing cells were co-stained using chicken anti-TH (1:1000) with goat anti-chicken 568 secondary (1:500). After staining, all sections were mounted on slides and cover slipped with Fluoromount plus DAPI (Southern Biotech). Images were collected on a Leica DM6000B epifluorescent upright microscope at 10x or 20x. Mice were excluded from analyses if they did not show viral expression in the LC, correct optic fiber targeting, and increased c-Fos expression in the LC compared to the control animals of the same cohort. No differences in c-fos expression between genotypes were observed.

Statistical Analysis

Data were found to be normally distributed using the D'Agostino-Pearson test and analyzed by two-way ANOVA for main effects and interaction effects, with Sidak's correction for multiple comparisons to examine planned comparisons between stress or virus treatment, where appropriate. Significance was set at $p<0.05$ and two-tailed variants of tests were used throughout. Data are presented as mean ± SEM. Calculations were performed and figures created using Prism Version 8 (GraphPad Software, San Diego, CA).

3.4 Results

$Dbh^{-/-}$ mice, but not $Gal^{cKO\text{-}Dbh}$ mice, are resistant to the acute anxiogenic effects of foot shock stress

To determine the relative importance of NE and noradrenergic-derived galanin for the acute behavioral response to a stressor, we subjected mice to 20 min of foot shock and then immediately tested them in the EZM. When we analyzed the percentage of time the animals spent in the open arms of the EZM by two-way ANOVA, we found a significant genotype x treatment interaction for $Dbh^{-/-}$ mice compared to their $Dbh^{+/-}$ littermates ($F_{1,29}=8.003$, $p=0.0084$), with post hoc testing showing a significant decrease in percent time spent in the open arms for $Dbh^{+/-}$ mice ($t_{29}=2.444$, $p=0.0413$), but no difference between stressed and non-stressed $Dbh^{-/-}$ mice ($t_{29}=1.541$, $p=0.2503$) (**Fig. 3.1a)**. For the $Gal^{cKO\text{-}Dbh}$ mice, there was a main effect of treatment ($F_{1,30}=17.89$, $p=0.0002$) but no genotype x treatment interaction ($F_{1,30}=0.00284$, $p=0.9580$), indicating that the mutants showed the same behavioral response in the EZM

immediately after foot shock stress as their WT counterparts (WT: t_{30}=3.028, p=0.0100, *Gal*$^{cKO\text{-}Dbh}$: t_{30}=2.953, p=0.0121) (**Fig. 3.1b**).

To confirm that the endocrine stress response was intact in mice lacking NE or NE-derived galanin, we measure levels of corticosterone (CORT) in the blood immediately after exposure to foot shock stress. For the *Dbh*$^{-/-}$ mice, there was a significant effect of treatment on CORT levels ($F_{1,21}$=48.49, p<0.0001), but no effect of genotype ($F_{1,21}$=1.854, p=0.1877), showing that both *Dbh*$^{-/-}$ mice and *Dbh*$^{+/-}$ controls have similar CORT responses to the foot shock stress (*Dbh*$^{+/-}$: t_{21}=4.759, p=0.0002, *Dbh*$^{-/-}$: t_{21}=5.088, p<0.0001) (**Fig. 3.1c**). We found a significant effect of treatment on CORT levels for the *Gal*$^{cKO\text{-}Dbh}$ mice ($F_{1,24}$=15.87, p=0.0005), but no effect of genotype ($F_{1,24}$=0.001293, p=0.9716), indicating that *Gal*$^{cKO\text{-}Dbh}$ mice have a normal CORT response to the foot shock stress itself and the neuroendocrine stress axis is functional (WT: t_{24}=2.942, p=0.0142, *Gal*$^{cKO\text{-}Dbh}$: t_{24}=2.722, p=0.0237) (**Fig. 3.1d**). Both the *Gal*$^{cKO\text{-}Dbh}$ mice and the *Dbh*$^{-/-}$ mice also showed normal freezing to the foot shocks compared to their littermate controls during the stress itself (*Dbh*$^{+/-}$ vs. *Dbh*$^{-/-}$: $F_{1,21}$=3.690, p=0.0684; WT vs. *Gal*$^{cKO\text{-}Dbh}$: $F_{1,10}$=0.000936, p=0.9925) (**Fig. 3.1e-f**).

Dbh$^{-/-}$ *mice, but not Gal*$^{cKO\text{-}Dbh}$ *mice, show reduced anxiogenic effects to optogenetic LC stimulation*

To complement the acute foot shock experiment and more selectively activate NE and galanin co-expressing cells, we optogenetically stimulated LC neurons in WT, *Dbh*$^{-/-}$, and *Gal*$^{cKO\text{-}Dbh}$ mice immediately before EZM testing (**Fig. 3.2a**). The stimulation and behavioral paradigm used here was based on a previously published paradigm of optogenetic LC activation-induced anxiety-like behavior (McCall et al., 2015). Mice received intra-LC infusion of virus expressing

either ChR2-mCherry or mCherry alone driven by the noradrenergic-specific PRSx8 promoter, resulting in high levels of viral expression selectively in the LC. Because more than 80% of LC neurons co-express galanin, we are confident that LC neurons containing galanin were activated using this viral strategy. Viral expression and optic ferrule placement were confirmed in all animals by histology (**Fig. 3.2b**), and successful activation of the LC was confirmed via an increase in c-Fos immunoreactivity (*Dbh* mice: t_{12}=5.055, p=0.0003; Gal mice: t_{17}=3.277, p=0.0044) (**Fig. 3.2c-d**). Because no differences in c-Fos expression after optogenetic stimulation were observed between genotypes (data not shown), controls and knockout animals were combined for c-Fos quantification. For the *Dbh*$^{-/-}$ mice, there were significant main effects of both virus ($F_{1,28}$=6.108, p=0.0198) and genotype ($F_{1,28}$=14.72, p=0.0006) on the percent time mice spent in the open arms of the EZM, with planned comparisons showing that *Dbh*$^{+/-}$ ChR2 mice spent significantly less time in the open arms compared to *Dbh*$^{+/-}$ mCherry mice (t_{28}=2.568, p=0.0314), while there was no significant difference between *Dbh*$^{-/-}$ mice expressing ChR2 or the control virus (t_{28}=1.030, p=0.5263) (**Fig. 3.2e**). While a significant interaction effect between genotype and virus was not observed in this experiment ($F_{1,28}$=0.8574, p=0.3624), the lack of a significant decrease in time spent in the open sections of the EZM for the *Dbh*$^{-/-}$ ChR2 mice suggests that the NE is involved in optogenetic LC stimulation-induced anxiety-like behavior. For the *Gal* mice, there was a significant main effect of virus ($F_{1,26}$=21.07, p<0.0001) but not genotype ($F_{1,26}$=0.0238, p=0.8786) on the percent time spent in the open arms of the EZM (**Fig. 3.2f**), demonstrating that the noradrenergic galanin is dispensable for the normal behavioral response to optogenetic LC activation.

Both Gal$^{cKO\text{-}Dbh}$ and Dbh $^{-/-}$ mice are resistant to the persistent anxiogenic effects of foot shock stress

Neuropeptides, such as galanin, have distinct dynamics compared to classic neurotransmitters such as NE, and may therefore exert their effects on a different timescale. To examine the relative roles of NE and noradrenergic-derived galanin in the persistent behavioral response to a stressor, we subjected mice to 20 min of foot shock and then tested them in the EZM 24 h later instead of immediately following the stressor (**Fig. 3.3a**). We found significant genotype x treatment interaction effects between stress and genotype in the percent time spent in the open segments for both *Dbh*$^{-/-}$ compared to *Dbh*$^{+/-}$ mice ($F_{1,38}$=6.211, p=0.0172) (**Fig. 3.3b**) and *Gal*$^{cKO\text{-}Dbh}$ mice compared to WT controls ($F_{1,38}$=4.694, p=0.0366) (**Fig. 3.3c**). Post hoc analyses revealed that the stress-exposed control animals in both experiments spent less time in the open arms of the EZM (*Dbh*$^{+/-}$: t_{38}=2.503, p=0.0332, WT: t_{38}=2.556, p=0.0292), while *Dbh*$^{-/-}$ and *Gal*$^{cKO\text{-}Dbh}$ mice were resistant to this effect (*Dbh*$^{-/-}$: t_{38}=1.054, p=0.5081, *Gal*$^{cKO\text{-}Dbh}$: t_{38}=0.4633, p=0.8745). These results demonstrate that both neuromodulators are important for the long-term (24 h) anxiogenic-like effects of foot shock stress.

3.5 Discussion

The discovery that a single neuron can release multiple neuromodulators has fundamentally changed our understanding of the nervous system. Co-transmission leads to an increase in the versatility and complexity of neural circuits in the brain, ultimately allowing an organism to respond adaptively across diverse situations, including to threatening or stressful events. In this study, we aimed to disentangle the roles of the LC co-transmitters NE and galanin by using knockout mice to dissociate the functional roles of NE and noradrenergic-derived galanin in

stress-induced behavior. This research is important because both of these transmitters play a role in regulating behavioral responses to stress in rodents, and have been implicated in stress-related neuropsychiatric disorders in humans (Karlsson and Holmes, 2006; Weinshenker and Holmes, 2016; Borodovitsyna et al., 2018; Hokfelt et al., 2018). More broadly, our results may also shed light on how other small molecule and peptide co-transmitter systems function throughout the nervous system. While both *Dbh*$^{-/-}$ and *Gal*$^{cKO\text{-}Dbh}$ mice responded similarly during the stressor itself, with high levels of freezing and increased plasma CORT, we found that that *Dbh*$^{-/-}$ mice were resistant to foot shock or optogenetic LC activation-induced anxiety-like behavior in the EZM immediately after the stressor, while the responses of *Gal*$^{cKO\text{-}Dbh}$ mice were similar to controls. However, when tested 24 h after stress exposure, we found that both *Dbh*$^{-/-}$ and *Gal*$^{cKO\text{-}Dbh}$ mice were resistant to the persistent effects of foot shock in EZM performance. These results suggest that NE, but not NE-derived galanin, is involved in behavioral changes immediately following stress exposure, but that an important role for NE-derived galanin emerges over a longer timescale.

Our findings that the *Dbh*$^{-/-}$ mice were resistant to stress-induced behavioral changes both immediately following the foot shock and 24 h later support an important role for NE in mediating stress-induced anxiety-like behavioral changes. Recent studies have found that LC projections to the BLA mediate foot shock stress-induced increases in BLA firing through βAR signaling, and local blockade of βAR signaling in the BLA immediately following foot shock leads to decreased freezing behavior in an immediate fear extinction paradigm (Giustino et al., 2017; Giustino et al., 2020). Furthermore, LC-NE mediated βAR signaling in the BLA was found to induce anxiety-like behavior on its own and modulate pain-related anxiety-like behavior (McCall et al., 2017; Llorca-Torralba et al., 2019). This acute action of NE in the BLA likely

explains the acute stress-induced anxiety-like effect in the EZM immediately following foot shock that we observed in WT and *Gal*$^{cKO\text{-}Dbh}$ mice, which is absent in the *Dbh*$^{-/-}$ mice. It is possible that acute NE release is also required for the expression of stress-induced anxiety-like behavior in the EZM 24 h after the stressor. Alternatively, the high levels of NE released during the stress itself may induce plasticity that facilitates anxiety-like behavior the following day. A series of experiments using L-3,4-dihydroxyphenylserine (DOPS) to acutely restore NE in *Dbh*$^{-/-}$ mice either during the foot shock exposure or during the EZM 24 h later could determine whether acute NE signaling is required during the EZM regardless of when the test is administered, or whether longer-term neurotrophic actions are in play 24 h after a stressor.

A previous study showed that selective optogenetic activation of galanin-containing LC neurons was sufficient to induce avoidance behavior and this behavioral effect could be prevented by a βAR antagonist, indicating a noradrenergic mechanism (McCall et al., 2015). However, the potential contribution from galanin was not explicitly examined. Here, we employed the same optogenetic protocol to selectively activate LC neurons and showed that *Gal*$^{cKO\text{-}Dbh}$ mutants an increased anxiety-like behavior in the EZM similar to WT animals, but this effect was absent in *Dbh*$^{-/-}$ mice, which had no change in EZM performance. Our results support the previous work by McCall and colleagues by showing that acute optogenetic LC stimulation-induced anxiety-like behavior is likely mediated by NE and expand on this finding by showing that NE-derived galanin is dispensable for this acute behavioral change.

Our data support recent studies indicating that activation of the LC is sufficient to drive anxiety-like behavior. Recent studies using optogenetic manipulation of LC neurons have shown that increasing high tonic, but not phasic, firing of the LC leads to aversion and anxiety-like behavior in mice, and that inhibiting LC activity using chemogenetics blocks stress-induced

anxiety-like behavior (McCall et al., 2015; Li et al., 2018). Furthermore, as mentioned previously, βAR signaling specifically in the BLA via LC projections has been found to induce anxiety-like behavior and modulate pain-induced anxiety-like behavior, adding support to the theory that increased NE release from the LC can induce anxiety (McCall et al., 2017; Llorca-Torralba et al., 2019). However, there is some evidence to the contrary. Several studies have suggested that lesioning the LC leads to decreased anxiety-like behavior (Nassif et al., 1983; Britton et al., 1984; Koob et al., 1984). Additionally, systemic administration of α2AR antagonists have been seen to have both anxiogenic and anxiolytic effects on behavior (Charney et al., 1983; Gower and Tricklebank, 1988; Holmes et al., 2002). Using a more specific manipulation, a previous study pharmacologically activated the LC via local infusion of the selective α2AR antagonist idazoxan, and found that this led to decreased anxiety-like behavior in an open field drinking test in rats (Weiss et al., 1994). It is likely that pharmacological and optogenetic manipulations of the LC result in different patterns of LC activation, and so this difference in effects may be due to different patterns of LC activation being elicited. While we did not directly measure the effects of our optogenetic manipulation on LC activity in this study, McCall and colleagues previously used *in vivo* electrophysiology combined with optogenetics to show that 5 Hz tonic stimulation of the LC leads to increased tonic activation patterns similar to those evoked by stress (Curtis et al., 1997; Curtis et al., 2012; McCall et al., 2015). It is possible that only manipulations that increase tonic firing sufficiently result in anxiogenic effects. If a stimulus preferentially increases phasic activity instead of high tonic activity, then anxiety may not manifest. It is also important to take LC circuitry into consideration. Recent studies have suggested that activation of distinct, projection-specific subsets of LC neurons can lead to different, even opposing, effects on behavior (Uematsu et al., 2015; Chandler, 2016; Hirschberg

et al., 2017). For example, activation of LC neurons that project to the amygdala promotes aversive learning, while activation of a separate, mPFC-projecting group of LC neurons extinguishes aversive responses (Uematsu et al., 2017). Therefore, it is likely that the LC may indeed be able to differentially modulate anxiety, depending on the exact pattern of LC activity elicited and which subpopulations of LC neurons are recruited.

There are many potential mechanisms by which galanin might be affecting behavior over a 24 h timescale. Neuropeptides, such as galanin, have different dynamics than classic neurotransmitters like NE due to divergent mechanisms controlling synthesis, release, and degradation of the molecules (see Chapter 1 for details). Because of their storage in large dense core vesicles (LDCV), neuropeptides are thought to be preferentially released when neurons fire at high frequencies, and previous research has suggested that galanin transmission occurs under conditions that strongly activate noradrenergic neurons (Bartfai et al., 1988; Sciolino and Holmes, 2012; Lang et al., 2015). NE, on the other hand, is stored in both small clear synaptic vesicles and LDCVs, which may account for our results showing that NE is important for both acute and long-term behavioral responses to stress. Given that both foot shock and 5 Hz optogenetic LC stimulation strongly activate the LC and should, in theory, cause both NE and galanin release, we must consider explanations for the delayed emergence of galanin-mediated behavioral effects. Galanin can act as an inhibitory neuromodulator by signaling immediately after release through galanin receptors, which are typically G_i-coupled, but galanin can also act as a neurotrophic factor, leading to changes in plasticity over time (Weinshenker and Holmes, 2016). One possible mechanism underlying our results is the initial high LC activity during the foot shock stress "primed" the LDCVs, which then were able to release galanin upon increased LC firing during EZM exposure the next day and resulted in enhanced neuromodulatory effects

on downstream regions (**Fig. 3.4**). This ability of galanin to drive anxiety-like behavior is consistent with the previously hypothesized role for galanin in promoting passive coping behaviors (Weiss et al., 1998; Tillage et al., 2020). An alternative, non-mutually exclusive, "neurotrophic" mechanism is that galanin released from LC terminals during the foot shock session had longer term effects (such as changes in dendritic spines, receptor distribution, etc.) on downstream brain regions involved in the stress response (e.g. amygdala, prefrontal cortex (PFC), etc.) (**Fig. 3.5**). These alterations in plasticity took time to develop and thus did not change behavior in the EZM test until 24 h after the stress, and failed to occur in the absence of galanin from the LC in the $Gal^{cKO\text{-}Dbh}$ mice. Previous research has shown that significant atrophy and remodeling of dendrites occurs in stress-sensitive regions, such as the PFC, as early as 24 h after a single foot shock stress, and that chronic intracerebroventricular infusions of galanin prevent foot shock-induced dendritic spines loss in the PFC (Sciolino et al., 2015; Nava et al., 2017; Musazzi et al., 2018).

The results described here suggest a role for NE-derived galanin in regulating behavioral consequences of stress over the course of hours to days. This raises many interesting questions for future experiments to address, such as when, where in the brain, and how could galanin be acting to increase stress susceptibility 24 h later? Experiments quantifying expression of the immediate early gene c-fos could determine which brain regions are differentially activated after the EZM test in the $Gal^{cKO\text{-}Dbh}$ mice compared to WT mice. Examining differences in synapse remodeling, such as dendritic spine alterations, following foot shock stress between $Gal^{cKO\text{-}Dbh}$ mice and WT mice would be helpful in determining whether a neurotrophic mechanism is occurring in this time frame. Behavioral pharmacology experiments will also be useful for elucidating the mechanisms and receptors in play. For example, galanin could be administered to

Gal$^{cKO\text{-}Dbh}$ mice either prior to foot shock or prior to EZM testing 24 h later to determine when galanin signaling is required for stress-induced anxiety-like behavior. A complementary approach would be to infuse a galanin receptor antagonist in WT mice at the same two time points to determine when blocking galanin signaling induces a stress-resilient phenotype. These experiments could also be done either brain-wide (e.g. intracerebroventricular infusions) or locally (e.g. BLA, PFC) to determine in which specific brain region galanin is acting to induce these changes and could employ compounds specific to individual galanin receptors (GalR1-3) in order to isolate which receptors are involved.

While there are significant benefits to using knockout models like the *Dbh*$^{-/-}$ and *Gal*$^{cKO\text{-}Dbh}$ mice, there are also important limitations to consider. First, neither of these genetic manipulations are specific to the LC. While the LC projects widely to brain regions known to control behavioral responses to stress (e.g. hippocampus, amygdala, prefrontal cortex) and is very likely the main source of galanin and NE that mediate stress-related behaviors, we cannot conclude that it is the only driver from the present study. Experiments using LC-specific genetic or viral-mediated knockouts would be needed to confirm this hypothesis. This is important because other noradrenergic regions, particularly the A2 neurons in the nucleus of the solitary tract (NTS), are known to play a role in mediating responses to stress (Myers et al., 2017), although very few of the noradrenergic neurons in the NTS appear to co-express galanin. Furthermore, because the knockout mice used here lack expression of NE or galanin throughout development, it is possible there may be compensatory mechanisms that alter the way these systems function. The pharmacological and viral-vector mediated approaches described above could help to overcome this limitation.

Our data indicate that both NE and NE-derived galanin are involved in mediating aspects of stress-induced anxiety-like behavior and appear to act over different timescales. These findings on the differential roles of co-transmitters in the LC-NE system may be applicable to other neuromodulatory systems that co-express neuropeptides, such as the serotonergic dorsal raphe neurons which express neuropeptide Y and galanin in some species, or the dopaminergic ventral tegmental area (VTA) neurons which express high levels of brain-derived neurotrophic factor (Hokfelt et al., 1999; Berton et al., 2006). Future studies will continue to disentangle the functional relationship between these co-expressed neuromodulators in the LC-NE system and determine the mechanism by which galanin regulates long-term stress responses.

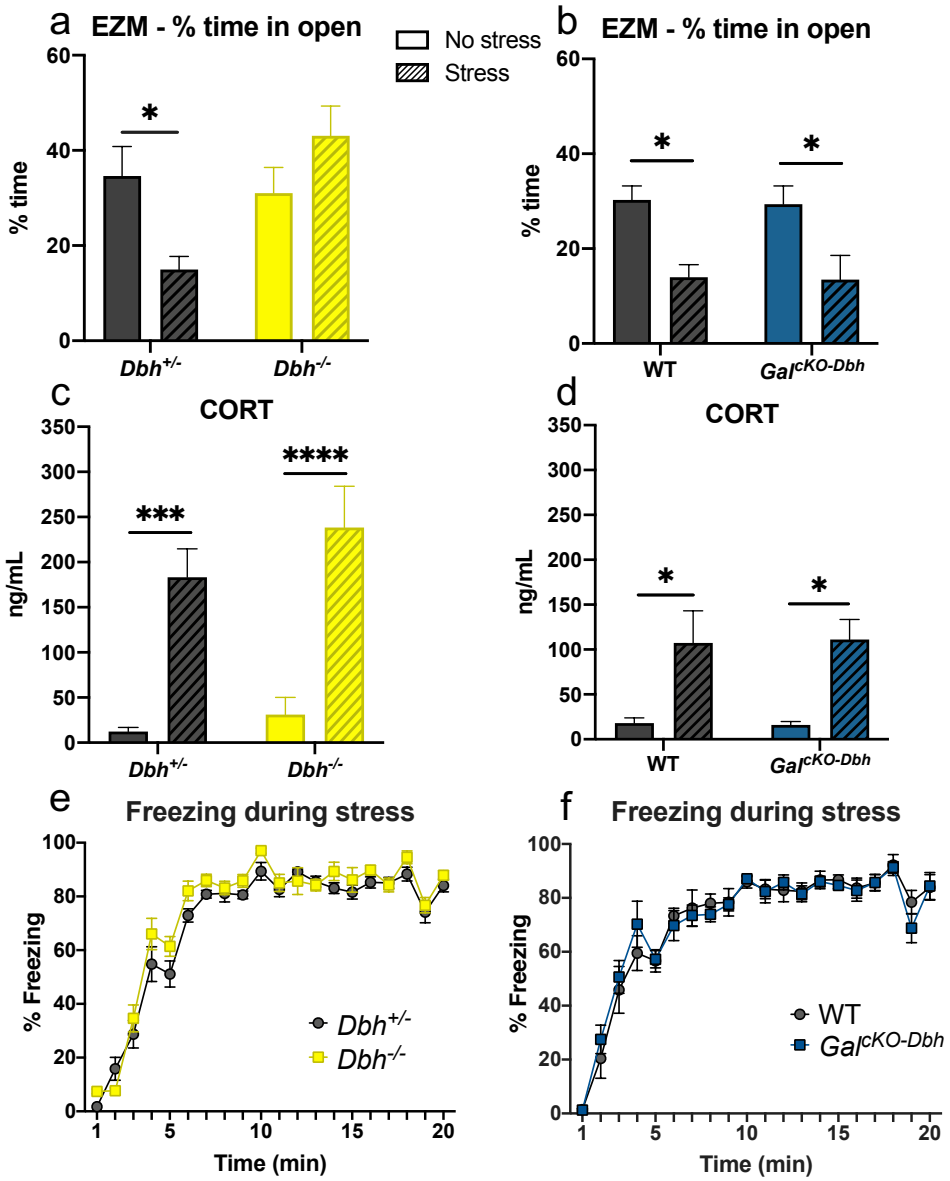

Figure 3.1. NE, but not noradrenergic-derived galanin, is required for anxiety-like behavior immediately following foot shock stress. *Dbh*$^{-/-}$, *Gal*$^{cKO\text{-}Dbh}$, and their respective control mice (*Dbh*$^{+/-}$ and WT) received 20 min of foot shock ("Stress") or no foot shock ("No Stress") and were tested in the elevated zero maze (EZM) immediately afterwards. A separate group of mice received foot shock or no foot shock, and blood was collected immediately afterwards for CORT measurements. (a) *Dbh*$^{+/-}$, but not *Dbh*$^{-/-}$ mice, showed a significant decrease in the percent time spent in the open segments of the EZM immediately after foot shock stress. (b) Both *Gal*$^{cKO\text{-}Dbh}$ and their WT littermates showed a significant decrease in the percent time spent in the open segments in the EZM immediately after foot shock stress. *Dbh*$^{-/-}$ and *Gal*$^{cKO\text{-}Dbh}$ mice showed increases in plasma CORT immediately following the foot shock stress (c-d) and similar freezing behavior during the foot shock stress (e-f) as their respective controls.

n = 5-8 mice per group for CORT analysis. *n* = 8-9 mice per group for behavior. Error bars show SEM. *p<0.05, ***p<0.001, ****p<0.0001.

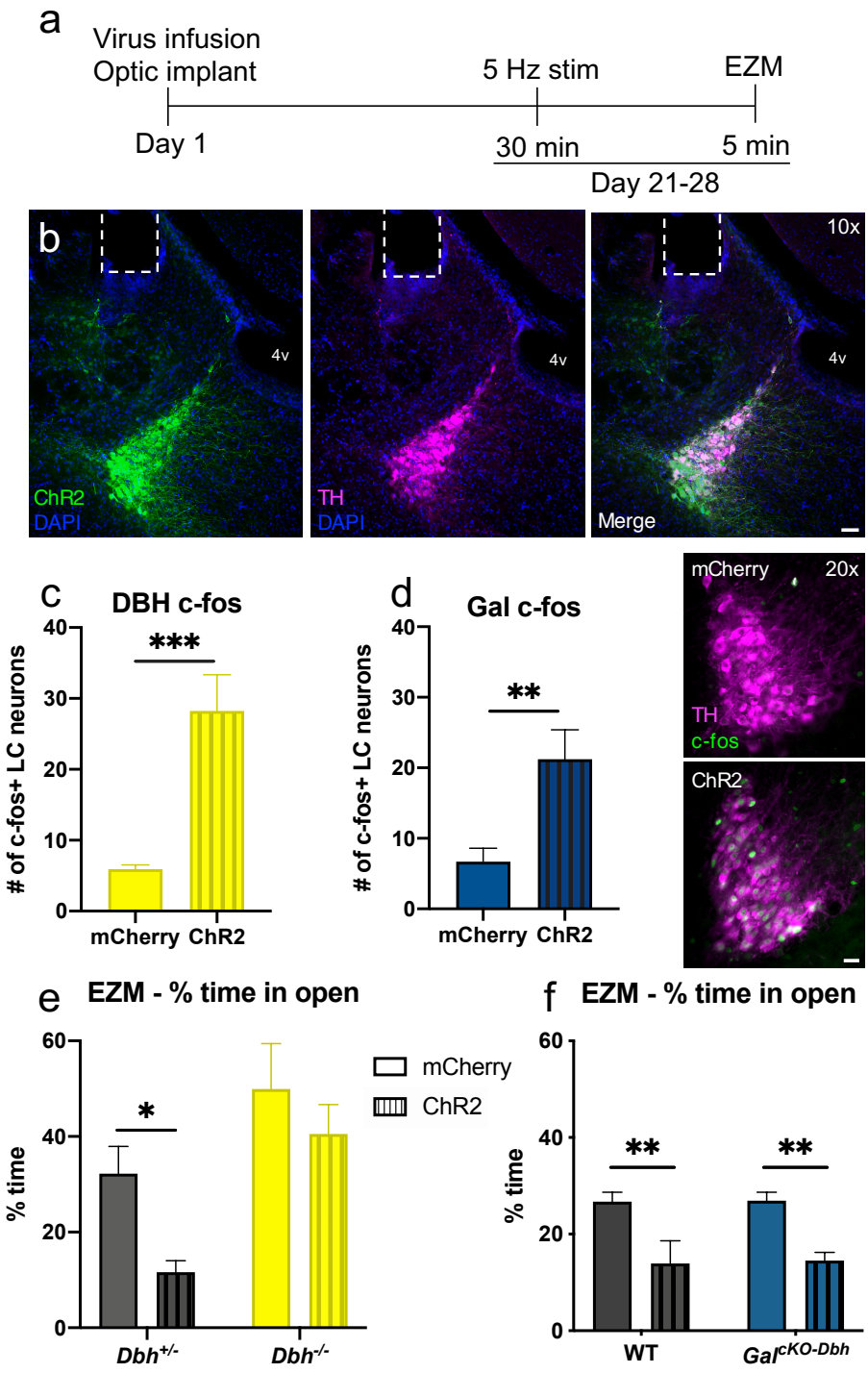

Figure 3.2. NE, but not noradrenergic-derived galanin, is required for anxiety-like behavior immediately following optogenetic LC stimulation. *Dbh*$^{-/-}$, *Gal*$^{cKO\text{-}Dbh}$, and their respective control mice (*Dbh*$^{+/-}$ and WT) expressing either ChR2-mCherry or mCherry alone in

the LC were given 30 min of optogenetic LC stimulation (5 Hz tonic) and then tested in the elevated zero maze (EZM). At least one week after the EZM, all mice were given 15 min of optogenetic LC stimulation, and brains were collected for c-fos immunohistochemistry 90 min later. (a) Optogenetic surgery and behavior timeline. (b) Representative image of ChR2 expression (green) and tyrosine hydroxylase (TH, magenta) overlap in the LC and optic fiber ferrule placement (scale bar, 50 μm; 4v, 4th ventricle). (c,d) Optogenetic stimulation of LC neurons expressing ChR2 results in greater c-fos expression compared with LC neurons expressing mCherry. Because no differences in c-fos expression between genotypes were observed, data were collapsed across genotype (TH, magenta; c-fos, green; scale bar, 20 μm). (e) *Dbh*$^{+/-}$ mice expressing ChR2 spent less percent time in the open segments of the EZM following optogenetic simulation compared to mCherry-expressing *Dbh*$^{+/-}$ mice, while optogenetic LC activation did not impact the behavior of *Dbh*$^{-/-}$ mice. (f) Both *Gal*$^{cKO\text{-}Dbh}$ and their WT littermates expressing ChR2 showed a significant decrease in percent time spent in the open segments of the EZM following optogenetic stimulation compared to those expressing mCherry. *n* = 7-9 mice per group. Error bars show SEM. *p<0.05, **p<0.01.

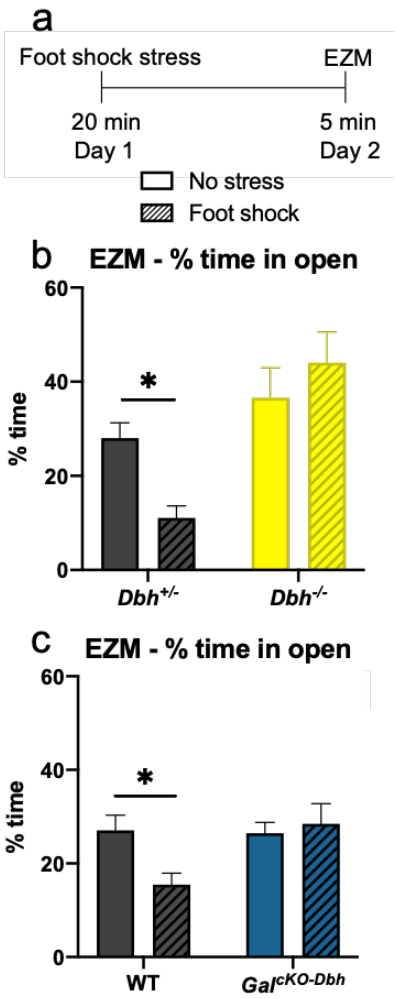

Figure 3.3. Both NE and noradrenergic-derived galanin are required for anxiety-like behavior 24 h following foot shock stress. (a) Foot shock stress paradigm timeline. (b, c) *Dbh*$^{+/-}$ and WT, but not *Dbh*$^{-/-}$ or *Gal*$^{cKO\text{-}Dbh}$ mice, showed a significant decrease in percent time spent in the open segments of the EZM 24 h after foot shock stress. *n* = 10-12 mice per group. Error bars show SEM. *p<0.05, **p<0.01.

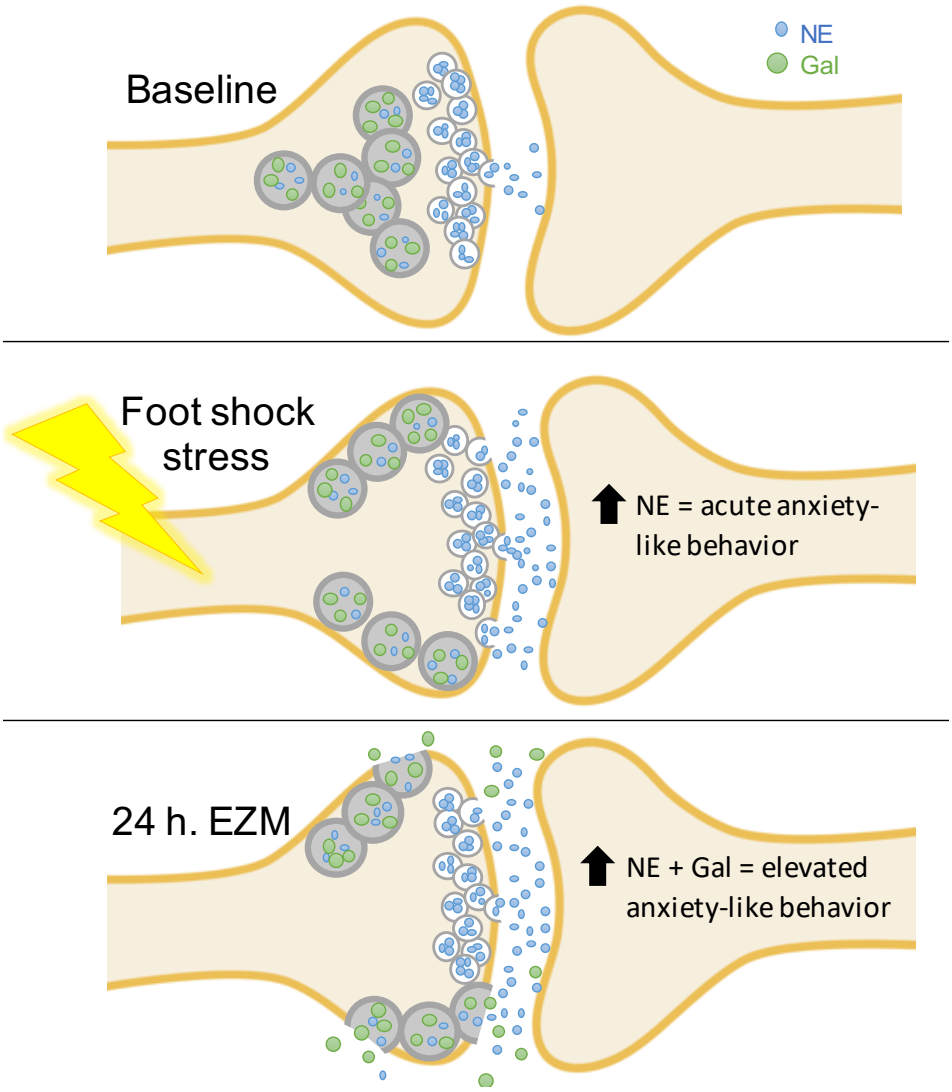

Figure 3.4. Potential neuromodulatory mechanism for how galanin may influence stress-induced behavior 24 h later. Initial high LC activity during the foot shock stress may "prime" the large dense core vesicles (LDCVs) that store galanin (Gal) along with norepinephrine (NE), which then would cause increased galanin release upon the heightened LC firing during elevated zero maze (EZM) exposure the next day and result in enhanced direct neuromodulatory effects on downstream brain regions. This increased neuromodulation by galanin may lead to the adaptive, anxiety-like behavioral effect seen in stressed WT mice that is absent in the *Gal*$^{cKO\text{-}Dbh}$ mice.

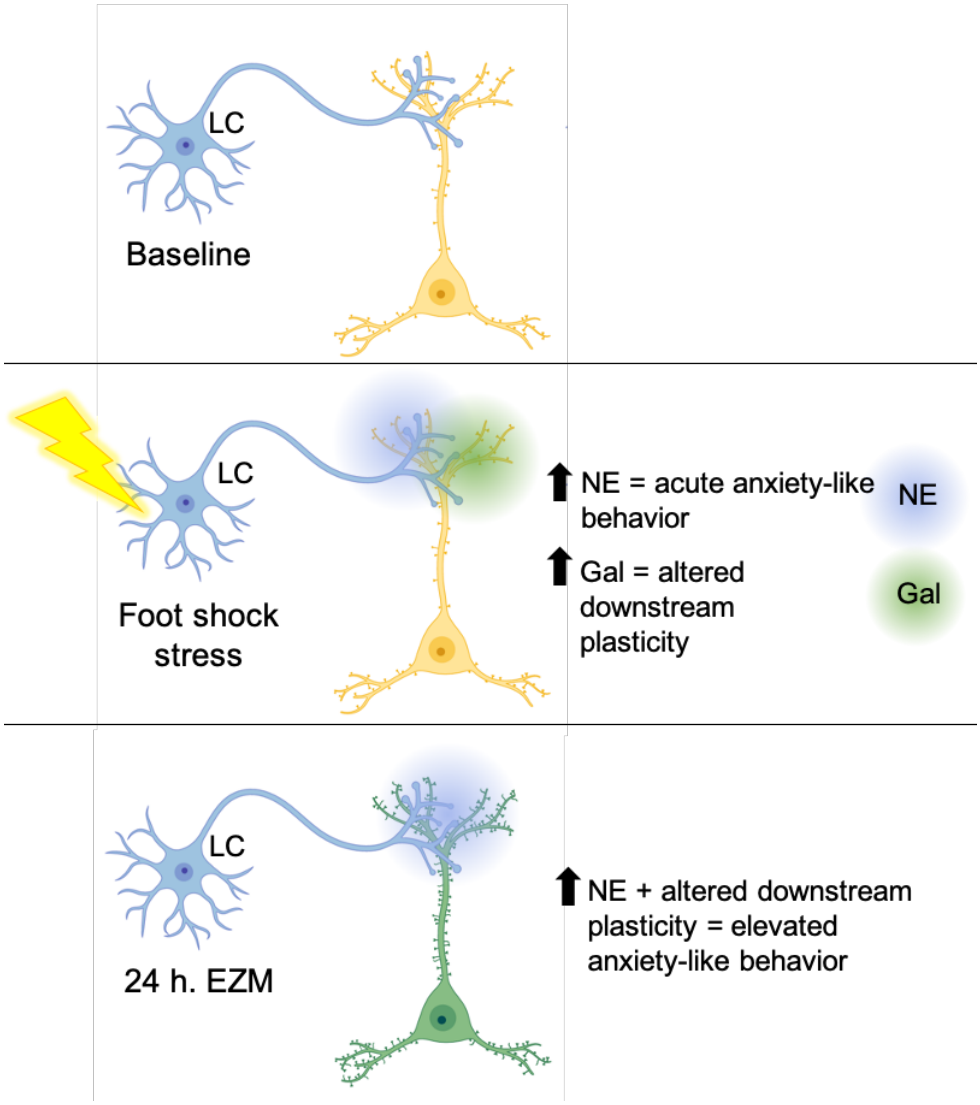

Figure 3.5. Potential neurotrophic mechanism for how galanin may influence stress-induced behavior 24 h later. Galanin (Gal) released from LC terminals during the foot shock stress may have persistent effects, such as changes in dendritic spines or receptor distribution, on downstream stress-sensitive brain regions. These alterations in plasticity could occur over the course of hours and thus affect elevated zero maze (EZM) behavior by acting in conjunction with acute norepinephrine (NE) signaling during the EZM test 24 h after stress exposure, but not affecting behavior immediately after the stressor.

CHAPTER 4:

Chronic environmental or genetic elevation of galanin in noradrenergic neurons confers stress resilience in mice

Adapted from:

R.P. Tillage, G.E. Wilson, L.C. Liles, P.V. Holmes, David Weinshenker

Chronic environmental or genetic elevation of galanin in noradrenergic neurons confers stress resilience in mice

Accepted for publication in Journal of Neuroscience, September 2020

4.1 Abstract

The neuropeptide galanin has been implicated in stress-related neuropsychiatric disorders in humans and rodent models. While pharmacological treatments for these disorders are ineffective for many individuals, physical activity is beneficial for stress-related symptoms. Galanin is highly expressed in the noradrenergic system, particularly the locus coeruleus (LC), which is dysregulated in stress-related disorders and activated by exercise. Galanin expression is elevated in the LC by chronic exercise, and blockade of galanin transmission attenuates exercise-induced stress resilience. However, most research on this topic has been done in rats, so it is unclear whether the relationship between exercise and galanin is species-specific. Moreover, use of intracerebroventricular galanin receptor antagonists in prior studies precluded defining a causal role for LC-derived galanin specifically. Therefore, the goals of this study were twofold. First, we investigated whether physical activity (chronic wheel running) increases stress resilience and galanin expression in the LC of male and female mice. Next, we used transgenic mice that overexpress galanin in noradrenergic neurons (Gal OX) to determine how chronically elevated noradrenergic-derived galanin, alone, alters anxiogenic-like responses to stress. We found that three weeks of *ad libitum* access to a running wheel in their home cage increased galanin mRNA in the LC of mice, which was correlated with and conferred resilience to stress. The effects of exercise were phenocopied by galanin overexpression in noradrenergic neurons, and Gal OX mice were resistant to the anxiogenic effect of optogenetic LC activation. These findings support a role for chronically increased noradrenergic galanin in mediating resilience to stress.

4.2 Introduction

Stress-related neuropsychiatric disorders affect approximately 600 million people worldwide, yet current pharmacological treatments have limited efficacy and cause adverse side effects for many people (Nestler et al., 2002; Rush et al., 2006; James et al., 2018). Clinical studies have consistently linked physical exercise to improvements in a wide array of neuropsychiatric disorders (Herring et al., 2010; Cooney et al., 2013; Ashdown-Franks et al., 2020). Individuals who regularly exercise are less likely to experience stress-related neuropsychiatric disorders, such as depression, anxiety, and post-traumatic stress disorder (Whitworth and Ciccolo, 2016; Chekroud et al., 2018; Harvey et al., 2018), and chronic voluntary wheel running increases resilience to various stressors in rodents (Sciolino et al., 2012; Kingston et al., 2018; Mul et al., 2018; Tanner et al., 2019). A multitude of biological changes occur as a result of chronically increased physical activity which may or may not be causally linked to alterations in stress resilience and mood; however, a promising candidate for mediating these beneficial effects is the neuropeptide galanin.

Galanin is abundant in the brain (Tatemoto, 1983; Kofler et al., 2004; Fang et al., 2015), and modulates stress, mood, cognition, food intake, nociception, and seizures (Mitsukawa et al., 2008; Lang et al., 2015). Human studies have implicated genetic variants in the genes encoding the galanin gene and its receptors (GalR1, 2, and 3) in conferring an increased risk of depression and anxiety, especially in the context of environmental stress exposure, and postmortem studies have similarly revealed galaninergic dysregulation in people with major depressive disorder (Barde et al., 2016).

While the pattern of galanin expression in the brain can vary from species to species, it is particularly rich in the noradrenergic locus coeruleus (LC) of both humans and rodents

(Skofitsch, 1985; Melander, 1986; Holets et al., 1988; Chan-Palay et al., 1990; Perez et al., 2001; Le Maitre et al., 2013). The LC is activated by stress, and norepinephrine (NE) release plays an important role in the stress response, coordinating a host of downstream effects via broad axonal projections required for the "fight-or-flight" response (Valentino and Van Bockstaele, 2008). Consistent with this role, the LC-NE system is dysregulated in stress-related neuropsychiatric disorders, such as anxiety, depression, and post-traumatic stress disorder (Roy et al., 1988; Ordway et al., 1994; Wong et al., 2000; Bissette et al., 2003; Ehnvall et al., 2003; Roy et al., 2017; Naegeli et al., 2018). In rats, galanin expression increases in the LC following chronic wheel running or treadmill exercise and correlates with running distance (O'Neal et al., 2001; Van Hoomissen et al., 2004; Holmes et al., 2006; Sciolino et al., 2012; Epps et al., 2013; Sciolino et al., 2015), and in Sciolino et al. (2015), we found that wheel running confers resilience to a stressor. Galanin has both acute neuromodulatory and chronic neurotrophic properties, and the beneficial effects of exercise in rats were blocked by chronic, but not acute, intracerebroventricular (ICV) infusion of a galanin antagonist and recapitulated by chronic ICV infusion of galanin alone, suggesting a neurotrophic mechanism of action (Sciolino et al., 2015). However, it is not known whether these phenomena can be extrapolated to other species or attributed to LC-derived galanin.

To investigate the contribution of chronically elevated noradrenergic galanin to stress resilience in mice, we investigated behavioral responses to foot shock in both an environmental (voluntary wheel running) and genetic (dopamine β-hydroxylase-galanin transgene; "Gal OX") model of LC galanin overexpression. To isolate anxiety-like responses mediated specifically by the LC, we also examined the behavior of Gal OX mice following optogenetic LC activation.

Our findings support a causal role for chronically elevated noradrenergic-derived galanin in promoting stress resilience.

4.3 Methods

Animals

All procedures related to the use of animals were approved by the Institutional Animal Care and Use Committee of Emory University and were in accordance with the National Institutes of Health guidelines for the care and use of laboratory animals. All mice were group housed and maintained on a 12/12-h light-dark cycle with access to food and water *ad libitum,* unless noted otherwise. All manipulations and behavioral tests occurred during the light cycle. Adult male and female mice (3-9 months), with equal numbers of both sexes, were used for all experiments. The Gal OX mice were generated with a transgene containing the mouse galanin gene driven by the human *dopamine β-hydroxylase* (*Dbh*) promoter, resulting in an approximately 5-fold increase in galanin mRNA in noradrenergic and adrenergic neurons and a 2-fold increase in galanin protein in LC-innervated forebrain regions compared to wild-type (WT) littermates (Jackson Labs stock #004996) (Steiner et al., 2001). All mice used in this study were on a C57BL/6J background.

Exercise

Both exercise and sedentary mice were singly housed for one week prior to the start of running wheel experiments. On the first day of the experiment, low-profile wireless running wheels (Med Associates, St. Albans, VT) were placed in the cage of the exercise mice. Sedentary animals had

no additions to their home cages, consistent with our previous studies in rats (Sciolino et al., 2012; Sciolino et al., 2015). All mice were monitored daily for 3 weeks.

Behavioral assays and corticosterone (CORT) measurement

For the behavioral battery following exercise, assays were conducted 24-48 h post-foot shock stress, with at least 2-3 h between tests, in order of least stressful to most stressful to minimize effects from the previous tests (**Fig. 4.2a**). Baseline behavioral assays (open field (OF), elevated plus maze (EPM), forced swim test (FST), fear conditioning, nestlet shredding, elevated zero maze (EZM), marble burying, novelty-suppressed feeding (NSF), locomotor activity, and shock-probe defensive burying (SPDB)) were conducted as previously described (Tillage et al., 2020) with at least 4-5 d between tests (**Fig. 4.4a**). The foot shock stress paradigm and CORT measurements were conducted as described in Chapter 3.

Galanin in situ hybridization and densitometry

To measure galanin mRNA in the LC following exercise, mice were deeply anesthetized with isoflurane and rapidly decapitated for brain extraction. Brains were collected, flash frozen in Tissue Freezing Medium, and stored at -80°C until processing. Brains were sectioned at 12-µm and collected on gelatin-coated slides (SouthernBiotech, Birmingham, AL). Slides were stored at -80°C. Galanin *in situ* hybridization was conducted and images were acquired as previously described (Sciolino et al., 2015). For quantification, images were converted to 16-bit in NIH ImageJ (https://imagej.nih.gov/ij/) and the mean grayscale value was measured in 3-4 LC sections per animal using a standardized region of interest to obtain an average measurement per

animal. The mean grayscale value of the background was subtracted out for each measurement. The experimenter was blind to treatment during image analysis.

Stereotaxic surgery, optogenetic stimulation, and histology

All stereotaxic surgeries, optogenetic stimulation, and histology for viral expression and optic fiber placement verification were conducted as described in Chapter 3.

Statistical analysis

Data were found to be normally distributed using the D'Agostino-Pearson test and analyzed by two-way ANOVA for main effects and interaction effects, with Sidak's correction for multiple comparisons to examine planned comparisons between stress or virus treatment, where appropriate. Significance was set at $p<0.05$ and two-tailed variants of tests were used throughout. Data are presented as mean ± SEM. Calculations were performed and figures created using Prism Version 8 (GraphPad Software, San Diego, CA).

4.4 Results

Wheel running characteristics

Singly housed WT C57BL6/J mice were given unrestricted access to a running wheel in their home cage for 21 d. Mice steadily increased their running distance over the first week, after which they ran approximately 10-16 km per day, which is comparable to distances seen for C57BL/6J mice in previous studies using similar running wheels (De Bono et al., 2006; Goh and Ladiges, 2015) (**Fig. 4.1a**). Female mice ran significantly more than males ($F_{1,12}=9.101$, $p=0.0107$) (**Fig. 4.1b**).

Exercise increases resilience to foot shock stress-induced anxiety-like behavior

At the end of the 3 weeks, half of the mice were subjected to a foot shock stressor. The following day, mice were put through a battery of behavioral tasks consisting of elevated zero maze (EZM), marble burying (MB), and shock-probe defensive burying (SPDB). Mice were then food-deprived overnight and tested in a novelty-suppressed feeding (NSF) assay the next day before euthanasia and tissue collection (**Fig. 4.2a**). These behavioral assays were chosen to cover a range of both active (e.g. digging in MB and SPDB) and passive (e.g. freezing in SPDB, decreased exploration in EZM, longer latency to feed in NSF) anxiety-like behaviors displayed by mice, as well as to align with the behavioral assays previously used in our studies on the anxiolytic effects of exercise in rats (Sciolino et al., 2012; Sciolino et al., 2015). For the EZM, a two-way ANOVA showed a significant exercise x stress interaction ($F_{1,25}$=5.718, p=0.0246), and post hoc tests revealed that sedentary mice had a significant decrease in the time spent in the open arms of the EZM after stress (p=0.0294), while stress had no effect on the exercise animals (p=0.6810) (**Fig. 4.2b**). No differences were seen in the MB test as a result of exercise ($F_{1,25}$=2.265, p=0.1448) or stress ($F_{1,25}$=0.06874, p=0.7953) (**Fig. 4.2c**).

In the SPDB assay, a two-way ANOVA showed a main effect of exercise ($F_{1,19}$=9.133, p=0.007) and stress ($F_{1,19}$=4.759, p=0.0419) on freezing behavior, with no significant interaction effect ($F_{1,19}$=3.107, p=0.0940). Planned comparisons indicated that stressed sedentary animals spending significantly more time freezing compared to non-stressed sedentary animals (p=0.021). The effects of stress were abrogated by exercise (p=0.9489) (**Fig. 4.2d**). There was a main effect of exercise on rearing behavior, showing that regardless of stress exposure ($F_{1,19}$=0.09776, p=0.7579), exercise mice displayed more rearing bouts in the SPDB task

($F_{1,19}$=16.24, p=0.0007) (**Fig. 4.2e**). Exercise mice also had a slight, but significant increase in the number of shock probe touches from the electrified probe compared to sedentary mice ($F_{1,19}$=6.004, p=0.0241), regardless of stress exposure ($F_{1,19}$=0.01144, p=0.9160) (**Fig. 4.2f**). There was no effect of exercise or stress on the amount of time mice spent grooming (exercise: $F_{1,19}$=3.917, p=0.0625; stress: $F_{1,19}$=0.9914, p=0.3319) or digging (exercise: $F_{1,19}$=0.08843, p=0.7694; stress: $F_{1,19}$=0.02293, p=0.8812) in the SPDB test (**Fig. 4.2g-h**).

In the NSF task, there was a main effect of exercise on the latency to eat the food in the novel environment ($F_{1,25}$=78.94, p<0.0001) but no main effect of stress ($F_{1,25}$=3.092, p=0.0909). Post hoc testing revealed that stressed sedentary animals had a significantly longer latency to eat compared to non-stressed sedentary animals (p=0.0243), with no effect of stress on the exercise animals (p=0.9825) (**Fig. 4.2i**). As a control, the amount of food consumed by each mouse in 1 h immediately after the NSF test was recorded. There were no significant differences due to exercise ($F_{1,25}$=2.371, p=0.1361) or stress ($F_{1,25}$=0.003919, p=0.9506) (**Fig. 4.2j**). There were no differences between males and females in any behavioral measures. Together, these results demonstrate that chronic wheel running affords protection from the anxiogenic-like effects of foot shock stress.

Exercise increases gal mRNA in the LC

Several previous studies have shown that chronic voluntary exercise increases prepro-galanin mRNA in the LC of rats (Van Hoomissen et al., 2004; Holmes et al., 2006; Sciolino et al., 2012; Sciolino et al., 2015), but this change has never been examined in mice. We measured prepro-galanin mRNA in the LC of exercise and sedentary mice using *in situ* hybridization and found a robust and significant increase in galanin mRNA in exercise mice compared to their sedentary

counterparts ($F_{1,23}$=58.24, p<0.0001), with no difference according to stress exposure ($F_{1,23}$=0.08014, p=0.7796) (**Fig. 4.3a-b**). Furthermore, we found a positive correlation between the average distance each mouse ran per day in the third week and the level of galanin mRNA in the LC (r^2=0.4196, p=0.0312) (**Fig. 4.3c**), but not in week 1 (r^2=0.08222, p=0.3926) or week 2 (r^2=0.2234, p=0.142) (**Fig. 4.3d-e**). There were no significant differences between male and females in galanin mRNA level in the LC at baseline (sedentary) or after exercise. These results indicate that elevation of galanin expression in the LC occurs as a result of chronic physical activity in mice, similar to what is observed in rats.

Galanin mRNA levels in the LC correlate with exercise-induced stress resilience

To further determine the relationship between galanin abundance in the LC and stress resilience, we examined whether the magnitude of galanin mRNA expression correlated with the exercise-induced stress resilience behavioral changes seen in the EZM, NSF, and SPDB assays. Strikingly, there was a non-significant trend towards a negative correlation between LC galanin expression and amount of time spent in the open arms of the EZM for non-stressed mice (r^2=0.1036, p=0.2553), but a strong, significant positive correlation for stressed mice between these two measures (r^2=0.7058, p=0.0152) (**Fig. 4.4a-b**). There were significant negative correlations between galanin mRNA levels in the LC and latency to eat in the NSF assay for both non-stressed (r^2=0.4873, p=0.0055) and stressed animals (r^2=0.6279, p=0.0036) (**Fig. 4.4c-d**). Finally, there was not a significant correlation between LC galanin mRNA levels and freezing during the SPDB assay for non-stressed mice (r^2=0.2638, p=0.0876), but there was a significant negative correlation between these measures for stressed mice (r^2=0.4981, p=0.0217) (**Fig. 4.4e-f**). For all three behaviors, the correlations with LC galanin mRNA levels were stronger (and in

the case of EZM, opposite) in the stressed mice compared to non-stressed mice. Together, these data support the idea that LC-derived galanin is less important for anxiety-like behavior at baseline but becomes preferentially engaged by stress to confer resilience.

Gal OX mice show normal baseline line behavior

Gal OX mice are reported to have normal performance in several canonical tests for anxiety-like behavior, including the elevated plus maze and open field test, but are resistant to yohimbine-induced anxiety-like behavior in a light-dark exploration task (Holmes et al., 2002). To confirm and expand on previous baseline behavioral studies conducted with the Gal OX mice, we conducted an extensive battery of anxiety-, depression-, learning-, and motor-related behavioral tasks (**Fig. 4.5a**). We observed no differences between Gal OX and littermate WT control mice in canonical tests of anxiety-like behavior (elevated plus maze, t_{17}=0.1641, p=0.8717; zero maze, t_{17}=0.6739, p=0.5095; open field, t_{17}=0.3211, p=0.7521) or depressive-like behavior (tail suspension test, t_{17}=1.578, p=0.1331; forced swim test, t_{17}=0.4564, p=0.6539) (**Fig. 4.5b-f**). They showed no difference from WT littermates in compulsive behaviors during the nestlet shredding task (t_7=0.07861, p=0.9395) or marble burying task (t_{17}=0.8051, p=0.4319) (**Fig. 4.5g-h**). Additionally, Gal OX behavior was comparable to WT in the novelty-suppressed feeding task (t_{17}=1.355, p=0.1933) (**Fig. 4.5i**). Gal OX mice exhibited normal cognitive responses in contextual ($F_{1,17}$=0.2773, p=0.6053) and cued fear conditioning ($F_{1,17}$=0.5667, p=0.4619) (**Fig. 4.5j-l**). The locomotor activity of Gal OX mice was normal ($F_{1,17}$=0.6486, p=0.4317). (**Fig. 4.5m**). In the shock probe defensive burying task, Gal OX mice were normal in most behaviors, including digging (t_{12}=0.7124, p=0.4899), freezing (t_{12}=0.7015, p=0.4964), rearing, (t_{12}=0.4402, p=0.6676), and number of probe touches (t_{12}=0.6455, p=0.5308) (**Fig. 4.6a-d**). The only

exception was that Gal OX mice spent significantly less time grooming during the task than their WT counterparts (t_{12}=3.152, p=0.0084) (**Fig. 4.6e**). There were no differences between males and females in any behavioral measures.

Gal OX mice are resistant to the behavioral effects of foot shock stress

Although chronic wheel running increased galanin expression in the LC, exercise has pleiotropic effects on brain neurochemistry. To determine whether we could recapitulate the exercise-induced stress resilience effect with chronically elevated noradrenergic galanin expression alone, we tested the response of Gal OX mice to the same foot shock stressor used in the exercise paradigm (**Fig. 4.7a**). We simplified the paradigm to include only the EZM because it revealed the most profound relationship between LC galanin expression and stress resilience in the exercise experiment (**Fig. 4.2, Fig. 4.4**), and activation of the LC vigorously and consistently increases anxiety-like behavior in this assay (McCall et al., 2015).

When tested in the EZM 24 h after foot shock, there was a main effect of genotype on the amount of time spent in the open arms ($F_{1,33}$=11.81, p=0.0016), but a non-significant interaction between genotype x stress ($F_{1,33}$=3.941, p=0.0555). Planned comparisons showed that WT mice spent significantly less time in the open arms of the EZM 24 h after stressor exposure compared to non-stressed WT mice (p=0.0191). However, Gal OX mice did not show this behavioral change after stress (p=0.9938) (**Fig. 4.7b**).

We conducted two control experiments to verify that galanin overexpression did not change the physiological responses to foot shock. First, we measured the amount of freezing during the administration of foot shocks and found no differences between WT and Gal OX mice ($F_{1,10}$=0.01299, p=0.9115) (**Fig. 4.7c**). Next, we measured foot shock-induced increases in

plasma corticosterone (CORT) levels and found a significant effect of stress ($F_{1,23}$=17.12, p=0.0004), but no effect of genotype ($F_{1,23}$=0.004147, p=0.9492), indicating that Gal OX mice have a normal CORT response to the foot shock stress itself and the neuroendocrine stress axis is functional in these mice (**Fig. 4.7d**). There were no differences between males and females. These results demonstrate that while Gal OX mice are initially affected by foot shock in the same way as their WT littermates, they are resistant to stress-induced behavioral changes 24 h later.

Gal OX mice are resistant to the anxiogenic effects of acute optogenetic LC activation

Foot shock stress engages many brain regions in addition to the LC. To more selectively target activation of the noradrenergic system, we used optogenetics to stimulate the LC immediately before EZM testing (**Fig. 4.8a**). The stimulation and behavioral protocols used here were based on a previously published paradigm of optogenetic LC activation-induced anxiety-like behavior (McCall et al., 2015). Mice received intra-LC infusion of virus expressing either ChR2-mCherry or mCherry alone. Viral expression and optic ferrule placement were confirmed in all animals by histology (**Fig. 4.8b**), and successful activation of the LC was confirmed via an increase in c-Fos expression (t_8=2.798, p=0.0233) (**Fig. 4.8c**). No differences in c-Fos expression after optogenetic stimulation were observed between genotypes. There were significant effects of both genotype ($F_{1,32}$=13.18, p=0.001) and virus ($F_{1,32}$=8.569, p=0.0062) on the amount of time mice spent in the open arms of the zero maze, with post hoc testing showing that WT ChR2 mice spent significantly less time in the open arms compared to WT mCherry mice (p=0.0234), while there was no difference between Gal OX mice that received the ChR2 and the mCherry virus (p=0.2809) (**Fig. 4.8d**). There were no differences between males and females. These results demonstrate that the Gal OX mice are resistant to LC stimulation-induced anxiety-like behavior.

4.5 Discussion

Although many studies have suggested a role for LC-derived galanin in stress resilience, most examined a single species (rat) and lacked direct evidence for the noradrenergic system as the functional source of the neuropeptide. To our knowledge, the present results are the first to demonstrate that (1) chronic exercise simultaneously increases both stress resilience and galanin expression in the LC of mice, and (2) increasing galanin in noradrenergic neurons ameliorates anxiogenic-like responses to stress and optogenetic LC stimulation.

We found that the level of galanin expression correlated with running distance in the third week, indicating that the relationship between physical activity and galanin abundance increases in a "dose-dependent" manner, as has been shown in rats (Holmes et al., 2006; Sciolino et al., 2012). Furthermore, we discovered that galanin mRNA expression in the LC correlated with the exercise-induced resilience in a stress-dependent manner. Stressed animals showed stronger (and in the case of EZM, opposite) correlations across all behavioral measures with galanin expression levels in the LC compared to non-stressed mice. In general, exercise had little effect on baseline behavior, but ameliorated the anxiogenic effects of foot shock stress, similar to what we have reported in rats (Sciolino et al., 2015). However, we did observe that wheel running increased exploratory drive in behavioral paradigms that were not modulated by stress, such as rearing and probe touches in the SPDB. The results from our chronic voluntary wheel running experiment are consistent with other previous studies that showed enhanced stress resilience after chronic increases in physical activity in rodents (Sciolino et al., 2012; Kingston et al., 2018; Mul et al., 2018; Tanner et al., 2019). Female mice in our study consistently ran farther than male mice, as has been reported previously (De Bono et al., 2006; Bartling et al., 2017), but no other sex differences were seen. Our results support the idea that LC-derived galanin is less important

for anxiety-like behavior at baseline but becomes preferentially engaged by stress to confer resilience.

Wheel running has wide-ranging effects on a variety of molecular and structural changes in the brain that may ameliorate the negative affective states induced by stress, including hippocampal neurogenesis and brain-derived neurotrophic factor (Li et al., 2008; Liu and Nusslock, 2018), so it is possible that the alterations in the galanin system as a result of exercise work in concert with other systems in the brain to lead to an increase in stress resilience. To determine whether increasing galanin in noradrenergic neurons, alone, could recapitulate the anxiolytic effects of exercise, we turned to Gal OX mice. Similar to chronic exercise, Gal OX mice showed minimal behavioral differences from their WT littermates at baseline, consistent with much of the previous research suggesting that galaninergic effects are primarily evoked under conditions of stress that elicit high levels of neuronal activity. Galanin, like other neuropeptides, is stored in large dense core vesicles that require high frequency neuronal firing, such as those evoked in LC neurons by stress, to induce release (Lang et al., 2015). Gal OX mice did display decreased grooming in the SPDB assay. Because stress can elicit increased grooming behaviors in mice (Kalueff and Tuohimaa, 2004), decreased grooming could be indicative of increased resilience in the face of a stressful environment like the shock-probe task. Gal OX mice had a typical CORT response to foot shock, indicating that their neuroendocrine stress response was functioning normally, and customary freezing behavior during the stress itself. However, the decrease in open arm time in the EZM evident 24 h after foot shock observed in WT animals were completely abolished in Gal OX mice, suggesting that noradrenergic galanin promotes stress resilience.

While foot shock is a powerful activator of LC neurons, this stressor engages many other nodes of the stress response circuitry (Kim et al., 2016; Lecca et al., 2016). To isolate LC-induced anxiogenesis, we used LC-specific optogenetic stimulation immediately before testing in the EZM. The optogenetic parameters we employed were based on previously reported electrophysiological recordings of LC activity in response to stress and optogenetic activation shown to induce anxiety-like behavior in the EZM. Importantly, that effect of optogenetic stimulation was blocked with β-adrenergic receptor antagonism, demonstrating that increased noradrenergic transmission was responsible for the anxiety-like behavior (McCall et al., 2015). Similar to the foot shock response, Gal OX mice did not display the anxiety-like behavior shown by their WT littermates following optogenetic LC activation. The fact that the Gal OX mice are resistant to this behavioral change suggests that increased noradrenergic galanin can dampen the stress-related behavioral effects of increased LC activity.

We consider two main mechanisms by which chronically elevated galanin in the LC leads to increased stress resilience: (1) acute neuromodulatory actions of excess galanin being released during the stressor and acting somatodendritically to inhibit the LC itself or downstream regions involved in mediating stress-induced behaviors, or (2) long-term neurotrophic changes in downstream brain regions mediated by chronically high levels of galanin signaling that confer anxiolysis. All three galanin receptors (GalR1-3) are G protein-coupled receptors that signal through inhibitory $G_{i/o}$ pathways, but GalR2 can also signal through $G_{q/11}$, giving it a more complicated role in downstream signal processing (Lang et al., 2015). GalR2 is thought to regulate the long-term trophic actions of galanin, whereas GalR1 and GalR3 seem to be more important in the acute inhibitory neuromodulation by galanin (Hobson et al., 2008; Holmes, 2014; Weinshenker and Holmes, 2016). We favor the chronic neurotrophic mechanism to

explain our present and previous findings. In our previous study (Sciolino et al., 2015), we found that either chronic exercise or chronic ICV galanin protected against stress-induced anxiogenic behavior and dendritic spine loss in the medial prefrontal cortex (mPFC) of rats. Importantly, chronic but not acute infusion of a galanin antagonist blocked the beneficial effects of exercise on neuroplasticity and behavior, supporting the idea that the stress resilience is caused by chronic elevated galanin leading to long-term neurotrophic adaptation, not acute increases in galanin's neuromodulatory actions. These data suggest that a similar neurotrophic mechanism likely underlies our present results.

There are several caveats associated with the Gal OX mice used in this study. The first is that the overexpression of galanin is not entirely noradrenergic-specific; they have some ectopic expression of galanin in non-noradrenergic neurons in the piriform and entorhinal cortex (Steiner et al., 2001). Additionally, galanin is not only overexpressed in noradrenergic nuclei that normally express galanin, such as the LC, but all noradrenergic and adrenergic cell groups, leading to high levels of galanin in neurons that do not contain it endogenously. Some of these (e.g. the *Hoxb1* cluster in the medulla and pons outside of the LC (Chen et al., 2019)) have been implicated in stress and anxiety-like responses. Thus, we cannot definitively ascribe the effects we obtained using the Gal OX mice specifically to the LC-derived galanin. Despite this, due to the LC's well-defined role in regulating the stress response, the broad projections of the LC to other stress-sensitive brain regions, the phenotypic similarities between the Gal OX mice and exercise mice that have elevated galanin exclusively in the LC, and our LC-specific optogenetic results, it seems likely that chronically elevated galanin in the LC contributes to enhanced stress resilience.

Combined with the existing literature, the results from the present study demonstrate that noradrenergic galanin promotes stress resilience across species, and that its enrichment can come from either an environmental (exercise) or genetic (transgenic overexpression) source. Future studies will further dissect how galaninergic transmission from noradrenergic sources underlie its anxiolytic properties. The critical galanin receptor (GalR1-3), the mode of signaling (acute neuromodulatory vs chronic neurotrophic), and the downstream targets in the stress response network (e.g. prefrontal cortex, amygdala) remain to be identified. The galanin system remains a promising target for both pharmacotherapies and non-drug treatments for affective disorders.

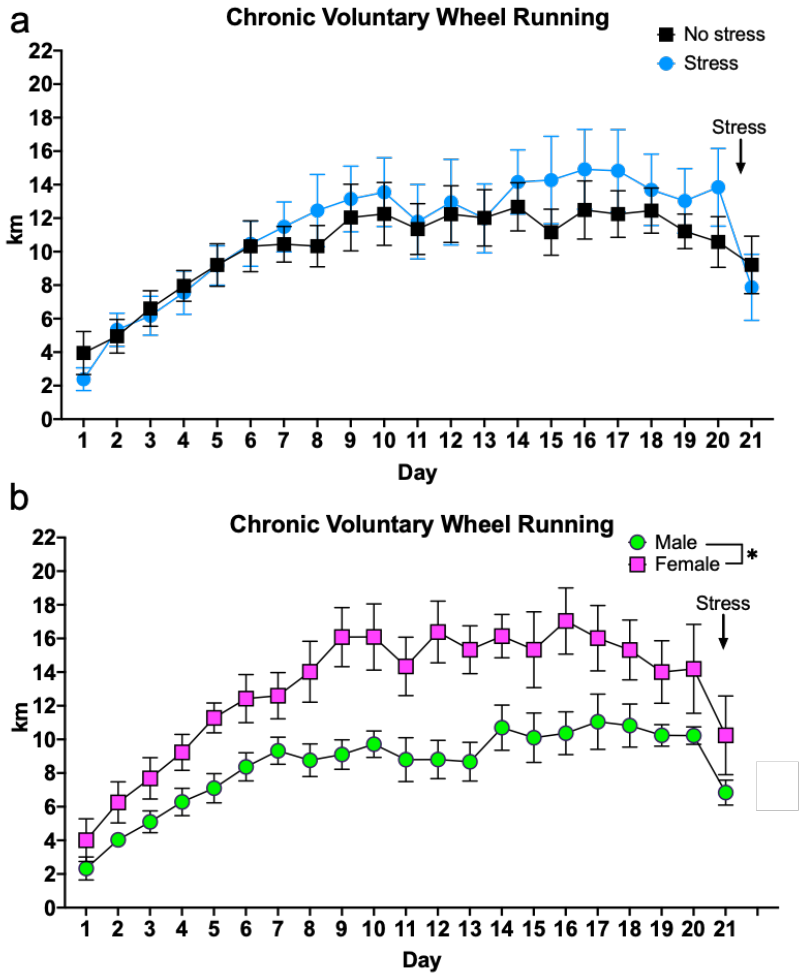

Figure 4.1. Distance traveled by mice with access to running wheels. (a) Wild-type C57Bl6/J mice were given ad libitum access to running wheels in their home cage for 3 weeks. (b) Female mice ran significantly more than males over three weeks of running wheel access. n = 7-8 mice per group. Error bars show SEM. *p<0.05.

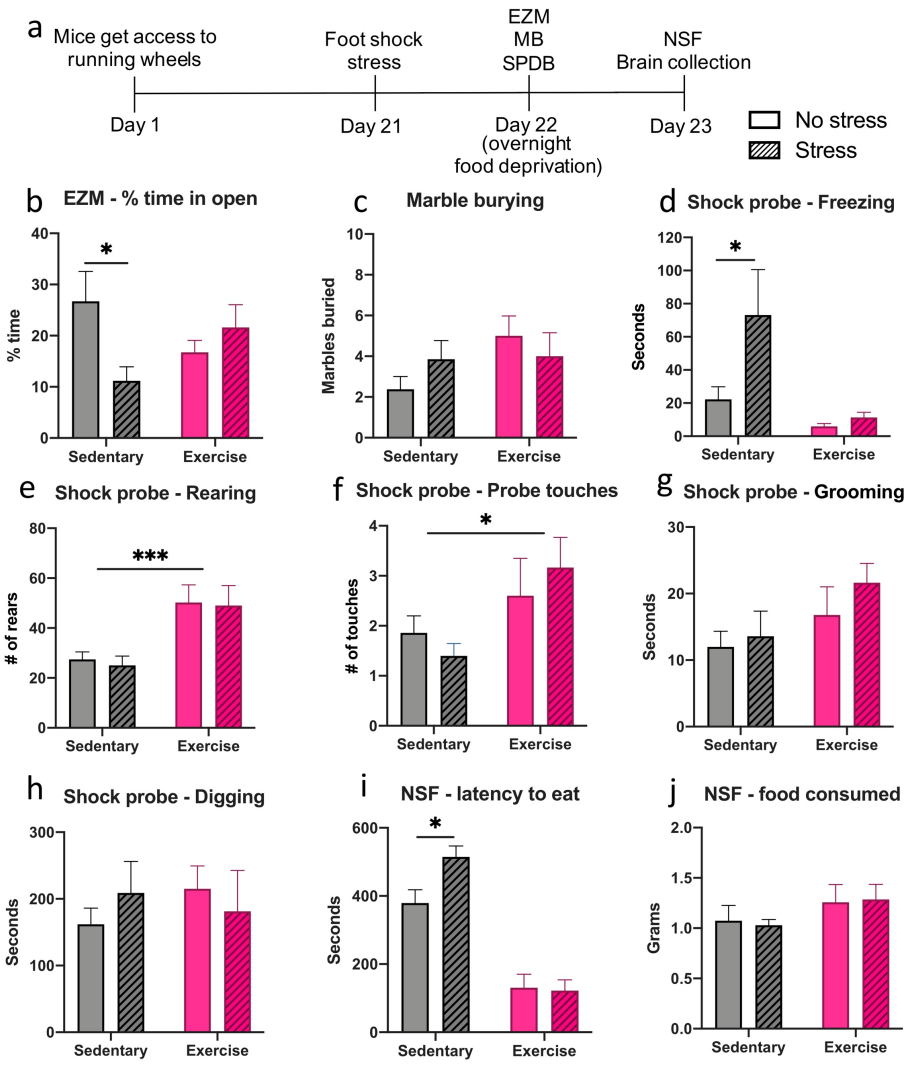

Figure 4.2. Exercise increases resilience to foot shock stress-induced anxiety-like behavior. Wild-type C57Bl6/J mice were given *ad libitum* access to running wheels in their home cage ("Exercise") or no running wheel ("Sedentary") for 3 weeks, then were tested in behavioral assays 24-48 h following foot shock ("Stress") or no foot shock ("No Stress"). (a) Exercise paradigm timeline. EZM, elevated zero maze. MB, marble burying. SPDB, shock probe defensive burying. NSF, novelty-suppressed feeding. (b) Sedentary mice show decreased time spent in the open arms of the EZM after stress, but exercise mice do not. (c) No significant differences were seen in the MB assay. (d) In the SPDB assay, sedentary stressed mice showed increased freezing compared to sedentary non-stressed mice, but there was no difference between stressed and non-stress exercise mice. (e) Exercise mice showed an overall increase in both rearing and (f) number of probe touches compared to sedentary mice, with no effect of stress. (g) There were no differences as a result of exercise or stress on grooming or (h) digging in the SPDB assay. (i) In the NSF test, sedentary mice took significantly longer to eat after stress compared to non-stressed sedentary mice, with no difference between stressed and non-stressed exercise mice. (j) Exercise mice tended to consume more food during the hour after the NSF test, but it was not significant. n = 7-8 mice per group, mixed males and females. Error bars show SEM. *p<0.05, ***p<0.001.

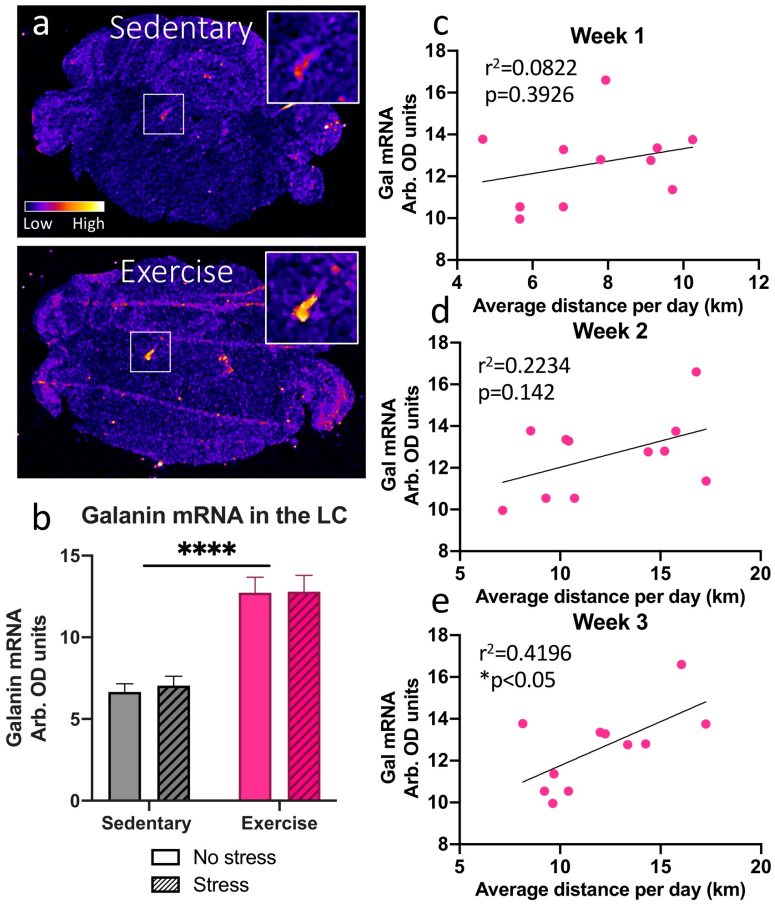

Figure 4.3. Exercise increases galanin mRNA in the LC of mice. Galanin mRNA levels in the LC were measured via *in situ* hybridization in wild-type C57Bl6/J mice following 3 weeks of *ad libitum* access to running wheels in their home cage ("Exercise") or no running wheels ("Sedentary"), foot shock ("Stress") or no foot shock ("No Stress"), and behavioral testing. (a) Representative images of galanin *in situ* hybridization. (b) Quantitative densitometry analysis revealed that exercise mice showed significantly elevated galanin mRNA in the LC compared to sedentary mice, with no effect of foot shock stress exposure. (c) Correlation analysis showed that the average distance ran per day during the third week for each mouse showed a significant positive correlation with the level of galanin mRNA expression in the LC. The average distance ran per day during the first (d) and second (e) weeks did not correlated with the level of galanin mRNA expression in the LC. n = 5-8 mice per group, mixed males and females. Error bars show SEM. ****p<0.0001.

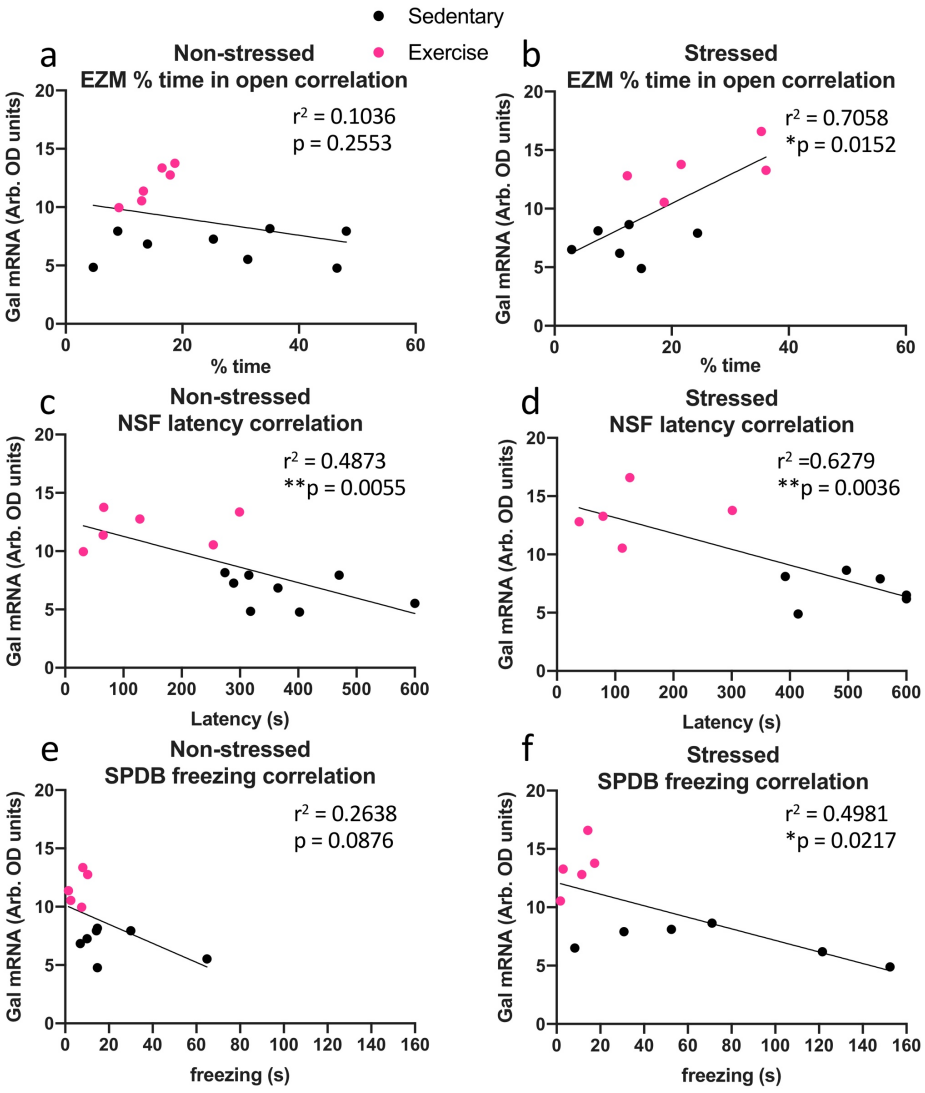

Figure 4.4. Galanin mRNA levels in the LC correlate with exercise-induced stress resilience. Correlation analysis of galanin mRNA measured by *in situ* hybridization and performance in tests of anxiety-like behavior. EZM, elevated zero maze. NSF, novelty-suppressed feeding. SPDB, shock probe defensive burying. There was no significant correlation between galanin mRNA levels in the LC and percent time spent in the open arms of the EZM for non-stressed mice, but there was a significant positive correlation for stressed mice (a-b). There were significant negative correlations between galanin mRNA levels in the LC and latency to eat in the NSF assay for both non-stressed and stressed animals (c-d). There was no significant correlation between LC galanin mRNA expression and freezing during the SPDB assay for non-stressed mice, but there was a significant negative correlation for stressed mice (e-f). *n* = 5-8 mice per group.

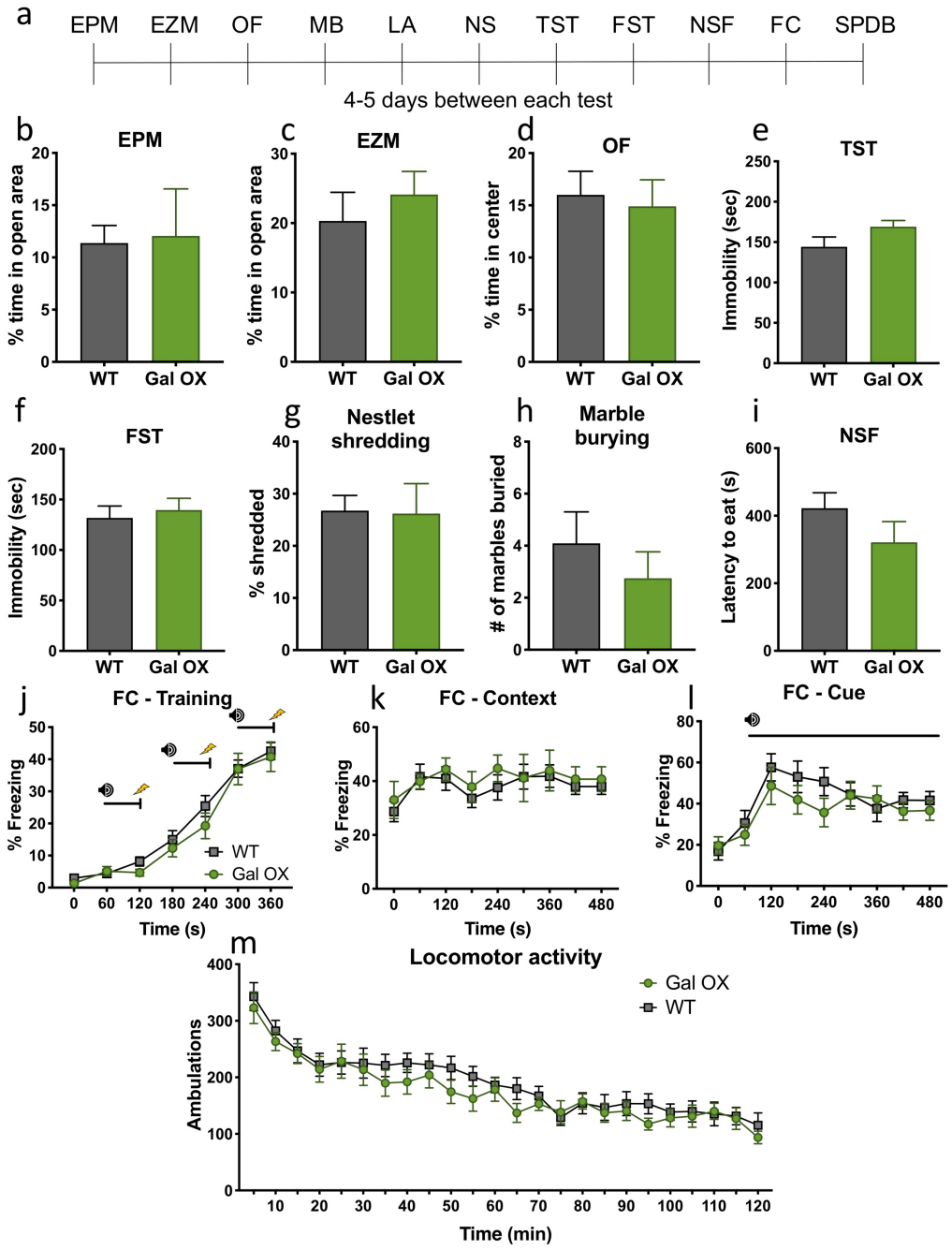

Figure 4.5. Gal OX mice display normal behavior at baseline. A battery of behavioral tests was conducted on Gal OX mice compared to their WT littermates. (a) Timeline showing order of tests. (b) EPM, elevated plus maze, (c) EZM, elevated zero maze, (d) OF, open field, (e) TST, tail suspension test, (f) FST, forced swim test, (g) NS, nestlet shredding, (h) MB, marble burying, (i) NSF, novelty-suppressed feeding, (j-l) FC, fear conditioning, (m) LA, locomotor activity. SPDB, shock probe defensive burying. Gal OX mice were normal in all measures. *n* = 8-11 mice per group, mixed males and females. Error bars show SEM.

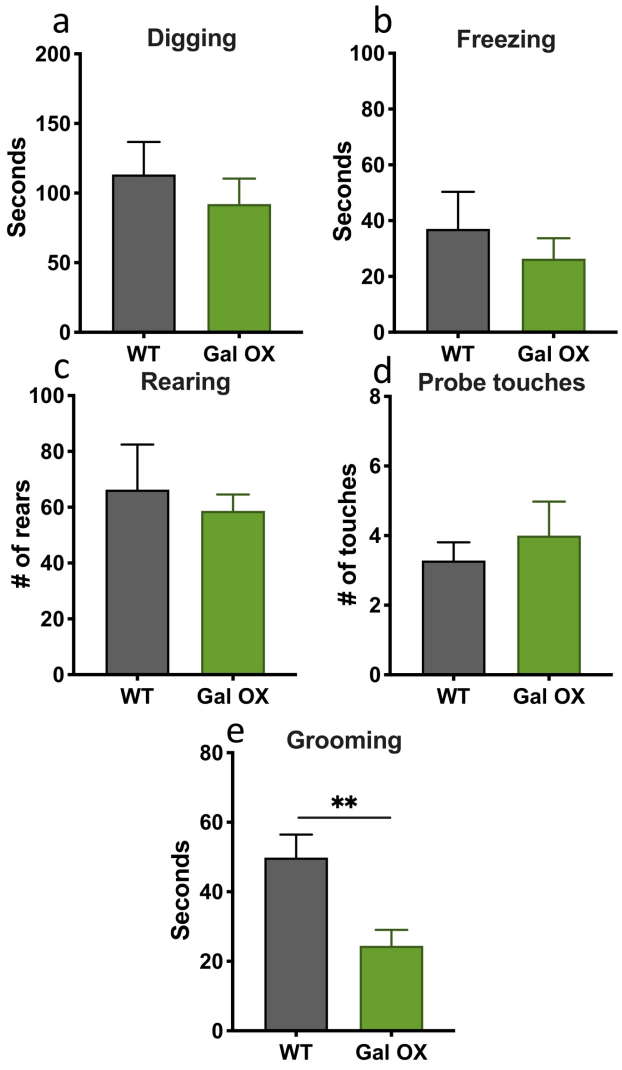

Figure 4.6. Gal OX mice display decreased grooming in the shock probe defensive burying task. Gal OX mice were normal in all measures in the shock probe defensive burying assay, including time spent digging (a), freezing (b), number of rears (c), and probe touches (d). However, they spent significantly more time grooming than WT controls (e). *n* = 7 mice per group, mixed males and females. Error bars show SEM. **p<0.01.

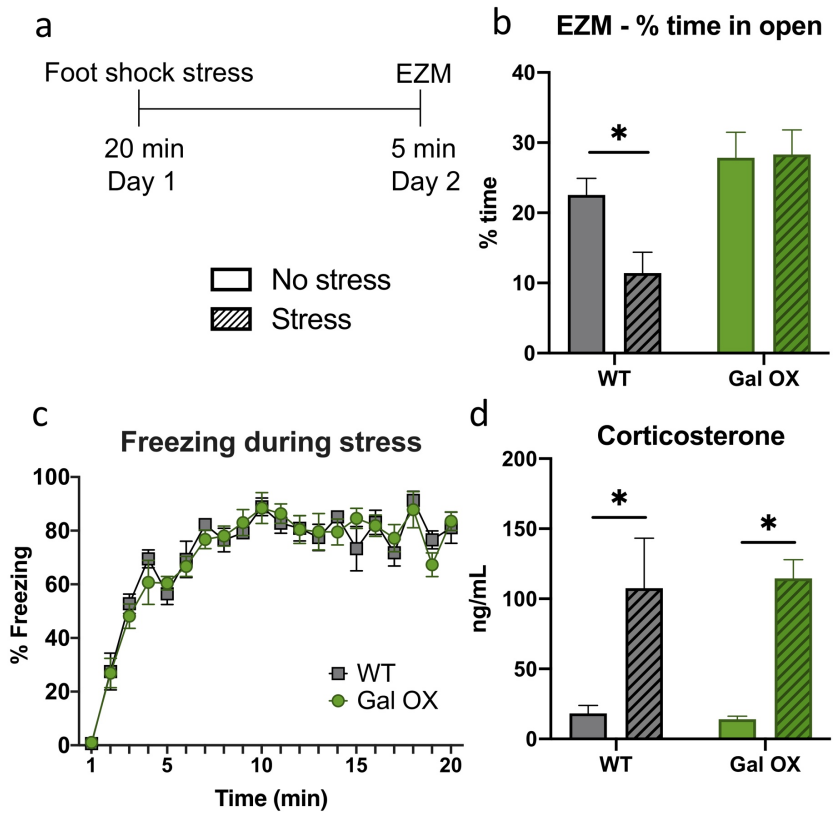

Figure 4.7. Gal OX mice are resistant to the anxiogenic effects of foot shock stress. Gal OX mice and wild-type littermate controls (WT) received 20 min of foot shock ("Stress") or no foot shock ("No Stress") and were tested in the elevated zero maze (EZM) 24 h later. A separate group of mice received foot shock or no foot shock, and blood was collected immediately afterwards for CORT measurements. (a) Foot shock stress paradigm timeline. WT, but not Gal OX mice, showed a significant decrease in time spent in the open arms of the EZM 24 h after foot shock stress (b). WT and Gal OX mice showed similar freezing behavior during the foot shock stress (c) and similar increases in plasma CORT immediately following the foot shock stress (d). *n* = 5-7 mice per group for CORT analysis. *n* = 8-10 mice per group for behavior, mixed males and females. Error bars show SEM. *p<0.05, ***p<0.001.

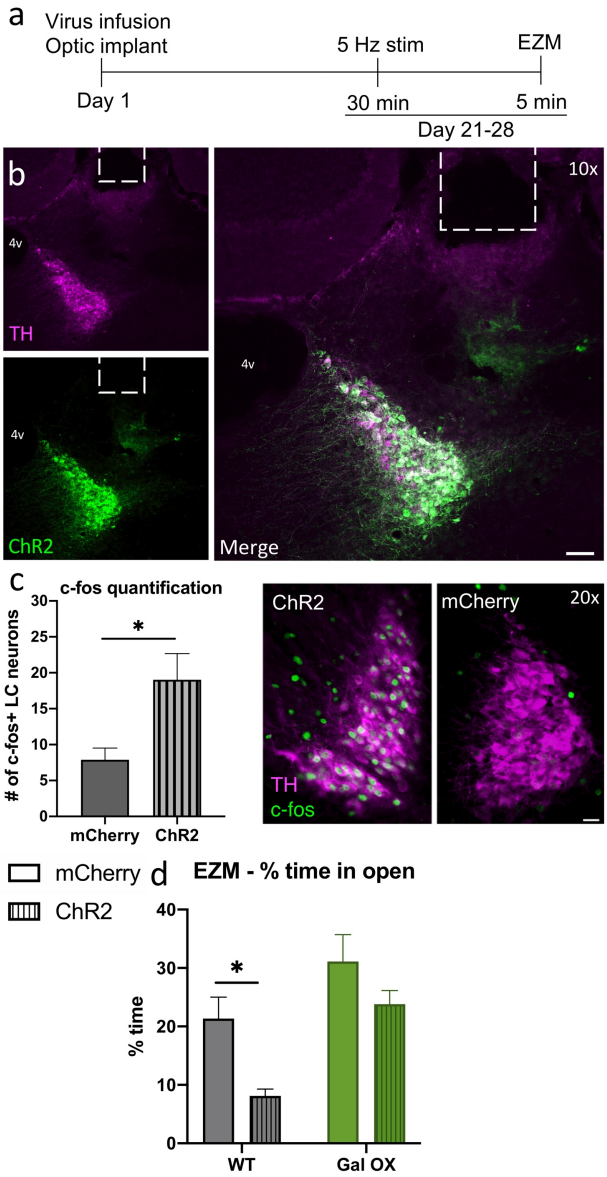

Figure 4.8. Gal OX mice are resistant to the anxiogenic effects of optogenetic LC activation. Gal OX and wild-type littermate controls (WT) were given 30 min of optogenetic LC stimulation and then tested in the elevated zero maze (EZM). At least one week later, all mice were given 15 min of optogenetic LC stimulation, and brains were collected for c-fos immunohistochemistry 90 min later. (a) Optogenetic surgery and behavior timeline. (b) Representative images of ChR2 viral expression (green) and tyrosine hydroxylase (TH, magenta) overlap in the LC and optic fiber ferrule placement (scale bar, 50 µm; 4v, 4th ventricle). (c) Optogenetic stimulation of the LC leads to increased c-fos expression in LC neurons with the ChR2 virus, but not in mice with the control mCherry virus. No differences in c-fos expression between genotypes were seen so data shown are collapsed across genotype (TH, magenta; c-fos, green; scale bar, 20 µm). Optogenetic stimulation causes WT-ChR2 mice to spend less time in the open arms of the EZM compared to WT-mCherry mice but does not impact the behavior of Gal OX mice (d). *n* = 8-10 mice per group, mixed males and females. Error bars show SEM. *p<0.05.

CHAPTER 5:

General Discussion and Future Directions

5.1 Summary

The galaninergic and noradrenergic systems are dysregulated in stress-related neuropsychiatric disorders, but the underlying neurobiological mechanisms involved are not well understood. Furthermore, we lack a complete understanding about the basic role of noradrenergic-derived galanin in regulating stress-responsive behaviors. The experiments described in this dissertation address this knowledge gap by using genetic and environmental manipulations of the galanin system to improve our understanding of how galanin from the LC modulates stress-induced behavior. In Chapter 2, we determined how a chronic lack of galanin in noradrenergic neurons affects both neurochemistry and behavior using $Gal^{cKO\text{-}Dbh}$ mice. We found that noradrenergic neurons are a significant source of galanin to the hippocampus and prefrontal cortex, and that noradrenergic-derived galanin regulates behavioral coping responses. In Chapter 3, we examined the distinct roles of noradrenergic-derived galanin compared to NE in regulating behavioral responses to stress. Using $Dbh^{-/-}$ and $Gal^{cKO\text{-}Dbh}$ mice, we found that NE and noradrenergic-derived galanin play partially overlapping, but distinguishable roles in behavioral responses to stress. NE is important for acute stress-induced anxiety-like behavior, while both NE and noradrenergic-derived galanin are required for persistent behavioral changes 24 h after a stressor. Finally, in Chapter 4, we studied how chronic elevation of galanin affects stress resilience. We found that chronic voluntary wheel running increased galanin levels in the LC of mice and conferred resilience to a stressor. The effects of exercise were phenocopied by transgenic mice with galanin overexpression in noradrenergic neurons, which showed enhanced stress resilience and resistance to the anxiogenic effect of optogenetic LC activation. Together, these three studies provide valuable information about the complex role of noradrenergic-derived galanin in regulating stress-induced behaviors.

5.2 Integration of key findings and future directions

The experiments conducted in this dissertation indicate a role for noradrenergic-derived galanin in regulating behavioral effects of stress in complex ways over time and support the conclusion that noradrenergic-derived galanin regulates stress-related coping behaviors. While the mechanisms underlying the effects discovered here are not yet clear, there are two non-mutually exclusive categories of possible mechanisms: acute, neuromodulatory effects due to immediate galanin transmission (**Fig 3.4**), and long-term neurotrophic effects involving enhanced downstream plasticity due to galanin signaling (**Fig. 3.5**). The data described in this dissertation raise many interesting questions for future experiments to address, such as when and where in the brain does galanin from the LC act to regulate stress susceptibility, and are these sites of action different for acute neuromodulatory actions compared to chronic neurotrophic actions? Behavioral pharmacology experiments will be necessary to elucidate these mechanisms, examine the brain regions involved, and investigate which galanin receptor subtypes are mediating the distinct behavioral effects. Delineating the precise roles of GalR1-3 in mediating the effects discussed here is necessary before galaninergic compounds can be considered as potential therapeutic options for patients.

In Chapter 2, we found that $Gal^{cKO\text{-}Dbh}$ mice displayed a more active coping strategy in three independent tasks measuring behavior in an anxiogenic context (marble burying, shock probe defensive burying, and novelty-suppressed feeding), suggesting that noradrenergic galanin normally promotes passive coping behaviors when a stressor is encountered. Interestingly, a recent paper by McEwan and colleagues used CRISPR genome editing to disrupt an enhancer sequence in the *GAL* gene in mice, leading to decreased galanin expression in several brain regions, and found that these mice showed an increase in marble burying and decreased latency

to feed in a novelty-suppressed feeding assay, mimicking our behavioral findings with the *Gal*$^{cKO\text{-}Dbh}$ mice (McEwan et al., 2020). It is possible that the loss of neuromodulatory and neurotrophic effects of noradrenergic-derived galanin in the *Gal*$^{cKO\text{-}Dbh}$ mice may contribute to the baseline phenotype. However, another possible explanation for the results found in Chapter 2 is the presence of compensatory mechanisms in the *Gal*$^{cKO\text{-}Dbh}$ mice that result from the chronic loss of noradrenergic galanin throughout development. These mechanisms may alter other systems that also regulate responses to stress in order to restore balance and normal functioning. While we confirmed that the noradrenergic system and systemic stress response are grossly intact in the *Gal*$^{cKO\text{-}Dbh}$ mice through c-fos expression, brain tissue NE levels (Chapter 2), and plasma corticosterone (Chapter 3), we did not examine potential changes to other transmitter systems known to play important roles in stress-induced behaviors, such as corticotropin-releasing factor and brain-derived neurotrophic factor (McEwen and Akil, 2020). Future studies should include pharmacology experiments with galanin receptor agonists and antagonists or the use of LC-specific viral-mediated galanin knockout during adulthood to overcome the potential limitation of compensatory mechanisms in the *Gal*$^{cKO\text{-}Dbh}$ mice.

In Chapter 3, we found that *Gal*$^{cKO\text{-}Dbh}$ mice displayed increased stress resilience 24 h after foot shock, but not immediately following the stressor or in response to acute optogenetic LC activation, indicating a role for noradrenergic galanin in mediating adaptive stress susceptibility over time. By contrast, we found that that *Dbh*$^{-/-}$ mice were resistant to displaying increased anxiety-like behavior following either an acute stressor, optogenetic LC activation, or 24 h after stressor exposure. These results suggest that NE is required for stress-induced anxiety-like behavior regardless of the time point, in accordance with a large body of previous literature indicating the importance of NE in mediating responses to stress (Valentino and Van Bockstaele,

2008; Borodovitsyna et al., 2018). A previous study showed that selective optogenetic activation of LC neurons was sufficient to induce anxiety-like behavior, and this effect could be blocked by a systemic β-adrenergic receptor antagonist, indicating a noradrenergic mechanism (McCall et al., 2015). Our data support this result by showing that NE is required for acute LC stimulation-induced anxiety-like behavior and expand on this finding by showing that NE-derived galanin is dispensable for this acute behavioral change. Recently, LC-NE mediated βAR signaling in the basolateral amygdala (BLA) was found to induce anxiety-like behavior on its own, and also regulate pain-related anxiety-like behavior (McCall et al., 2017; Llorca-Torralba et al., 2019). Additionally, LC projections to the BLA mediate foot shock stress-induced increases in BLA firing through βAR signaling, and local blockade of βAR signaling in the BLA immediately following foot shock leads to decreased freezing behavior in an immediate fear extinction paradigm (Giustino et al., 2017; Giustino et al., 2020). This acute action of NE in the BLA likely explains the acute stress-induced anxiety-like effect in the EZM immediately following foot shock that we observed in WT and $Gal^{cKO\text{-}Dbh}$ mice, which is absent in the $Dbh^{-/-}$ mice. It is possible that acute NE release is also required for the expression of stress-induced anxiety-like behavior in the EZM 24 h after the stressor. Alternatively, the high levels of NE released during the stress itself may induce plasticity that facilitates anxiety-like behavior the following day. A series of experiments using L-3,4-dihydroxyphenylserine (DOPS) to acutely restore NE in $Dbh^{-/-}$ mice either during the foot shock exposure or during the EZM 24 h later could determine whether acute NE signaling is required during the EZM regardless of when the test is administered, or whether longer-term neurotrophic actions are in play 24 h after a stressor.

The stress resilience effect displayed by $Gal^{cKO\text{-}Dbh}$ mice 24 h after stressor exposure in Chapter 3 could be due to either the lack of acute, neuromodulatory effects of increased galanin

release 24 h after stress (**Fig 3.4**), or the lack of neurotrophic effects of enhanced downstream plasticity due to increased galanin release during the stressor (**Fig. 3.5**). Behavioral pharmacology experiments will be useful for elucidating the mechanisms underlying this effect. For example, galnon, a galanin receptor agonist, could be administered to *Gal*$^{cKO\text{-}Dbh}$ mice either prior to the foot shock exposure or prior to EZM testing 24 h later to determine when galanin signaling is required for stress-induced anxiety-like behavior. If galnon administration immediately prior to the stressor restored the 24 h stress effect in the EZM, this would support the neurotrophic hypothesis that galaninergic action over the course of the 24 h alters stress-induced anxiety-like behavior. However, if galnon administration only restores the 24 h stress effect when given immediately prior to EZM testing, this would suggest that the acute, neuromodulatory effects of galanin are driving the stress-induced behavioral change. If neither of these manipulations restores the 24 h stress effect in the *Gal*$^{cKO\text{-}Dbh}$ mice, it might suggest that the chronic lack of noradrenergic galanin in these animals causes long-term changes in galanin receptor expression patterns or general stress circuitry function, meaning that a single galnon treatment cannot restore the stress effect. A complementary approach to the galnon experiment would be to infuse a galanin receptor antagonist, such as M40, in WT mice at the same two time points to determine if blocking galanin signaling induces a stress-resilient phenotype. Additionally, these approaches would overcome any developmental compensatory mechanisms present in the *Gal*$^{cKO\text{-}Dbh}$ mice. This combination of pharmacological and genetic approaches will help isolate the mechanism leading to increased stress resilience displayed by *Gal*$^{cKO\text{-}Dbh}$ mice.

Our findings from Chapters 2 and 3 suggest that noradrenergic galanin mediates stress susceptibility and passive coping behaviors. Because the LC innervates most of the brain, and galanin receptors are widely expressed across the CNS, there are many potentially interesting

downstream, stress-sensitive regions where noradrenergic galanin could be acting to exert its effects. Future studies should measure c-fos expression in stress-sensitive brain regions downstream from the LC to isolate regions that are differentially activated after the EZM test in the $Gal^{cKO\text{-}Dbh}$ mice compared to WT mice. The behavioral pharmacology experiments described above using galnon and M40 could also be done using site-specific infusions to further test the role of candidate brain regions such as the ventral tegmental area (VTA) and the amygdala, both of which have been implicated in stress regulation and stress-related disorders in humans and animal models (McEwen et al., 2012; Duval et al., 2015; Knowland and Lim, 2018; Koo et al., 2019). Previous work by Weiss and colleagues has suggested that galanin may increase passive coping or stress susceptibility by acute inhibition of VTA dopamine neurons that play a crucial role in motivation and reward. Administration of galanin directly into the VTA of rats increased passive immobility in the forced swim test, while blockade of galanin receptors in the VTA reversed stress-induced behavioral changes, suggesting that acute, neuromodulatory effects of galanin in the VTA result in stress susceptibility (Weiss et al., 2005). While the LC was the suspected source of galanin for mediating these effects, it was never directly tested. The amygdala regulates stress responses through aversive signal processing and promoting defensive behaviors. In clinical studies, amygdala hyperactivity has been associated with PTSD, anxiety disorders, and depression, and increased connectivity between the LC and amygdala have been associated with excessive worry in generalized anxiety disorder (Shin et al., 2006; Hamilton et al., 2012; McLaughlin et al., 2014; Meeten et al., 2016; Stevens et al., 2017). Furthermore, optogenetic activation of LC fibers in the BLA modulates BLA activity and increases anxiety-like behavior, indicating that the LC is an important regulator of amygdala excitability, and rodent studies have shown that acute intra-amygdala infusion of galanin dose-dependently

suppresses punished responding (Moller et al., 1999; McCall et al., 2017). Together, these findings suggest that the VTA and amygdala could be important regions for the acute, neuromodulatory galaninergic actions and provide justification for examining the role of noradrenergic galanin in these regions in future studies.

In Chapter 4, we found increased stress resilience in both the exercise and Gal OX mice. A potential explanation for this is enhanced autoinhibition of LC activity caused by increased galanin suppressing stress-induced LC activity and NE output, therefore leading to decreased anxiety-like behavior (Sciolino and Holmes, 2012). Slice electrophysiology studies have shown that galanin has an inhibitory effect on LC neuron activity. Both galanin and GalR1 agonists potently hyperpolarize LC neurons, suppress spontaneous firing, and enhance α2AR negative feedback via GalR1 (Seutin et al., 1989; Pieribone et al., 1995; Ma et al., 2001; Xu et al., 2001). Furthermore, amperometric studies have shown that LDCVs are released from the soma of LC-NE neurons during high activation, and high resolution *in situ* hybridization imaging in combination with tannic acid application has indicated that galanin is both synthesized and released from LDCVs in the dendrites of LC neurons (Huang et al., 2007; Vila-Porcile et al., 2009). These findings suggest that galanin can be released somatodentritically from LC-NE neurons and produce an autoinhibitory effect on LC neuron activity. However, we do not think that this neuromodulatory mechanism is the main driver behind the stress resilience effect seen in Chapter 4. Sciolino et al. (2015) previously showed that chronic exercise or chronic intracerebroventricular galanin protected against stress-induced anxiogenic behavior and dendritic spine loss in the medial prefrontal cortex (mPFC) of rats. Additionally, chronic, but not acute, infusion of a galanin antagonist blocked the beneficial effects of exercise on behavior and neuroplasticity, supporting the idea that the stress resilience is caused by chronically elevated

galanin leading to long-term neurotrophic adaptation, likely through GalR2 activation, not acute increases in galanin's neuromodulatory actions inhibiting the LC or downstream regions.

The LC is the primary source of NE and galanin to the mPFC and the hippocampus, indicating that both of these regions could be promising sites of action for noradrenergic galanin (Tillage et al., 2020). These two regions have also been consistently implicated in stress regulation and stress-related disorders in humans and animal models (McEwen et al., 2012; Duval et al., 2015). The hippocampus encodes contextual information associated with threats, and the mPFC provides crucial top-down inhibitory control over amygdala activity to regulate stress-related behaviors. Clinical studies have shown that both the mPFC and hippocampus are involved in stress-related disorders. For example, patients with PTSD, depression, or anxiety disorders show reduced hippocampal volume, and PTSD patients have decreased mPFC activity and decreased functional connectivity between the PFC and amygdala (Videbech and Ravnkilde, 2004; Shin et al., 2006). Finally, as mentioned above, chronic exercise or chronic intracerebroventricular galanin infusion protects against stress-induced dendritic spine loss in the mPFC of rats, suggesting an important neurotrophic role for galanin in regulating the long-term neuroplasticity in this region and providing strong rationale for investigating the mPFC in future studies (Sciolino et al., 2015).

One of the most surprising and paradoxical findings from the experiments in this dissertation was that either a lack of galanin in the LC (*Gal*$^{cKO\text{-}Dbh}$ mice, Chapter 3) or high galanin in the LC (exercise and Gal OX mice, Chapter 4) each led to *increased* resilience in the 24 h foot shock stress paradigm compared to controls (summarized in **Fig. 5.1**). At first glance, this is perplexing because it shows an inconsistency in the valence of how noradrenergic galanin modulates stress resilience. However, this finding actually fits with the complexity reported in

the galanin literature, and aligns with contrasting roles that galanin plays across distinct mechanisms and timescales (Weinshenker and Holmes, 2016). One possibility is that the different effects of galanin line up with the neuromodulatory and neurotrophic actions of galanin and are mediated through distinct signaling pathways. For example, the neuromodulatory effects of galanin are generally mediated by GalR1 and GalR3 signaling through $G_{i/o}$ proteins leading to fast neuronal inhibition, while the longer-term neurotrophic actions of galanin require GalR2 and G_q signaling (Wang et al., 1998; Hobson et al., 2008). Thus, the increased stress resilience in the *Gal*$^{cKO\text{-}Dbh}$ mice could reflect the lack of acute, inhibitory neuromodulation via GalR1 and GalR3 activation. By contrast, the increased stress resilience caused by environmental or genetic galanin overexpression in noradrenergic neurons may reflect chronic neurotrophic effects mediated by GalR2 signaling (**Fig. 5.2**). Another possibility is that both of these effects are due to altered plasticity in downstream, stress-sensitive regions, such as changes in dendritic spines or receptor distribution, caused by the neurotrophic actions by galanin, but that these effects are different over time and result in opposite outcomes for stress susceptibility over timescales of hours (Chapter 3) compared to weeks (Chapter 4). In other words, increased neurotrophic galanin activity over a 24 h period following foot shock stress might cause changes that lead to increased sensitivity to stress signals and result in enhanced anxiety-like behavior, but chronically elevated galanin activity for several weeks could cause different, longer term changes that result in resiliency to stressors. Previous research has shown that significant atrophy and remodeling of dendrites occurs in stress-sensitive regions, such as the mPFC, as early as 24 h after a single foot shock stress, supporting the hypothesis that neurotrophic changes could occur during this time frame (Nava et al., 2017; Musazzi et al., 2018).

Given the contrasting roles noradrenergic galanin plays in regulating stress resilience over different timescales, it would be interesting to use a chronic stress paradigm in future studies to dissect the role of galanin in chronic stress-induced behavioral changes, such as social defeat stress or chronic unpredictable stress. Galanin expression is increased in the LC by chronic social stress in rats (Holmes et al., 1995). Isingrini et al. (2016) showed that chronic, but not acute, activation of LC terminals in the VTA promotes resilience to social defeat stress. The effects were assumed to be caused by increased NE transmission, but a role for noradrenergic galanin transmission should be examined. Similar to our experiments in Chapter 3 of this dissertation, future experiments could compare the resiliency of $Gal^{cKO\text{-}Dbh}$ mice to $Dbh^{-/-}$ mice in a chronic social defeat stress paradigm to determine whether NE or noradrenergic galanin is involved in mediating stress resilience under chronic stress conditions. The foot shock stress paradigm we employed here allowed us to measure adaptive stress-induced behavioral changes, as it is reasonable for mice to show increased anxiety-like behavior after experiencing a stressor. In contrast, by using a paradigm such as social defeat stress, which allows the separation of resilient and susceptible animals over time, studies could focus on the role of noradrenergic galanin in regulating maladaptive stress-induced behavioral changes. Chronic stress paradigms more closely model some human neuropsychiatric disorders, such as depression, compared to acute stress models, and recent research has shown that chronic social defeat stress in mice can reproduce the some of the same transcriptional changes seen in humans with depression (Scarpa et al., 2020). Thus, studies such as this could help isolate the specific role of noradrenergic-derived galanin in affective disorders.

5.3 Clinical implications

Given the important role of galanin in regulating stress-induced behavior, the galaninergic system may be a potential target for the development of novel pharmacotherapeutics for stress-related neuropsychiatric disorders, such as depression and anxiety. Both genome-wide association studies and post-mortem human tissue studies have indicated that the galanin system is dysregulated in these disorders, but more research in both humans and animal models is needed to further our understanding of stress-related galaninergic mechanisms before a pharmacotherapeutic approach can be established. No clinical studies on the effects of galanin agonist or antagonist administration in anxiety disorders have been conducted, but one study has examined this in depression. A placebo-controlled clinical study showed preliminary evidence that intravenous administration of galanin has acute antidepressant effects for people with MDD, and the authors suggested this effect may be due to a mechanism related to therapeutic sleep deprivation because of similar changes to sleep EEGs (Murck et al., 2004). However, this study included only 10 participants and no other studies have attempted to replicate this result. Additionally, it is unlikely that galanin administered intravenously can cross the blood-brain-barrier. In contrast to that finding, another study showed a significant positive correlation between plasma galanin levels and MDD severity in women (Wang et al., 2014). Clearly, more research on the galanin system in humans and its relation to stress-related disorders is necessary. Future studies should employ a variety of approaches including human genomic analyses, genetically modified animal models, and post-mortem human tissue to isolate the specific disruptions to the galanin system that occur in stress-related disorders and determine the roles of individual galanin receptors in order potentially create a targeted galanin pharmacotherapeutic.

Genome-wide association studies have revealed that genetic variants in both coding and non-coding regions of the *GAL* and galanin receptor genes confer increased risk of depression and anxiety in humans (Wray et al., 2012; da Conceicao Machado et al., 2018; Keszler et al., 2019). The associations for several of these variants were found to be especially strong when researchers took environmental stress exposures in to account, such as childhood adversity and recent negative life events, indicating a role for gene x environment interactions (Juhasz et al., 2014; Gonda et al., 2018). The functional effects of these genetic variants on galanin transmission are still largely unknown. Interestingly, a recent study identified an interaction between allelic variation in highly conserved *GAL* enhancer sequence and alcohol intake and anxiety in men, then used CRISPR genome editing to disrupt the same enhancer sequence in mice, which led to reduced galanin expression in the amygdala and hypothalamus and a corresponding reduction in ethanol intake and anxiety-like behavior in male mice, mirroring the patterns seen in humans (McEwan et al., 2020). This approach of developing genetic animal models to test specific variants in the *GAL* and galanin receptors genes identified in humans should be used in future research and will be necessary for determining the functional and physiological effects of these variants.

One post-mortem human tissue study has pointed towards dysregulation of the galanin system in stress-related disorders. Analyses of brain tissue from individuals with MDD who committed suicide compared to healthy controls uncovered evidence of significant alterations in the galanin system, including increased galanin and GalR3 mRNA expression and corresponding decreases in DNA methylation at the *GAL* and *GALR3* genes in the LC, suggesting dysregulation specifically in the noradrenergic system (Barde et al., 2016). Despite this evidence indicating a role for galanin in the pathophysiology of stress-related disorders, the specific mechanisms

involved are still unclear, and these epigenetic alterations of the galanin system in MDD have not yet been studied in animal models or connected to the genomic variations in these genes associated with anxiety and depression in humans. Furthermore, as this was only a single study, additional post-mortem research on the state of the galanin system in people who died with affective and anxiety disorders is necessary to confirm these results and further our knowledge on this topic.

Based on current research, the most promising pharmacological target for the treatment of stress-related disorders in the galanin system is the GalR2 receptor. Rodent studies have indicated that GalR2 stimulation has anti-depressant effects whereas GalR1 and GalR3 activation may induce pro-depressive behaviors (Millon et al., 2017). These opposite, receptor-specific effects may explain the conflicting results often found in the literature on the role of galanin in anxiety- and depressive-like behavior, and are likely due to the distinct signaling pathways triggered by these receptors (Bartfai et al., 2004; Holmes et al., 2005; Lu et al., 2005; Kuteeva et al., 2008a; Kuteeva et al., 2008b; Le Maitre et al., 2011; Saar et al., 2013). Additionally, as discussed above, it is likely that the stress resilience effects presented in Chapter 4 are caused by galanin's neurotrophic properties acting through the GalR2 receptor. While more research is necessary to study this hypothesis, treatment with GalR2-specific agonists could be a potential future therapeutic strategy to mimic the beneficial, pro-stress resilience effects of exercise in patients. Difficulty in generating small molecule compounds that pass through the blood-brain-barrier and act selectively on specific galanin receptors has slowed this area of research. Several such compounds have now been developed, however, including a GalR2 positive allosteric modulator, CYM2503, and a synthetic peptide, J18, with high relative affinity for GalR2 (Lu et al., 2010; Saar et al., 2013). Furthermore, J18 was shown to have potent antidepressant-like

effects in the forced swim and tail suspension tests in mice, suggesting potential therapeutic efficacy and indicating the importance of continuing to study these compounds in future research (Saar et al., 2013).

5.4 Conclusion

Because the galanin system is dysregulated in affective and anxiety disorders, it has been proposed as a target for novel therapeutic development. However, we lack a comprehensive understanding of the role of galanin in the stress response. The results presented in this dissertation indicate that noradrenergic-derived galanin plays an important and complex role in regulating stress-induced behaviors. Our data in Chapter 2 using noradrenergic-specific galanin knockout mice highlight a role for noradrenergic galanin in regulating stress-related coping behaviors. Our results in Chapter 3 show that noradrenergic galanin and NE have distinct roles in regulating short-term behavioral responses to stress, and act over different timescales. Finally, in Chapter 4, our data support a role for noradrenergic galanin acting over long time scales to increase stress resilience. The complex effects of galanin point towards the importance of continuing to advance our understanding of the mechanisms involved before considering the galanin system as a target for novel pharmacotherapies for stress-related disorders.

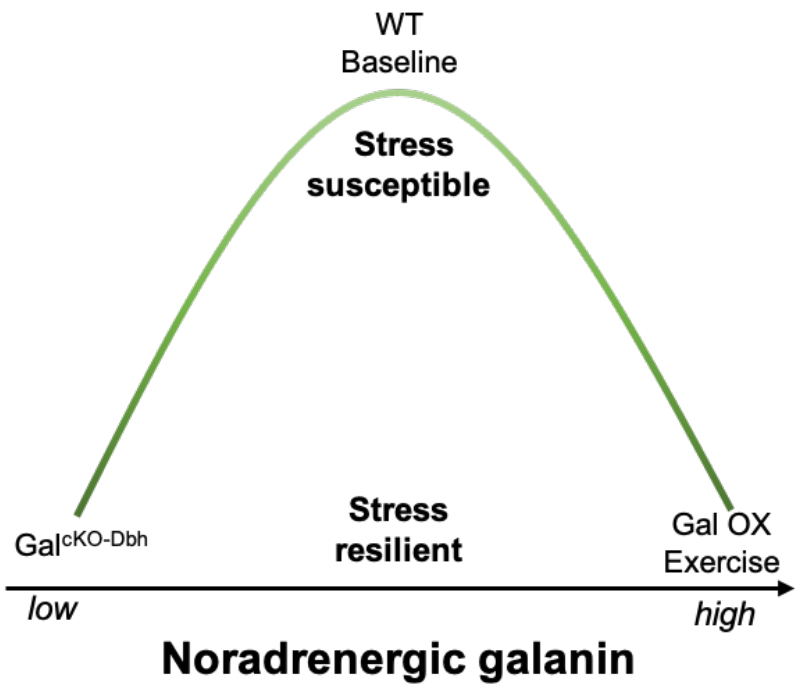

Figure 5.1. Summary of 24 h stress behavioral effects. Either lack of galanin in the LC (*Gal*$^{cKO\text{-}Dbh}$ mice, Chapter 3) or high galanin in the LC (exercise and Gal OX mice, Chapter 4) led to increased resilience after 24 h foot shock stress compared to controls.

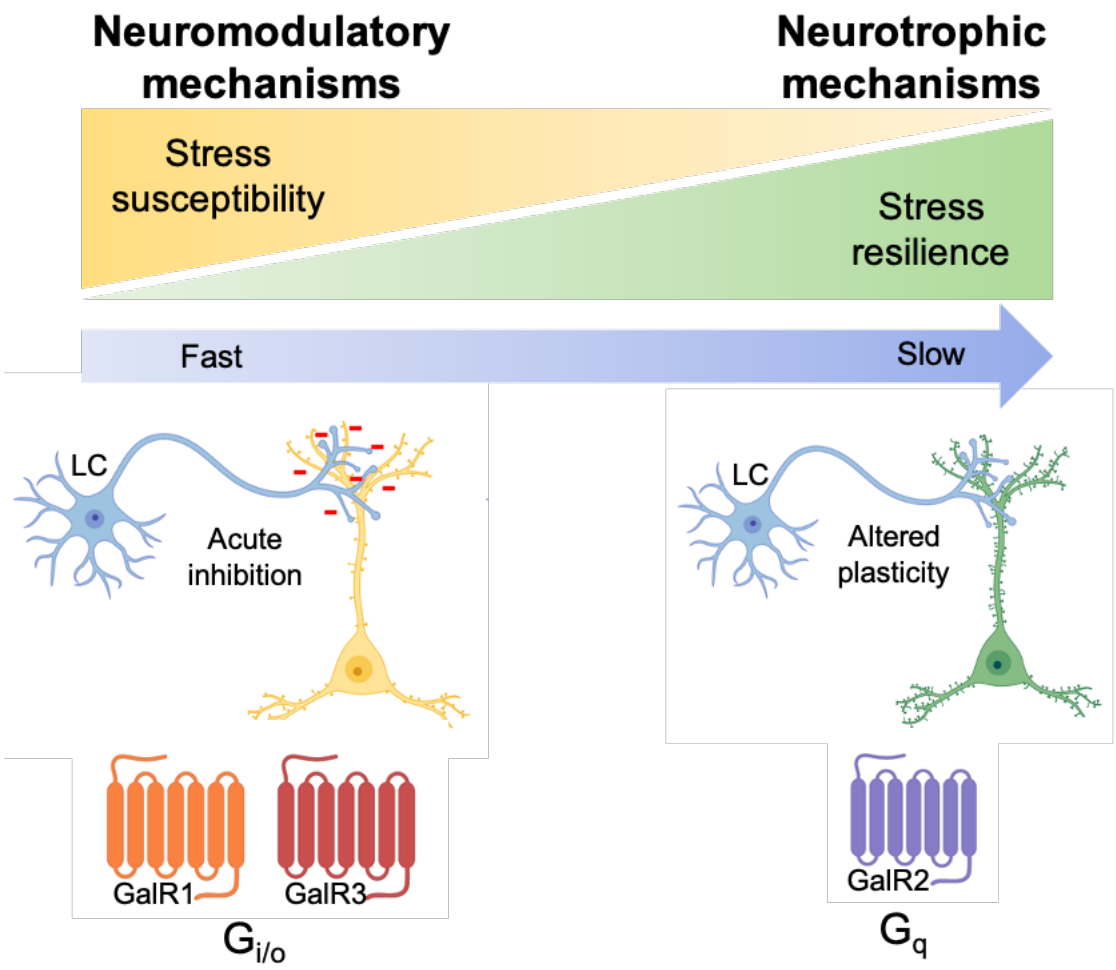

Figure 5.2. Potential explanation of differing galaninergic effects over time. Opposing effects of galanin may align with the distinct neuromodulatory and neurotrophic actions of galanin. (Left) The increased stress resilience observed in *Gal*$^{cKO\text{-}Dbh}$ mice could reflect the lack of acute, neuromodulatory galanin transmission, resulting in stress resilience likely caused by the decreased GalR1 and GalR3 activation. (Right) The stress resilience effects observed after chronic exercise or in the Gal OX mice could be due to the chronically increased neurotrophic effects of galanin leading to altered neuroplasticity, such as changes to dendritic spine densities or receptor distributions, mediated by GalR2.

REFERENCES

Adams AC, Clapham JC, Wynick D, Speakman JR (2008) Feeding behaviour in galanin knockout mice supports a role of galanin in fat intake and preference. J Neuroendocrinol 20:199-206.

Ahren B, Pacini G, Wynick D, Wierup N, Sundler F (2004) Loss-of-function mutation of the galanin gene is associated with perturbed islet function in mice. Endocrinology 145:3190-3196.

Amaral DG, Routtenberg A (1975) Locus coeruleus and intracranial self-stimulation: a cautionary note. Behav Biol 13:331-338.

Angoa-Perez M, Kane MJ, Briggs DI, Francescutti DM, Kuhn DM (2013) Marble burying and nestlet shredding as tests of repetitive, compulsive-like behaviors in mice. J Vis Exp:50978.

Angoa-Perez M, Kane MJ, Briggs DI, Sykes CE, Shah MM, Francescutti DM, Rosenberg DR, Thomas DM, Kuhn DM (2012) Genetic depletion of brain 5HT reveals a common molecular pathway mediating compulsivity and impulsivity. J Neurochem 121:974-984.

Anyan J, Amir S (2018) Too Depressed to Swim or Too Afraid to Stop? A Reinterpretation of the Forced Swim Test as a Measure of Anxiety-Like Behavior. Neuropsychopharmacology 43:931-933.

Ashdown-Franks G, Firth J, Carney R, Carvalho AF, Hallgren M, Koyanagi A, Rosenbaum S, Schuch FB, Smith L, Solmi M, Vancampfort D, Stubbs B (2020) Exercise as Medicine for Mental and Substance Use Disorders: A Meta-review of the Benefits for Neuropsychiatric and Cognitive Outcomes. Sports Med 50:151-170.

Association AP (2013) Diagnostic and Statistical Manual of Mental

Disorders, Fifth ed. Edition. Arlington, VA.

Aston-Jones G, Waterhouse B (2016) Locus coeruleus: From global projection system to adaptive regulation of behavior. Brain Res 1645:75-78.

Bale TL, Abel T, Akil H, Carlezon WA, Jr., Moghaddam B, Nestler EJ, Ressler KJ, Thompson SM (2019) The critical importance of basic animal research for neuropsychiatric disorders. Neuropsychopharmacology 44:1349-1353.

Bandelow B, Michaelis S, Wedekind D (2017) Treatment of anxiety disorders. Dialogues Clin Neurosci 19:93-107.

Barde S, Ruegg J, Prud'homme J, Ekstrom TJ, Palkovits M, Turecki G, Bagdy G, Ihnatko R, Theodorsson E, Juhasz G, Diaz-Heijtz R, Mechawar N, Hokfelt TG (2016) Alterations in the neuropeptide galanin system in major depressive disorder involve levels of transcripts, methylation, and peptide. Proc Natl Acad Sci U S A 113:E8472-E8481.

Bari BA, Chokshi V, Schmidt K (2020) Locus coeruleus-norepinephrine: basic functions and insights into Parkinson's disease. Neural Regen Res 15:1006-1013.

Bartfai T, Iverfeldt K, Fisone G, Serfozo P (1988) Regulation of the release of coexisting neurotransmitters. Ann Rev Pharmacol Toxicol 28:285-310.

Bartfai T, Lu X, Badie-Mahdavi H, Barr AM, Mazarati A, Hua XY, Yaksh T, Haberhauer G, Ceide SC, Trembleau L, Somogyi L, Krock L, Rebek J, Jr. (2004) Galmic, a nonpeptide galanin receptor agonist, affects behaviors in seizure, pain, and forced-swim tests. Proc Natl Acad Sci U S A 101:10470-10475.

Bartling B, Al-Robaiy S, Lehnich H, Binder L, Hiebl B, Simm A (2017) Sex-related differences in the wheel-running activity of mice decline with increasing age. Exp Gerontol 87:139-147.

Bernard R, Kerman IA, Thompson RC, Jones EG, Bunney WE, Barchas JD, Schatzberg AF, Myers RM, Akil H, Watson SJ (2011) Altered expression of glutamate signaling, growth factor, and glia genes in the locus coeruleus of patients with major depression. Mol Psychiatry 16:634-646.

Berridge CW, Waterhouse BD (2003) The locus coeruleus–noradrenergic system: modulation of behavioral state and state-dependent cognitive processes. Brain Research Reviews 42:33-84.

Berton O, McClung CA, Dileone RJ, Krishnan V, Renthal W, Russo SJ, Graham D, Tsankova NM, Bolanos CA, Rios M, Monteggia LM, Self DW, Nestler EJ (2006) Essential role of BDNF in the mesolimbic dopamine pathway in social defeat stress. Science 311:864-868.

Bing O, Möller C, Engel J, Söderpalm B, Heilig M (1993) Anxiolytic-like action of centrally administered galanin. Neurosci Lett 164:17-20.

Bissette G, Klimek V, Pan J, Stockmeier C, Ordway G (2003) Elevated concentrations of CRF in the locus coeruleus of depressed subjects. Neuropsychopharmacology 28:1328-1335.

Borodovitsyna O, Joshi N, Chandler D (2018) Persistent Stress-Induced Neuroplastic Changes in the Locus Coeruleus/Norepinephrine System. Neural Plast 2018:1892570.

Bourdelat-Parks BN, Anderson GM, Donaldson ZR, Weiss JM, Bonsall RW, Emery MS, Liles LC, Weinshenker D (2005) Effects of dopamine beta-hydroxylase genotype and disulfiram inhibition on catecholamine homeostasis in mice. Psychopharmacology (Berl) 183:72-80.

Bousman C, Maruf AA, Muller DJ (2019) Towards the integration of pharmacogenetics in psychiatry: a minimum, evidence-based genetic testing panel. Curr Opin Psychiatry 32:7-15.

Britton DR, Ksir C, Britton KT, Young D, Koob GF (1984) Brain norepinephrine depleting lesions selectively enhance behavioral responsiveness to novelty. Physiol Behav 33:473-478.

Can A, Dao DT, Terrillion CE, Piantadosi SC, Bhat S, Gould TD (2012) The tail suspension test. J Vis Exp:e3769.

Carek PJ, Laibstain SE, Carek SM (2011) Exercise for the Treatment of Depression and Anxiety. The International Journal of Psychiatry in Medicine 41:15-28.

Carter ME, Yizhar O, Chikahisa S, Nguyen H, Adamantidis A, Nishino S, Deisseroth K, de Lecea L (2010) Tuning arousal with optogenetic modulation of locus coeruleus neurons. Nat Neurosci 13:1526-1533.

Chan-Palay V, Jentsch B, Lang W, Hochli M, Asan E (1990) Distribution of neuropeptide Y, C-terminal flanking peptide of NPY and galanin coexistence with catecholamine in the locus coeruleus of normal human, Alzheimer's dementia and Parkinson's disease brains. . Dementia and Geriatric Cognitive Disorders 1:18-31.

Chandler DJ (2016) Evidence for a specialized role of the locus coeruleus noradrenergic system in cortical circuitries and behavioral operations. Brain Res 1641:197-206.

Chandley MJ, Szebeni A, Szebeni K, Crawford JD, Stockmeier CA, Turecki G, Kostrzewa RM, Ordway GA (2014) Elevated gene expression of glutamate receptors in noradrenergic neurons from the locus coeruleus in major depression. Int J Neuropsychopharmacol 17:1569-1578.

Charney DS, Heninger GR, Redmond DE, Jr. (1983) Yohimbine induced anxiety and increased noradrenergic function in humans: effects of diazepam and clonidine. Life Sci 33:19-29.

Chekroud SR, Gueorguieva R, Zheutlin AB, Paulus M, Krumholz HM, Krystal JH, Chekroud AM (2018) Association between physical exercise and mental health in 1·2 million individuals in the USA between 2011 and 2015: a cross-sectional study. The Lancet Psychiatry 5:739-746.

Chen YW, Das M, Oyarzabal EA, Cheng Q, Plummer NW, Smith KG, Jones GK, Malawsky D, Yakel JL, Shih YI, Jensen P (2019) Genetic identification of a population of noradrenergic neurons implicated in attenuation of stress-related responses. Mol Psychiatry 24:710-725.

Cheung C, Hohmann J, Clifton D, Steiner R (2001) Distribution of galanin messenger RNA-expressing cells in murine brain and their regulation by leptin in regions of the hypothalamus. Neuroscience 103:423-432.

Chisholm D, Sweeny K, Sheehan P, Rasmussen B, Smit F, Cuijpers P, Saxena S (2016) Scaling-up treatment of depression and anxiety: a global return on investment analysis. The Lancet Psychiatry 3:415-424.

Christiansen SH (2011) Regulation of the galanin system in the brainstem and hypothalamus by electroconvulsive stimulation in mice. Neuropeptides 45:337-341.

Cooney GM, Dwan K, Greig CA, Lawlor DA, Rimer J, Waugh FR, McMurdo M, Mead GE (2013) Exercise for depression. Cochrane Database Syst Rev:CD004366.

Crow TJ, Spear PJ, Arbuthnott GW (1972) Intracranial self-stimulation with electrodes in the region of the locus coeruleus. Brain Res 36:275-287.

Cryan JF, Sweeney FF (2011) The age of anxiety: role of animal models of anxiolytic action in drug discovery. Br J Pharmacol 164:1129-1161.

Curtis AL, Lechner SM, Pavcovich LA, Valentino RJ (1997) Activation of the locus coeruleus noradrenergic system by intracoerulear microinfusion of corticotropin-releasing factor: effects on discharge rate, cortical norepinephrine levels and cortical electroencephalographic activity. J Pharmacol Exp Ther 281:163-172.

Curtis AL, Leiser SC, Snyder K, Valentino RJ (2012) Predator stress engages corticotropin-releasing factor and opioid systems to alter the operating mode of locus coeruleus norepinephrine neurons. Neuropharmacology 62:1737-1745.

da Conceicao Machado F, de Souza LV, Rangel M, Jara ZP, do Carmo Franco M (2018) Implication of galanin gene rs948854 polymorphism in depressive symptoms in adolescents. Horm Behav 97:14-17.

Daviu N, Bruchas MR, Moghaddam B, Sandi C, Beyeler A (2019) Neurobiological links between stress and anxiety. Neurobiol Stress 11:100191.

De Bono JP, Adlam D, Paterson DJ, Channon KM (2006) Novel quantitative phenotypes of exercise training in mouse models. Am J Physiol Regul Integr Comp Physiol 290:R926-934.

de Kloet ER, Molendijk ML (2016) Coping with the Forced Swim Stressor: Towards Understanding an Adaptive Mechanism. Neural Plast 2016:6503162.

Degroot A, Nomikos GG (2004) Genetic deletion and pharmacological blockade of CB1 receptors modulates anxiety in the shock-probe burying test. Eur J Neurosci 20:1059-1064.

Duval ER, Javanbakht A, Liberzon I (2015) Neural circuits in anxiety and stress disorders: a focused review. Ther Clin Risk Manag 11:115-126.

Echevarria DJ, Hernandez A, Diogenes A, Morilak DA (2005) Administration of the galanin antagonist M40 into lateral septum attenuates shock probe defensive burying behavior in rats. Neuropeptides 39:445-451.

Ehnvall A, Sjogren M, Zachrisson OCG, Agren H (2003) Lifetime burden of mood swings and activation of brain norepinephrine turnover in patients with treatment-refractory depressive illness. Journal of Affective Disorders 74:185-189.

Epps SA, Kahn AB, Holmes PV, Boss-Williams KA, Weiss JM, Weinshenker D (2013) Antidepressant and anticonvulsant effects of exercise in a rat model of epilepsy and depression comorbidity. Epilepsy Behav 29:47-52.

Fang P, He B, Shi M, Zhu Y, Bo P, Zhang Z (2015) Crosstalk between exercise and galanin system alleviates insulin resistance. Neurosci Biobehav Rev 59:141-146.

Gaval-Cruz M, Liles LC, Iuvone PM, Weinshenker D (2012) Chronic inhibition of dopamine beta-hydroxylase facilitates behavioral responses to cocaine in mice. PLoS One 7:e50583.

George SH, Gertsenstein M, Vintersten K, Korets-Smith E, Murphy J, Stevens ME, Haigh JJ, Nagy A (2007) Developmental and adult phenotyping directly from mutant embryonic stem cells. Proc Natl Acad Sci U S A 104:4455-4460.

Gerfen CR, Paletzki R, Heintz N (2013) GENSAT BAC cre-recombinase driver lines to study the functional organization of cerebral cortical and basal ganglia circuits. Neuron 80:1368-1383.

Gilsbach R, Hein L (2008) Presynaptic Metabotropic Receptors for Acetylcholine and Adrenaline/Noradrenaline. In: Pharmacology of Neurotransmitter Release, pp 261-288: Springer.

Giustino TF, Ramanathan KR, Totty MS, Miles OW, Maren S (2020) Locus Coeruleus Norepinephrine Drives Stress-Induced Increases in Basolateral Amygdala Firing and Impairs Extinction Learning. J Neurosci 40:907-916.

Giustino TF, Seemann JR, Acca GM, Goode TD, Fitzgerald PJ, Maren S (2017) beta-Adrenoceptor Blockade in the Basolateral Amygdala, But Not the Medial Prefrontal Cortex, Rescues the Immediate Extinction Deficit. Neuropsychopharmacology 42:2537-2544.

Goh J, Ladiges W (2015) Voluntary Wheel Running in Mice. Curr Protoc Mouse Biol 5:283-290.

Gonda X, Hullam G, Antal P, Eszlari N, Petschner P, Hokfelt TG, Anderson IM, Deakin JFW, Juhasz G, Bagdy G (2018) Significance of risk polymorphisms for depression depends on stress exposure. Sci Rep 8:3946.

Gower AJ, Tricklebank MD (1988) Alpha 2-adrenoceptor antagonist activity may account for the effects of buspirone in an anticonflict test in the rat. Eur J Pharmacol 155:129-137.

Granger AJ, Wang W, Robertson K, El-Rifai M, Zanello AF, Bistrong K, Saunders A, Chow BW, Nunez V, Turrero Garcia M, Harwell CC, Gu C, Sabatini BL (2020) Cortical ChAT(+) neurons co-transmit acetylcholine and GABA in a target- and brain-region-specific manner. Elife 9.

Hamilton JP, Etkin A, Furman DJ, Lemus MG, Johnson RF, Gotlib IH (2012) Functional Neuroimaging of Major Depressive Disorder: A Meta-Analysis and New Integration of Baseline Activation and Neural Response Data. American Journal of Psychiatry 169:693-703.

Harvey SB, Overland S, Hatch SL, Wessely S, Mykletun A, Hotopf M (2018) Exercise and the Prevention of Depression: Results of the HUNT Cohort Study. Am J Psychiatry 175:28-36.

Herring M, O'Connor P, Dishman R (2010) The Effect of Exercise Training on Anxiety Symptoms Among Patients. Arch Intern Med 170:321–331.

HHS USDo (2019) Key substance use and mental health indicators in the United States: Results from the 2018 National Survey on Drug Use and Health In: (HHS Publication No. PEP19-5068 NSH-, ed). Rockville, MD: Center for Behavioral Health Statistics and Quality, Substance Abuse and Mental Health Services Administration.

Hirschberg S, Li Y, Randall A, Kremer EJ, Pickering AE (2017) Functional dichotomy in spinal- vs prefrontal-projecting locus coeruleus modules splits descending noradrenergic analgesia from ascending aversion and anxiety in rats. Elife 6.

Hobson SA, Vanderplank PA, Pope RJ, Kerr NC, Wynick D (2013) Galanin stimulates neurite outgrowth from sensory neurons by inhibition of Cdc42 and Rho GTPases and activation of cofilin. J Neurochem 127:199-208.

Hobson SA, Bacon A, Elliot-Hunt CR, Holmes FE, Kerr NC, Pope R, Vanderplank P, Wynick D (2008) Galanin acts as a trophic factor to the central and peripheral nervous systems. Cell Mol Life Sci 65:1806-1812.

Hokfelt T, Broberger C, Diez M, Xu ZQ, Shi T, Kopp J, Zhang X, Holmberg K, Landry M, Koistinaho J (1999) Galanin and NPY, two peptides with multiple putative roles in the nervous system. Horm Metab Res 31:330-334.

Hokfelt T, Barde S, Xu ZD, Kuteeva E, Ruegg J, Le Maitre E, Risling M, Kehr J, Ihnatko R, Theodorsson E, Palkovits M, Deakin W, Bagdy G, Juhasz G, Prud'homme HJ, Mechawar

N, Diaz-Heijtz R, Ogren SO (2018) Neuropeptide and Small Transmitter Coexistence: Fundamental Studies and Relevance to Mental Illness. Front Neural Circuits 12:106.

Hökfelt T, Xu Z, Shi T, Holmberg K, Zhang X (1998) Galanin in ascending systems. Focus on coexistence with 5-hydroxytryptamine and noradrenaline. Ann N Y Acad Sci 21:252-263.

Holets VR, Hokfelt T, Rokaeus A, Terenius L, Goldstein M (1988) Locus coeruleus neurons in the rat containing neuropeptide Y, tyrosine hydroxylase or galanin and their efferent projections to the spinal cord, cerebral cortex and hypothalamus. Neuroscience 24:893-906.

Holmes A, Yang RJ, Crawley JN (2002) Evaluation of an Anxiety-Related Phenotype in Galanin Overexpressing Transgenic Mice. Journal of Mol Neuroscience 18:151-165.

Holmes A, Li Q, Koenig EA, Gold E, Stephenson D, Yang RJ, Dreiling J, Sullivan T, Crawley JN (2005) Phenotypic assessment of galanin overexpressing and galanin receptor R1 knockout mice in the tail suspension test for depression-related behavior. Psychopharmacology (Berl) 178:276-285.

Holmes FE, Armenaki A, Iismaa TP, Einstein EB, Shine J, Picciotto MR, Wynick D, Zachariou V (2012) Galanin negatively modulates opiate withdrawal via galanin receptor 1. Psychopharmacology (Berl) 220:619-625.

Holmes FE, Mahoney S, King VR, Bacon A, Kerr NC, Pachnis V, Curtis R, Priestley JV, Wynick D (2000) Targeted disruption of the galanin gene reduces the number of sensory neurons and their regenerative capacity. Proc Natl Acad Sci U S A 97:11563-11568.

Holmes PV (2014) Trophic Mechanisms for Exercise-Induced Stress Resilience: Potential Role of Interactions between BDNF and Galanin. Front Psychiatry 5:90.

Holmes PV, Yoo HS, Dishman RK (2006) Voluntary exercise and clomipramine treatment elevate prepro-galanin mRNA levels in the locus coeruleus in rats. Neurosci Lett 408:1-4.

Holmes PV, Blanchard DC, Blanchard RJ, Brady LS, Crawley JN (1995) Chronic social stress increases levels of preprogalanin mRNA in the rat locus coeruleus. Pharmacol Biochem Behav 50:655-660.

Huang HP, Wang SR, Yao W, Zhang C, Zhou Y, Chen XW, Zhang B, Xiong W, Wang LY, Zheng LH, Landry M, Hokfelt T, Xu ZQ, Zhou Z (2007) Long latency of evoked quantal transmitter release from somata of locus coeruleus neurons in rat pontine slices. Proc Natl Acad Sci U S A 104:1401-1406.

Hwang DY, Carlezon WA, Isacson O, Kim KS (2001) A high-efficiency synthetic expression selectively promoter that drives transgene in noradrenergic neurons. Human Gene Therapy 12:1731-1740.

Isingrini E, Perret L, Rainer Q, Amilhon B, Guma E, Tanti A, Martin G, Robinson J, Moquin L, Marti F, Mechawar N, Williams S, Gratton A, Giros B (2016) Resilience to chronic stress is mediated by noradrenergic regulation of dopamine neurons. Nature Neuroscience 19:560-563.

James SL et al. (2018) Global, regional, and national incidence, prevalence, and years lived with disability for 354 diseases and injuries for 195 countries and territories, 1990–2017: a systematic analysis for the Global Burden of Disease Study 2017. The Lancet 392:1789-1858.

Jedema HP, Grace AA (2004) Corticotropin-releasing hormone directly activates noradrenergic neurons of the locus ceruleus recorded in vitro. J Neurosci 24:9703-9713.

Jorm AF, Patten SB, Brugha TS, Mojtabai R (2017) Has increased provision of treatment reduced the prevalence of common mental disorders? Review of the evidence from four countries. World Psychiatry 16:90-99.

Juhasz G, Hullam G, Eszlari N, Gonda X, Antal P, Anderson IM, Hokfelt TG, Deakin JF, Bagdy G (2014) Brain galanin system genes interact with life stresses in depression-related phenotypes. Proc Natl Acad Sci U S A 111:E1666-1673.

Kalueff AV, Tuohimaa P (2004) Grooming analysis algorithm for neurobehavioural stress research. Brain Res Brain Res Protoc 13:151-158.

Kandel E, Schwarts J, Jessell T, Siegelbaum S, Hudspeth A (2013) Neurotransmitters. In: Principals of Neural Science, Fifth Edition, pp 289-306: Elseiver Health Sciences.

Karlsson RM, Holmes A (2006) Galanin as a modulator of anxiety and depression and a therapeutic target for affective disease. Amino Acids 31:231-239.

Karlsson RM, Holmes A, Heilig M, Crawley JN (2005) Anxiolytic-like actions of centrally-administered neuropeptide Y, but not galanin, in C57BL/6J mice. Pharmacol Biochem Behav 80:427-436.

Kebschull JM, Garcia da Silva P, Reid AP, Peikon ID, Albeanu DF, Zador AM (2016) High-Throughput Mapping of Single-Neuron Projections by Sequencing of Barcoded RNA. Neuron 91:975-987.

Kendler KS (2012) The dappled nature of causes of psychiatric illness: replacing the organic-functional/hardware-software dichotomy with empirically based pluralism. Mol Psychiatry 17:377-388.

Kessler RC, Chiu WT, Demler O, Merikangas KR, Walters EE (2005) Prevalence, severity, and comorbidity of 12-month DSM-IV disorders in the National Comorbidity Survey Replication. Arch Gen Psychiatry 62:617-627.

Keszler G, Molnar Z, Ronai Z, Sasvari-Szekely M, Szekely A, Kotyuk E (2019) Association between anxiety and non-coding genetic variants of the galanin neuropeptide. PLoS One 14:e0226228.

Kim Y, Perova Z, Mirrione MM, Pradhan K, Henn FA, Shea S, Osten P, Li B (2016) Whole-Brain Mapping of Neuronal Activity in the Learned Helplessness Model of Depression. Front Neural Circuits 10:3.

Kingston RC, Smith M, Lacey T, Edwards M, Best JN, Markham CM (2018) Voluntary exercise increases resilience to social defeat stress in Syrian hamsters. Physiol Behav 188:194-198.

Knowland D, Lim BK (2018) Circuit-based frameworks of depressive behaviors: The role of reward circuitry and beyond. Pharmacol Biochem Behav 174:42-52.

Kofler B, Berger A, Santic R, Moritz K, Almer D, Tuechler C, Lang R, Emberger M, Klausegger A, Sperl W, Bauer JW (2004) Expression of neuropeptide galanin and galanin receptors in human skin. J Invest Dermatol 122:1050-1053.

Koo JW, Chaudhury D, Han MH, Nestler EJ (2019) Role of Mesolimbic Brain-Derived Neurotrophic Factor in Depression. Biol Psychiatry 86:738-748.

Koob GF, Thatcher-Britton K, Britton DR, Roberts DC, Bloom FE (1984) Destruction of the locus coeruleus or the dorsal NE bundle does not alter the release of punished responding by ethanol and chlordiazepoxide. Physiol Behav 33:479-485.

Kordower JH, Le HK, Mufson EJ (1992) Galanin immunoreactivity in the primate central nervous system. J Comp Neurol 319:479-500.

Kruijshaar MKB, J. Vos, T., de Graaf R, Spijker J, Andrews G (2005) Lifetime prevalence estimates of major depression- An indirect estimation method and a quantification of recall bias. Eur J of Epidemiology 20:103-111.

Kuehl LK, Deuter CE, Hellmann-Regen J, Kaczmarczyk M, Otte C, Wingenfeld K (2020) Enhanced noradrenergic activity by yohimbine and differential fear conditioning in patients with major depression with and without adverse childhood experiences. Prog Neuropsychopharmacol Biol Psychiatry 96:109751.

Kuteeva E, Hokfelt T, Wardi T, Ogren SO (2008a) Galanin, galanin receptor subtypes and depression-like behaviour. Cell Mol Life Sci 65:1854-1863.

Kuteeva E, Wardi T, Lundstrom L, Sollenberg U, Langel U, Hokfelt T, Ogren SO (2008b) Differential role of galanin receptors in the regulation of depression-like behavior and monoamine/stress-related genes at the cell body level. Neuropsychopharmacology 33:2573-2585.

Lang R, Gundlach AL, Holmes FE, Hobson SA, Wynick D, Hokfelt T, Kofler B (2015) Physiology, signaling, and pharmacology of galanin peptides and receptors: three decades of emerging diversity. Pharmacol Rev 67:118-175.

Le Maitre E, Barde SS, Palkovits M, Diaz-Heijtz R, Hokfelt TG (2013) Distinct features of neurotransmitter systems in the human brain with focus on the galanin system in locus coeruleus and dorsal raphe. Proc Natl Acad Sci U S A 110:E536-545.

Le Maitre TW, Xia S, Le Maitre E, Dun XP, Lu J, Theodorsson E, Ogren SO, Hokfelt T, Xu ZQ (2011) Galanin receptor 2 overexpressing mice display an antidepressive-like phenotype: possible involvement of the subiculum. Neuroscience 190:270-288.

Lecca S, Pelosi A, Tchenio A, Moutkine I, Lujan R, Herve D, Mameli M (2016) Rescue of GABAB and GIRK function in the lateral habenula by protein phosphatase 2A inhibition ameliorates depression-like phenotypes in mice. Nat Med 22:254-261.

Lenze EJ, Goate AM, Nowotny P, Dixon D, Shi P, Bies RR, Lotrich FK, Rollman BL, Shear MK, Thompson PA, Andreescu C, Pollock BG (2010) Relation of serotonin transporter genetic variation to efficacy of escitalopram for generalized anxiety disorder in older adults. J Clin Psychopharmacol 30:672-677.

Lerner JT, Sankar R, Mazarati AM (2008) Galanin and epilepsy. Cell Mol Life Sci 65:1864-1871.

Levran O, Londono D, O'Hara K, Nielsen DA, Peles E, Rotrosen J, Casadonte P, Linzy S, Randesi M, Ott J, Adelson M, Kreek MJ (2008) Genetic susceptibility to heroin addiction: a candidate gene association study. Genes Brain Behav 7:720-729.

Lewandoski M, Meyers EN, Martin GR (1997) Analysis of Fgf8 gene function in vertebrate development. Cold Spring Harb Symp Quant Biol 62:159-168.

Li L, Feng X, Zhou Z, Zhang H, Shi Q, Lei Z, Shen P, Yang Q, Zhao B, Chen S, Li L, Zhang Y, Wen P, Lu Z, Li X, Xu F, Wang L (2018) Stress Accelerates Defensive Responses to Looming in Mice and Involves a Locus Coeruleus-Superior Colliculus Projection. Curr Biol.

Li Y, Luikart BW, Birnbaum S, Chen J, Kwon CH, Kernie SG, Bassel-Duby R, Parada LF (2008) TrkB regulates hippocampal neurogenesis and governs sensitivity to antidepressive treatment. Neuron 59:399-412.

Liu PZ, Nusslock R (2018) Exercise-Mediated Neurogenesis in the Hippocampus via BDNF. Front Neurosci 12:52.

Llorca-Torralba M, Suarez-Pereira I, Bravo L, Camarena-Delgado C, Garcia-Partida JA, Mico JA, Berrocoso E (2019) Chemogenetic Silencing of the Locus Coeruleus-Basolateral Amygdala Pathway Abolishes Pain-Induced Anxiety and Enhanced Aversive Learning in Rats. Biol Psychiatry 85:1021-1035.

Lu X, Ross B, Sanchez-Alavez M, Zorrilla EP, Bartfai T (2008) Phenotypic analysis of GalR2 knockout mice in anxiety- and depression-related behavioral tests. Neuropeptides 42:387-397.

Lu X, Barr AM, Kinney JW, Sanna P, Conti B, Behrens MM, Bartfai T (2005) A role for galanin in antidepressant actions with a focus on the dorsal raphe nucleus. Proc Natl Acad Sci U S A 102:874-879.

Lu X, Roberts E, Xia F, Sanchez-Alavez M, Liu T, Baldwin R, Wu S, Chang J, Wasterlain CG, Bartfai T (2010) GalR2-positive allosteric modulator exhibits anticonvulsant effects in animal models. Proc Natl Acad Sci U S A 107:15229-15234.

Lustberg D, Iannitelli AF, Tillage RP, Pruitt M, Liles LC, Weinshenker D (2020) Central norepinephrine transmission is required for stress-induced repetitive behavior in two rodent models of obsessive-compulsive disorder. Psychopharmacology (Berl) 237:1973-1987.

Ma X, Tong YG, Schmidt R, Brown W, Payza K, Hodzic L, Pou C, Godbout C, Hokfelt T, Xu ZQ (2001) Effects of galanin receptor agonists on locus coeruleus neurons. Brain Res 919:169-174.

Maeda T (2000) The Locus Coeruleus: History. Journal of Chemical Neuroanatomy 18:57–64.

Marino MD, Bourdelat-Parks BN, Cameron Liles L, Weinshenker D (2005) Genetic reduction of noradrenergic function alters social memory and reduces aggression in mice. Behav Brain Res 161:197-203.

Matsushita N, Kobayashi K, Miyazaki J, Kobayashi K (2004) Fate of transient catecholaminergic cell types revealed by site-specific recombination in transgenic mice. J Neurosci Res 78:7-15.

Mazarati AM, Hohmann JG, Bacon A, Liu H, Sankar R, Steiner RA, Wynick D, Wasterlain CG (2000) Modulation of hippocampal excitability and seizures by galanin. J Neurosci 20:6276-6281.

McCall JG, Al-Hasani R, Siuda ER, Hong DY, Norris AJ, Ford CP, Bruchas MR (2015) CRH Engagement of the Locus Coeruleus Noradrenergic System Mediates Stress-Induced Anxiety. Neuron 87:605-620.

McCall JG, Siuda ER, Bhatti DL, Lawson LA, McElligott ZA, Stuber GD, Bruchas MR (2017) Locus coeruleus to basolateral amygdala noradrenergic projections promote anxiety-like behavior. Elife 6.

McClung CA, Nestler EJ, Zachariou V (2005) Regulation of gene expression by chronic morphine and morphine withdrawal in the locus ceruleus and ventral tegmental area. J Neurosci 25:6005-6015.

McEwan AR, Davidson C, Hay E, Turnbull Y, Erickson JC, Marini P, Wilson D, McIntosh AM, Adams MJ, Murgatroyd C, Barrett P, Delibegovic M, Clarke TK, MacKenzie A (2020) CRISPR disruption and UK Biobank analysis of a highly conserved polymorphic enhancer suggests a role in male anxiety and ethanol intake. Mol Psychiatry.

McEwen BS, Akil H (2020) Revisiting the Stress Concept: Implications for Affective Disorders. J Neurosci 40:12-21.

McEwen BS, Eiland L, Hunter RG, Miller MM (2012) Stress and anxiety: structural plasticity and epigenetic regulation as a consequence of stress. Neuropharmacology 62:3-12.

McLaughlin KA, Busso DS, Duys A, Green JG, Alves S, Way M, Sheridan MA (2014) Amygdala response to negative stimuli predicts PTSD symptom onset following a terrorist attack. Depress Anxiety 31:834-842.

Meeten F, Davey GC, Makovac E, Watson DR, Garfinkel SN, Critchley HD, Ottaviani C (2016) Goal Directed Worry Rules Are Associated with Distinct Patterns of Amygdala Functional Connectivity and Vagal Modulation during Perseverative Cognition. Front Hum Neurosci 10:553.

Mefford I (1988) Epinephrine in the Mammalian Brain. Progress in Neuro-Psychopharmacology and Biological Psychiatry 12:365-388.

Melander T, Hokfelt, T., Rokaeus, A., Cuello, A., Oertel, W., Verhofstad, A., Goldstein, M. (1986) Coexistence of Galanin-like lmmunoreactivity with Catecholamines, 5-Hydroxytryptamine, GABA and Neuropeptides in the Rat CNS. Journal of Neuroscience 6:3640–3654.

Menard J, Treit D (1996) Lateral and medial septal lesions reduce anxiety in the plus-maze and probe-burying tests. Physiol Behav 60:845-853.

Mennicken F, Hoffert C, Pelletier M, Ahmad S, O'Donnell D (2002) Restricted distribution of galanin receptor 3 (GalR3) mRNA in the adult rat central nervous system. J Chem Neuroanat 24:257-268.

Millon C, Flores-Burgess A, Narvaez M, Borroto-Escuela DO, Gago B, Santin L, Castilla-Ortega E, Narvaez JA, Fuxe K, Diaz-Cabiale Z (2017) The neuropeptides Galanin and Galanin(1-15) in depression-like behaviours. Neuropeptides 64:39-45.

Mitsukawa K, Lu X, Bartfai T (2008) Galanin, galanin receptors and drug targets. Cell Mol Life Sci 65:1796-1805.

Moller C, Sommer W, Thorsell A, Heilig M (1999) Anxiogenic-like action of galanin after intra-amygdala administration in the rat. Neuropsychopharmacology 21:507-512.

Morey RA, Dunsmoor JE, Haswell CC, Brown VM, Vora A, Weiner J, Stjepanovic D, Wagner HR, 3rd, LaBar KS (2015) Fear learning circuitry is biased toward generalization of fear associations in posttraumatic stress disorder. Transl Psychiatry 5:e700.

Morris LS, McCall JG, Charney DS, Murrough JW (2020) The role of the locus coeruleus in the generation of pathological anxiety. Brain and Neuroscience Advances 4:1-18.

Muir J, Lopez J, Bagot RC (2019) Wiring the depressed brain: optogenetic and chemogenetic circuit interrogation in animal models of depression. Neuropsychopharmacology 44:1013-1026.

Mul JD, Soto M, Cahill ME, Ryan RE, Takahashi H, So K, Zheng J, Croote DE, Hirshman MF, la Fleur SE, Nestler EJ, Goodyear LJ (2018) Voluntary wheel running promotes resilience to chronic social defeat stress in mice: a role for nucleus accumbens DeltaFosB. Neuropsychopharmacology 43:1934-1942.

Murck H, Held K, Ziegenbein M, Kunzel H, Holsboer F, Steiger A (2004) Intravenous administration of the neuropeptide galanin has fast antidepressant efficacy and affects the sleep EEG. Psychoneuroendocrinology 29:1205-1211.

Musazzi L, Tornese P, Sala N, Popoli M (2018) What Acute Stress Protocols Can Tell Us About PTSD and Stress-Related Neuropsychiatric Disorders. Front Pharmacol 9:758.

Myers B, Scheimann JR, Franco-Villanueva A, Herman JP (2017) Ascending mechanisms of stress integration: Implications for brainstem regulation of neuroendocrine and behavioral stress responses. Neurosci Biobehav Rev 74:366-375.

Naegeli C, Zeffiro T, Piccirelli M, Jaillard A, Weilenmann A, Hassanpour K, Schick M, Rufer M, Orr SP, Mueller-Pfeiffer C (2018) Locus Coeruleus Activity Mediates Hyperresponsiveness in Posttraumatic Stress Disorder. Biol Psychiatry 83:254-262.

Nassif S, Kempf E, Cardo B, Velley L (1983) Neurochemical lesion of the locus coeruleus of the rat does not suppress the sedative effect of clonidine. Eur J Pharmacol 91:69-76.

Nava N, Treccani G, Alabsi A, Kaastrup Mueller H, Elfving B, Popoli M, Wegener G, Nyengaard JR (2017) Temporal Dynamics of Acute Stress-Induced Dendritic Remodeling in Medial Prefrontal Cortex and the Protective Effect of Desipramine. Cereb Cortex 27:694-705.

Nestler EJ, Hyman SE (2010) Animal models of neuropsychiatric disorders. Nat Neurosci 13:1161-1169.

Nestler EJ, Hyman SE, Holtzman DM, Malenka RC (2015) Widely Projecting Systems: Monoamines, Acetylinecholine, and Orexin. In: Molecular Neuropharmacology Third Edition, pp 149-183: McGraw-Hill

Nestler EJ, Barrot M, DiLeone RJ, Eisch AJ, Gold SJ, Monteggia LM (2002) Neurobiology of Depression. Neuron 34:13-25.

Nusbaum MP, Blitz DM, Marder E (2017) Functional consequences of neuropeptide and small-molecule co-transmission. Nat Rev Neurosci 18:389-403.

O'Neal HA, Van Hoomissen JD, Holmes PV, Dishman RK (2001) Prepro-galanin messenger RNA levels are increased in rat locus coeruleus after treadmill exercise training. Neurosci Lett 299:69-72.

Ogbonmwan YE, Schroeder JP, Holmes PV, Weinshenker D (2015) The effects of post-extinction exercise on cocaine-primed and stress-induced reinstatement of cocaine seeking in rats. Psychopharmacology (Berl) 232:1395-1403.

Oh J, Petersen C, Walsh CM, Bittencourt JC, Neylan TC, Grinberg LT (2019) The role of co-neurotransmitters in sleep and wake regulation. Mol Psychiatry 24:1284-1295.

Ordway G, Widdowson P, Smith K, A H (1994) Agonist Binding to a2-Adrenoceptors Is Elevated in the Locus Coeruleus from Victims of Suicide. Journal of Neurochemistry 63:617-624.

Paxinos G, Franklin KBJ (2013) The Mouse Brain in Sterotaxic Coordinates. San Diego, CA: Academic Press.

Perez SE, Wynick D, Steiner RA, Mufson EJ (2001) Distribution of Galaninergic Immunoreactivity in the Brain of the Mouse. Journal of Comparative Neurology 434:158-185.

Petruzzello SJ, Landers DM, Hatfield BD, Kubitz KA, Salazar W (1991) A Meta-Analysis on the Anxiety-Reducing Effects of Acute and Chronic Exercise. Sports Medicine 11:143-182.

Pieribone V, Xu Z, Zhang X, Grillner S, Bartfai T, Hökfelt T (1995) Galanin induces a hyperpolarization of norepinephrine-containing locus coeruleus neurons in the brainstem slice. Neuroscience 64:861-874.

Plummer NW, Scappini EL, Smith KG, Tucker CJ, Jensen P (2017) Two Subpopulations of Noradrenergic Neurons in the Locus Coeruleus Complex Distinguished by Expression of the Dorsal Neural Tube Marker Pax7. Front Neuroanat 11:60.

Pomrenze MB, Giovanetti SM, Maiya R, Gordon AG, Kreeger LJ, Messing RO (2019) Dissecting the Roles of GABA and Neuropeptides from Rat Central Amygdala CRF Neurons in Anxiety and Fear Learning. Cell Rep 29:13-21 e14.

Powell JM, Plummer NW, Scappini EL, Tucker CJ, Jensen P (2018) DEFiNE: A method for enhancement and quantification of fluorescently labeled axons. Front Neuroanat.

Rajarao SJ, Platt B, Sukoff SJ, Lin Q, Bender CN, Nieuwenhuijsen BW, Ring RH, Schechter LE, Rosenzweig-Lipson S, Beyer CE (2007) Anxiolytic-like activity of the non-selective galanin receptor agonist, galnon. Neuropeptides 41:307-320.

Raymond CS, Soriano P (2007) High-efficiency FLP and PhiC31 site-specific recombination in mammalian cells. PLoS One 2:e162.

Ritter S, Stein L (1973) Self-stimulation of noradrenergic cell group (A6) in locus coeruleus of rats. J Comp Physiol Psychol 85:443-452.

Robertson SD, Plummer NW, de Marchena J, Jensen P (2013) Developmental origins of central norepinephrine neuron diversity. Nat Neurosci 16:1016-1023.

Rodriguez CI, Buchholz F, Galloway J, Sequerra R, Kasper J, Ayala R, Stewart AF, Dymecki SM (2000) High-efficiency deleter mice show that FLPe is an alternative to Cre-loxP. Nat Genet 25:139-140.

Roshanaei-Moghaddam B, Pauly MC, Atkins DC, Baldwin SA, Stein MB, Roy-Byrne P (2011) Relative effects of CBT and pharmacotherapy in depression versus anxiety: is medication somewhat better for depression, and CBT somewhat better for anxiety? Depress Anxiety 28:560-567.

Ross JA, Reyes BAS, Van Bockstaele EJ (2019) Amyloid beta peptides, locus coeruleus-norepinephrine system and dense core vesicles. Brain Res 1702:46-53.

Rovin ML, Boss-Williams KA, Alisch RS, Ritchie JC, Weinshenker D, West CH, Weiss JM (2012) Influence of chronic administration of antidepressant drugs on mRNA for galanin, galanin receptors, and tyrosine hydroxylase in catecholaminergic and serotonergic cell-body regions in rat brain. Neuropeptides 46:81-91.

Roy A, Pickar D, De Jong J, Karoum F, Linnoila M (1988) Norepinephrine and its metabolites in cerebrospinal fluid, plasma, and urine. Relationship to hypothalamic-pituitary-adrenal axis function in depression. Arch Gen Psychiatry 45:849-857.

Roy B, Wang Q, Palkovits M, Faludi G, Dwivedi Y (2017) Altered miRNA expression network in locus coeruleus of depressed suicide subjects. Sci Rep 7:4387.

Rush AJ, Trivedi MH, Wisniewski SR, Nierenberg AA, Stewart JW, Warden D, Niederehe G, Thase ME, Lavori PW, Lebowitz BD, McGrath PJ, Rosenbaum JF, Sackeim HA, Kupfer DJ, Luther J, Fava M (2006) Acute and longer-term outcomes in depressed outpatients requiring one or several treatment steps: A STAR*D report. American Journal of Psychiatry 163:1905-1917.

Saar I, Lahe J, Langel K, Runesson J, Webling K, Jarv J, Rytkonen J, Narvanen A, Bartfai T, Kurrikoff K, Langel U (2013) Novel systemically active galanin receptor 2 ligands in depression-like behavior. J Neurochem 127:114-123.

Samuels ER, Szabadi E (2008) Functional Neuroanatomy of the Noradrenergic Locus Coeruleus- Its Roles in the Regulation of Arousal and Autonomic Function Part II- Physiological and Pharmacological Manipulations and Pathological Alterations of Locus Coeruleus Activity in Humans. Curr Neuropharmacology 6:254-285.

Scarpa JR, Fatma M, Loh YE, Traore SR, Stefan T, Chen TH, Nestler EJ, Labonte B (2020) Shared Transcriptional Signatures in Major Depressive Disorder and Mouse Chronic Stress Models. Biol Psychiatry 88:159-168.

Schank JR, Liles LC, Weinshenker D (2008) Norepinephrine signaling through β-adrenergic receptors is critical for expression of cocaine-induced anxiety. Biol Psychiatry 63:1007–1012.

Schmidt KT, Weinshenker D (2014) Adrenaline rush: the role of adrenergic receptors in stimulant-induced behaviors. Mol Pharmacol 85:640-650.

Schwarz LA, Luo L (2015) Organization of the locus coeruleus-norepinephrine system. Curr Biol 25:R1051-1056.

Sciolino NR, Holmes PV (2012) Exercise offers anxiolytic potential: a role for stress and brain noradrenergic-galaninergic mechanisms. Neurosci Biobehav Rev 36:1965-1984.

Sciolino NR, Dishman RK, Holmes PV (2012) Voluntary exercise offers anxiolytic potential and amplifies galanin gene expression in the locus coeruleus of the rat. Behav Brain Res 233:191-200.

Sciolino NR, Smith JM, Stranahan AM, Freeman KG, Edwards GL, Weinshenker D, Holmes PV (2015) Galanin mediates features of neural and behavioral stress resilience afforded by exercise. Neuropharmacology 89:255-264.

Sciolino NR, Plummer NW, Chen YW, Alexander GM, Robertson SD, Dudek SM, McElligott ZA, Jensen P (2016) Recombinase-Dependent Mouse Lines for Chemogenetic Activation of Genetically Defined Cell Types. Cell Rep 15:2563-2573.

Selye H (1995) Stress and Disease. Science 122:625-631.

Seutin V, Verbanck P, Massotte L, Dresse A (1989) Galanin decreases the activity of locus coeruleus neurons in vitro. Eur J Pharmacol 164:373-376.

Shepherd JK, Grewal SS, Fletcher A, Bill DJ, Dourish CT (1994) Behavioural and pharmacological characterisation of the elevated "zero-maze" as an animal model of anxiety. Psychopharmacology (Berl) 116:56-64.

Shin LM, Rauch SL, Pitman RK (2006) Amygdala, medial prefrontal cortex, and hippocampal function in PTSD. Ann N Y Acad Sci 1071:67-79.

Simon H, Le Moal M, Cardo B (1975) Self-stimulation in the dorsal pontine tegmentum in the rat. Behav Biol 13:339-347.

Skofitsch G, Jacobowitz D (1985) Immunohistochemical Mapping of Galanin-Like Neurons in the Rat Central Nervous System. Peptides 6:509–546.

Skofitsch G, Jacobowitz, D. (1985) Immunohistochemical Mapping of Galanin-Like Neurons in the Rat Central Nervous System. Peptides 6:509-546.

Steiner RA, Hohmann JG, Holmes A, Wrenn CC, Cadd G, Jureus A, Clifton DK, Luo M, Gutshall M, Ma SY, Mufson EJ, Crawley JN (2001) Galanin transgenic mice display cognitive and neurochemical deficits characteristic of Alzheimer's disease. Proc Natl Acad Sci U S A 98:4184-4189.

Stevens JS, Kim YJ, Galatzer-Levy IR, Reddy R, Ely TD, Nemeroff CB, Hudak LA, Jovanovic T, Rothbaum BO, Ressler KJ (2017) Amygdala Reactivity and Anterior Cingulate

Habituation Predict Posttraumatic Stress Disorder Symptom Maintenance After Acute Civilian Trauma. Biol Psychiatry 81:1023-1029.

Szot P, Weinshenker D, White S, Robbins C, Rust N, Schwartzkroin P, Palmiter R (1999) Norepinephrine-Deficient Mice Have Increased Susceptibility to Seizure-Inducing Stimuli. J Neurosci 19:10985-10992.

Tanner MK, Fallon IP, Baratta MV, Greenwood BN (2019) Voluntary exercise enables stress resistance in females. Behav Brain Res 369:111923.

Tatemoto K, Rökaeus A, Jörnvall H, McDonald T, Mutt V (1983) Galanin - a novel biologically active peptide from porcine intestine. FEBS letters 164:124-128.

Tatemoto K, Rökaeus, A., Jörnvall, H., McDonald, T., Mutt, V. (1983) Galanin - a novel biologically active peptide from porcine intestine. FEBS Letters 164:124-128.

Thomas A, Burant A, Bui N, Graham D, Yuva-Paylor LA, Paylor R (2009) Marble burying reflects a repetitive and perseverative behavior more than novelty-induced anxiety. Psychopharmacology (Berl) 204:361-373.

Thomas SA, Palmiter RD (1997) Disruption of the Dopamine p-Hydroxylase Gene in Mice Suggests Roles for Norepinephrine in Motor Function, Learning, and Memory. Behav Neurosci 111:579-589.

Thomas SA, Matsumoto AM, Palmiter RD (1995) Noradrenaline Is Essential for Mouse Fetal Development. Nature 374:643-646.

Thomas SA, Marck BT, Palmiter RD, Matsumoto AM (1998) Restoration of norepinephrine and reversal of phenotypes in mice lacking dopamine beta-hydroxylase. J Neurochem 70:2468-2476.

Tillage RP, Sciolino NR, Plummer NW, Lustberg D, Liles LC, Hsiang M, Powell JM, Smith KG, Jensen P, Weinshenker D (2020) Elimination of galanin synthesis in noradrenergic neurons reduces galanin in select brain areas and promotes active coping behaviors. Brain Struct Funct 225:785-803.

Uematsu A, Tan BZ, Johansen JP (2015) Projection specificity in heterogeneous locus coeruleus cell populations: implications for learning and memory. Learn Mem 22:444-451.

Uematsu A, Tan BZ, Ycu EA, Cuevas JS, Koivumaa J, Junyent F, Kremer EJ, Witten IB, Deisseroth K, Johansen JP (2017) Modular organization of the brainstem noradrenaline system coordinates opposing learning states. Nat Neurosci 20:1602-1611.

Valentino RJ, Foote SL (1988) Corticotropin-releasing Hormone Increases Tonic but Not Sensory-Evoked Activity of Noradrenergic Locus Coeruleus Neurons in Unanesthetized Rats. J Neurosci 8:1016–1025.

Valentino RJ, Van Bockstaele E (2008) Convergent Regulation of Locus Coeruleus Activity as an adaptive Response to Stress. Eur J Pharmacol 583:194-203.

Van Hoomissen JD, Holmes PV, Zellner AS, Poudevigne A, Dishman RK (2004) Effects of beta-adrenoreceptor blockade during chronic exercise on contextual fear conditioning and mRNA for galanin and brain-derived neurotrophic factor. Behav Neurosci 118:1378-1390.

Videbech P, Ravnkilde B (2004) Hippocampal volume and depression: A meta-analysis of MRI studies. American Journal of Psychiatry 161:1957-1966.

Vila-Porcile E, Xu ZQ, Mailly P, Nagy F, Calas A, Hokfelt T, Landry M (2009) Dendritic synthesis and release of the neuropeptide galanin: morphological evidence from studies on rat locus coeruleus neurons. J Comp Neurol 516:199-212.

Wang S, Hashemi T, Fried S, Clemmons AL, Hawes BE (1998) Differential intracellular signaling of the GalR1 and GalR2 galanin receptor subtypes. Biochemistry 37:6711-6717.

Wang YJ, Yang YT, Li H, Liu PZ, Wang CY, Xu ZQ (2014) Plasma galanin is a biomarker for severity of major depressive disorder. Int J Psychiatry Med 48:109-119.

Waterhouse BD, Chandler DJ (2016) Heterogeneous organization and function of the central noradrenergic system. Brain Res 1641:v-x.

Weinshenker D, Holmes PV (2016) Regulation of neurological and neuropsychiatric phenotypes by locus coeruleus-derived galanin. Brain Res 1641:320-337.

Weiss J, Stout J, Aaron M, Quan N, Owens M, Butler P, Nemeroff C (1994) Depression and Anxiety- Role of the Locus Coeruleus and Corticotropin-releasing Factor. Brain Res Bulletin 35:561-572.

Weiss JM, Bonsall RW, Demetrikopoulos MK, Emery MS, West CH (1998) Galanin: A Significant Role in Depression? Annals of the New York Academy of Sciences 863:364-382.

Weiss JM, Boss-Williams KA, Moore JP, Demetrikopoulos MK, Ritchie JC, West CH (2005) Testing the hypothesis that locus coeruleus hyperactivity produces depression-related changes via galanin. Neuropeptides 39:281-287.

Whitworth JW, Ciccolo JT (2016) Exercise and Post-Traumatic Stress Disorder in Military Veterans: A Systematic Review. Mil Med 181:953-960.

Willner P (2017) The chronic mild stress (CMS) model of depression: History, evaluation and usage. Neurobiology of Stress 6:78-93.

Wong M, Kling M, Munsone P, Listwak S, Licinio J, Prolo P, Karp B, McCutcheon I, Geracioti T, DeBellis M, Rice K, Goldstein D, Veldhuis J, Chrousos G, Oldfield E, McCann S, Gold P (2000) Pronounced and sustained central hypernoradrenergic function in major depression with melancholic features- Relation to hypercortisolism and corticotropin-releasing hormone. PNAS 97:325-330.

Wray NR et al. (2012) Genome-wide association study of major depressive disorder: new results, meta-analysis, and lessons learned. Mol Psychiatry 17:36-48.

Wynick D, Bacon A (2002) Targeted disruption of galanin: new insights from knock-out studies. Neuropeptides 36:132-144.

Wynick D, Small CJ, Bacon A, Holmes FE, Norman M, Ormandy CJ, Kilic E, Kerr NC, Ghatei M, Talamantes F, Bloom SR, Pachnis V (1998) Galanin regulates prolactin release and lactotroph proliferation. Proc Natl Acad Sci U S A 95:12671-12676.

Wyrofsky RR, Reyes BAS, Zhang XY, Bhatnagar S, Kirby LG, Van Bockstaele EJ (2019) Endocannabinoids, stress signaling, and the locus coeruleus-norepinephrine system. Neurobiol Stress 11:100176.

Xu Z, Tong Y, Hökfelt T (2001) Galanin enhances noradrenaline-induced outward current on locus coeruleus noradrenergic neurons. Neuroreport 12:1779-1782.

Xu ZQ, Shi TJ, Hokfelt T (1998) Galanin: GMAP- and NPY-LikeImmunoreactivities in Locus Coeruleusand Noradrenergic Nerve Terminalsin the Hippocampal Formationand Cortex With Notes on the Galanin-R1and -R2 Receptors. Journal of Comparative Neurology 392:227-251.

Xu ZQ, Zheng K, Hokfelt T (2005) Electrophysiological studies on galanin effects in brain--progress during the last six years. Neuropeptides 39:269-275.

Zachariou V, Thome J, Parikh K, Picciotto MR (2000) Upregulation of galanin binding sites and GalR1 mRNA levels in the mouse locus coeruleus following chronic morphine treatments and precipitated morphine withdrawal. Neuropsychopharmacology 23:127-137.

Zachariou V, Brunzell DH, Hawes J, Stedman DR, Bartfai T, Steiner RA, Wynick D, Langel U, Picciotto MR (2003) The neuropeptide galanin modulates behavioral and neurochemical signs of opiate withdrawal. Proc Natl Acad Sci U S A 100:9028-9033.

Zhu M-Y, Klimek V, Dilley GE, Haycock JW, Stockmeier C, Overholser JC, Meltzer HY, Ordway GA (1999) Elevated Levels of Tyrosine Hydroxylase in the Locus Coeruleus in Major Depression. Biol Psychiatry 26:1275-1286.

APPENDIX

APPENDIX 1:

Inflammation-induced depressive-like behavior in mice

A1.1 Abstract

Depression is one of the most prevalent neuropsychiatric disorders, but the neurobiological changes that cause depression are not well understood. Recent research has linked increased inflammation to depression and shown that a large subset of people with depression have elevated proinflammatory markers. Stress, which is linked to the onset of a depressive episode, can activate inflammatory responses in humans. The locus coeruleus (LC), the major noradrenergic nucleus in the brain, plays an important role in the stress response, is thought to be hyperactive in depression, and can also be activated by proinflammatory cytokines. We sought to investigate the causal role of increased inflammation in elevated LC activity and depressive-like behavior by using lipopolysaccharide (LPS) to induce a systemic inflammatory response and depressive-like behavior in mice, and then test the role of LC hyperactivity in this response. Despite testing two serotypes of LPS, two strains of mice, and several behavioral assays, we were unable to recapitulate the depressive-like behavior reported in the literature. Thus, the contribution of LC hyperactivity could not be assessed. In the future, a different paradigm should be employed to study this topic, such as a chronic dosing regimen.

A1.2 Introduction

Major depressive disorder (MDD) is the leading cause of disability worldwide and affects approximately 30% of the population at some point in their lives (Nestler et al., 2002; Kruijshaar et al., 2005). Clinical studies have shown that markers of immune activation are elevated by stress in humans and present at high levels in the blood of many people with MDD, such as interleukin-6 (IL-6), tumor necrosis factor α and interferon γ, and there are suggestions from the human literature that inflammation plays a causal role in the development of depression (Maes et al., 1998; Wohleb et al., 2016). For example, patients receiving pro-inflammatory cytokine immunotherapies for cancer have an elevated risk of developing depression, and there is high comorbidity between MDD and chronic inflammatory diseases such as diabetes and cardiovascular disease (Wohleb et al., 2016). Because studying the causal link between inflammation and depression in humans is incredibly complex and challenging, many researchers have turned to animal models to begin disentangling this relationship.

Rodent models of inflammation-induced depressive-like behavior have frequently used application of a systemic inflammatory mediator, such as lipopolysaccharide (LPS), to study the resulting behavioral and molecular changes. LPS, or endotoxin, is a molecule found on the surface of gram-negative bacteria and elicits a strong immune response in many animals, including rodents and humans. Different bacterial strains produce different serotypes of LPS with structural variations in the O sidechain, leading to diverse hydrophobic properties. Previous studies have shown that a single peripheral injection of LPS in mice can lead to increased depressive-like behavior in the tail suspension test (TST), forces swim test (FST), and sucrose preference test up to 48 h post-injection (Frenois et al., 2007; O'Connor et al., 2009; Sekio and Seki, 2014). Acute exposure to LPS in both humans and rodents leads to a range of “flu-like”

physical symptoms including fever, anhedonia, anorexia, fatigue, and poor sleep, collectively termed “sickness behavior” (De La Garza, 2005). These symptoms overlap substantially with behaviors related to depression and can confound results from animal studies aiming to examine inflammation-induced depression-like behavior. Therefore, previous researchers have suggested that the initial elevation of proinflammatory cytokines caused by LPS leads to a short bout of sickness behavior in mice, during which time locomotor activity and food consumption is reduced. However, by 24-48 h post-LPS, locomotion and food consumption should have returned to normal but depressive-like behaviors, such as increased immobility in the FST and TST and decreased sucrose preference, may still remain, suggesting that depression-like behavior remains after sickness behavior abates (Frenois et al., 2007; Dantzer et al., 2008) (**Fig A1.1**). LPS-induced sickness behavior can therefore be thought of as a transient and adaptive state to help the body recover from the initial inflammatory insult, whereas LPS-induced depression-like behavior is longer lasting and maladaptive.

Inflammation can increase activity of the locus coeruleus (LC), the main noradrenergic nucleus in the brain and an important mediator of the central stress response. In rats, one systemic injection of LPS was found to increase LC activity for up to 3 weeks and microinjections of the cytokine interleukin-1 into the LC region increased activity of LC neurons (Borsody and Weiss, 2002, 2004). Several studies in mice have also shown increased c-fos expression, indicative of increased neuronal activity, in the LC immediately after systemic LPS injection (Stone et al., 2006; Kurosawa et al., 2016). Both human and rodent studies have suggested that LC hyperactivity occurs in MDD. In clinical studies, people with MDD showed increased levels of norepinephrine (NE) and its metabolites in cerebrospinal fluid as well as increased expression of tyrosine hydroxylase (TH), the rate-limiting enzyme in NE synthesis, in

the LC compared to non-depressed controls, indicating elevated LC activity (Roy et al., 1988; Ordway et al., 1994; Zhu et al., 1999; Wong et al., 2000; Ehnvall et al., 2003). Multiple rodent models of depression also showed evidence of LC hyperactivity, including a rat model of stress-induced depression-like behavior (Simson and Weiss, 1988) and a mouse model of learned helplessness (Kim et al., 2016). Similarly, all known efficacious antidepressant therapies, including separate classes of drugs and electroconvulsive shock, decreased LC activity in rodents, supporting the idea that LC hyperactivity plays a causal role in depressive-like behavior (Grant and Weiss, 2001; West et al., 2009). Most convincingly, administration of drugs that increased LC activity induced depression-like behaviors in rats and mice, whereas drugs that decreased LC activity attenuated these effects (Weiss et al., 1986; Stone et al., 2009). Because inflammation increases LC activity, and LC hyperactivity is linked to increased depressive-like behavior, we aimed to investigate a causal relationship between inflammation-induced LC hyperactivity and depressive-like behavior.

The goals of this study were to (1) use acute LPS treatment to induce depressive-like behavior in mice, (2) examine changes in LC activity via the immediate early gene c-fos, and (3) modulate LC activity using designer receptors activated by designer drugs (DREADDs) to study the causal role of LC hyperactivity in inflammation-induced depression-like behavior. Unfortunately, we were unable to replicate previous studies that reported depressive-like behavior in mice following LPS treatment and unable reliably distinguish depressive-like behavior from sickness behavior. Therefore, because our first goal was never accomplished, we did not attempt to address our second and third goals.

A1.3 Methods

Animals

All procedures related to the use of animals were approved by the Institutional Animal Care and Use Committee of Emory University and were in accordance with the National Institutes of Health guidelines for the care and use of laboratory animals. Mice were maintained on a 12/12 h light-dark cycle with access to food and water ad libitum. The first two experiments were done using adult (4-6 months) male and female C57BL/6J mice (Jackson Lab stock no. 00664), and the third experiment was done using male CD-1 mice (Charles River stock no. 022).

Locomotor activity

Mice were singly housed in automated locomotor recording chambers (transparent Plexiglas cages on a rack; San Diego Instruments, La Jolla, CA), and ambulations (consecutive photobeam breaks) were recorded for the duration of the experiment in 90 min time bins. For data analysis, the 90 min bins were collapsed into 12 h bins.

Sucrose preference

Two small water bottles (modified 15mL conical tubes), one filled with 1% sucrose water and the other with plain tap water, were placed in the cage. Bottles were weighed every 12 h, refilled as necessary, and the location of the bottles was switched every 24 h to control for potential side bias. The amount of water consumed from the bottles during each 12-h period was calculated by subtracting the weight from the previous measurement. Percent sucrose preference was then calculated as (sucrose water consumed) ÷ (normal + sucrose water consumed) × 100%.

LPS

After 48 h of measurements to collect baseline weight, locomotor activity, food intake, and sucrose preference, mice were injected with either saline or LPS (1 mg/kg, i.p) at 7:00 pm. LPS solutions were prepared fresh the day of injection by dissolving the compound in sterile saline. Two different strains of LPS were tried during this study: O26-B6 (Sigma, L8274) and O127-B8 (Sigma, L3129). Experiment 1 used LPS strain O26-B6, and Experiments 2 and 3 used LPS strain O127-B8.

Forced swim test

36 h after LPS injections, mice were placed in a 3.5 L beaker with 3 L of water (25ºC), and behavior was videotaped for 6 min. Behavior in the last 4 min of the test was scored by an observer blind to treatment, with immobility defined as lack of any movements besides those which were required for balance and to keep the animal's head above water.

Brain collection

90 min after the FST in experiments 1 and 2, mice were anesthetized with isoflurane and transcardially perfused with KPBS followed by 4% PFA in PBS. Brains were postfixed overnight by immersion in 4% PFA at 4°C, and then transferred to 30% sucrose in KPBS for 48 h at 4°C. No further processing of this tissue took place because of the lack of a strong behavioral effect.

Statistical analysis

All data were analyzed by two-way ANOVA (time x treatment) with Sidak's correction for multiple comparisons when appropriate, except for the FST data which was analyzed by unpaired t-test. Significance was set at $p<0.05$ and two-tailed variants of tests were used throughout. Data are presented as mean ± SEM. Calculations were performed and figures created using Prism Version 8 (GraphPad Software, San Diego, CA).

A1.4 Results

Experiment 1

In order to investigate whether we could reliably induce a depressive-like phenotype in mice by acutely increasing systemic inflammation, we treated C57BL/6J mice with 1 mg/kg LPS (serotype O26-B6). We collected 48 h of baseline behavior (weight, food consumed, locomotor activity, and sucrose preference) prior to LPS treatment and continued to collect data for 36 h post-LPS (**Fig. A1.2**). Data collection occurred every 12 h at 7 am and 7 pm. Because mice are nocturnal and therefore are most active during the dark cycle starting at 7 pm, diurnal variations in weight, food intake, locomotion, and rearing activity were evident, as expected. We found a significant interaction between time and treatment for weight change ($F_{6,84}=8.906$, $p<0.0001$), and post hoc tests showed a significant decrease in weight for LPS-treated mice compared to controls at 12 h post-LPS ($p<0.0001$), but not at other timepoints (**Fig A1.3a**). Similarly, there was a significant interaction effect for food intake ($F_{6,84}=29.16$, $p<0.0001$), with a significant decrease in food consumed for LPS treated mice during the first 12 h post-LPS ($p<0.0001$), but no difference at any other timepoint (**Fig A1.3b**). The same pattern was seen in both locomotor activity and rearing, with significant interaction effects (locomotion: $F_{6,84}=4.719$, $p<0.001$; rearing: $F_{6,84}=2.069$, $p<0.05$), and significantly lower ambulations ($p<0.01$) and number of rears

($p<0.05$) at 12 h post-injection for LPS mice compared to saline mice, but no differences at other timepoints (**Fig A1.3c-d**). For sucrose preference, there was a significant interaction effect ($F_{6,84}=2.707$, $p<0.05$) and post hoc analyses revealed significant decreases in sucrose preference at both 12 h ($p<0.001$) and 24 h ($p<0.05$) post-LPS compared to saline treated mice (**Fig A1.3e**). There were no significant differences between LPS and saline mice in amount of time spent immobile ($t_{14}=0.984$, $p=0.3418$) or latency to the first float ($t_{14}=0.7789$, $p=0.449$) in the FST 36 h post-LPS (**Fig A1.3f-g).**

Experiment 2

To determine if a different serotype of LPS would illicit a more robust and long-lasting depressive-like behavioral response, we repeated the same experiment with O127-B8 LPS, which has been used in previous studies to induce depressive-like behavior (Frenois et al., 2007; O'Connor et al., 2009; Sekio and Seki, 2014; Kurosawa et al., 2016). However, the results were nearly identical to those from Experiment 1. There was a significant interaction between time and treatment in weight change of the mice ($F_{6,84}=15.50$, $p<0.0001$) and post hoc analysis showed a significant decrease in weight for LPS treated mice compared to saline treated animals at 12 h post-injection ($p<0.0001$), but not other timepoints (**Fig A1.4a**). There was a significant interaction effect for food intake ($F_{6,84}=21.56$, $p<0.0001$), with a decrease in food consumed for LPS treated mice 12 h ($p<0.0001$) and 36 h post-injection ($p<0.001$) (**Fig A1.4b**). We found a significant interaction effect for locomotor activity ($F_{6,84}=3.893$, $p<0.01$), with significantly lower ambulations ($p<0.01$) at 12 h post-injection for LPS mice compared to saline mice, but no differences at other timepoints (**Fig A1.4c**). There were no significant differences in rearing behavior ($F_{6,84}=1.544$, $p=0.1741$) (**Fig A1.4d**). For sucrose preference, there was a significant

interaction ($F_{6,84}$=7.724, p<0.0001), and post hoc analyses showed significant decreases in sucrose preference for LPS treated mice 12 h (p<0.001) post-injection (**Fig A1.4e**). Again, there were no significant differences between LPS and saline treated mice in amount of time spent immobile (t_{13}=0.9027, p=0.3831) or latency to the first float (t_{13}=1.626, p=0.1279) in the FST (**Fig A1.4f-g).**

Experiment 3

We next wanted to determine if the outbred CD-1 mouse strain would produce a stronger depressive-like behavioral response to the LPS immune challenge compared to the inbred C57BL/6J mice used for the previous experiments, so we repeated the experiment with male CD-1 mice, using serotype O127-B8 LPS. CD-1 mice have been used previously for acute LPS-induced depressive-like behavior (Frenois et al., 2007; O'Connor et al., 2009; Sekio and Seki, 2014; Kurosawa et al., 2016). This experiment was only run once, and so had fewer animals per group (*n* = 4) compared to Experiments 1 and 2 (*n* = 8), and only male mice were used instead of half males and half females. There was a significant interaction between time and treatment for change in weight of the mice ($F_{6,36}$=3.600, p<0.01), and post hoc tests revealed a significant decrease in weight for LPS treated mice compared to saline treated mice at 12 h post-LPS (p<0.0001) (**Fig A1.5a**). There was also a significant interaction effect for food intake ($F_{6,36}$=5.809, p<0.001), with a significant decrease in food consumed for LPS treated mice during the first 12 h post-LPS (p<0.0001), but no difference at other timepoints (**Fig A1.5b**). There were no significant interaction effects in locomotion ($F_{6,36}$=1.413, p=0.2366), rearing behavior ($F_{6,36}$=0.5892, p=0.7366) or sucrose preference ($F_{6,36}$=0.4064, p=0.8698) (**Fig A1.5c-e**). There were also no significant differences between LPS and saline mice in amount of time spent

immobile (t_6=1.139, p=0.298) or latency to float (t_6=0.01991, p=0.9848) in the FST (**Fig A1.3f-g).**

A1.5 Discussion

In these experiments, we attempted to replicate data from previous studies showing an increase in depressive-like behavior 24-36 h after a single systemic dose of LPS. While we saw an initial decrease in locomotor activity, food consumption, weight, and sucrose preference following LPS administration in some experiments, these changes were not consistent and normalized 24-36 h post-injection. Ideally, we would have seen the locomotor and food consumption effects return to normal by 24 h post-LPS, showing sickness behavior resolving, but the decreased sucrose preference effect remain present though 36 h, indicative of longer lasting anhedonia. Furthermore, we did not see any significant depressive-like behavioral changes in the FST (i.e. increased immobility or shorter latency to float) at 36 h post-injection. Future investigations on this topic should be careful to appropriately design and test the paradigm used to ensure robustness. It would also be interesting to employ a chronic LPS dosing paradigm to potentially induce a more substantial, longer lasting behavioral effect or combine LPS administration with chronic mild stress exposure (Kubera et al., 2013; Couch et al., 2016).

One of the main difficulties in this project was our inability to distinguish depressive-like behavior, a longer lasting and maladaptive state, from sickness behavior, a transient and adaptive state, because none of the behavioral effects persisted until the 36-h time point. This inability to distinguish between sickness behavior and depressive-like behavior has been described previously (Biesmans et al., 2013). Some studies using inflammation-induced depressive-like behavioral models did not address the occurrence of sickness behavior with LPS

treatment, and reported all behavioral changes as depressive-like effects without appropriate evidence (O'Connor et al., 2009; Sekio and Seki, 2014). It is important to be cautious when interpreting data from these studies.

We tested two LPS strains (O26-B6 in experiment 1 and O127-B8 in experiments 2 and 3). Many previously published studies did not specify which serotype of LPS was used, but those that did often used O127-B8. When we did not achieve robust behavioral changes with O26-B6 in experiment 1, we switch to O127-B8 in an attempt to more closely replicate the methods used successfully in previous studies. However, we did not see any major differences between our results in experiment 1 (**Fig. A1.3**) and experiment 2 (**Fig. A1.4**).

We tried two different strains of mice in this study: C57BL/6J for experiments 1 and 2, and CD-1 mice for experiment 3. C57BL/6J are an inbred strain and one of the most commonly used mouse strains in research. However, because of the lack of a substantial behavioral effect after LPS treatment, we switched to the outbred CD-1 strain for the last experiment. Several previous studies showing depressive-like behavioral effects of LPS used CD-1 mice, and previous research has shown that CD-1 mice have increased neuroinflammation after microglial activation (Nikodemova and Watters, 2011). However, in our pilot study with CD-1 mice (**Fig. A1.5**), we did not see evidence of increased depressive-like behavior compared to our previous experiments.

In conclusion, because we failed to replicate data from previous studies showing an increase in depressive-like behavior after a single systemic dose of LPS, the causal relationship between inflammation, LC hyperactivity, and depression remains unresolved. It is possible that this failure to replicate effects was due to differences in the specific behavioral paradigm used or differences in animal facilities as housing conditions have been shown to affect depressive-like

behaviors after LPS (Painsipp et al., 2011). Future investigations on this topic should proceed cautiously and thoroughly test the paradigm used to ensure robustness.

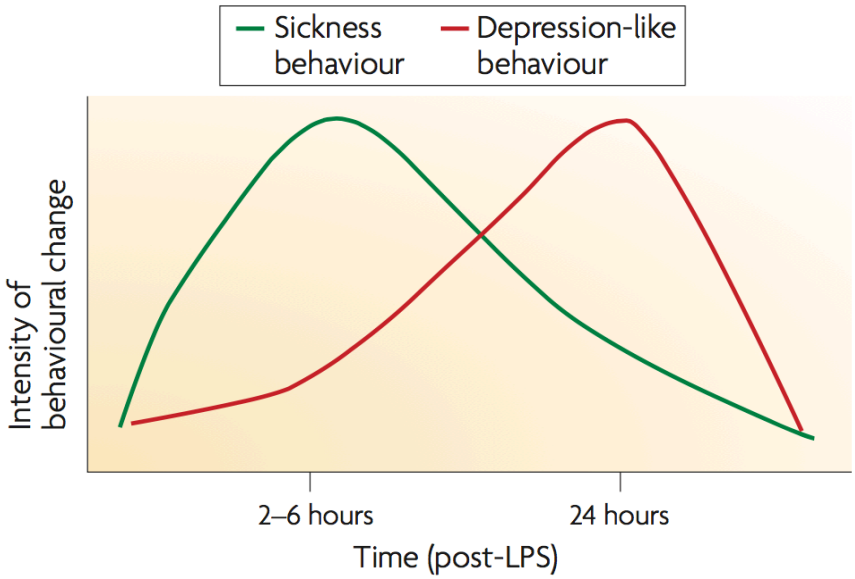

Figure A1.1 Sickness behavior and depression-like behavior after LPS. LPS causes sickness behavior in mice, during which locomotor activity and food consumption is reduced. However, by 24 h post-LPS, locomotion and food consumption have returned to normal but depression-like behavior (increased immobility in the FST and TST and decreased sucrose preference) still remains, suggesting that the study of depression-like behavior can be isolated during a window of time after sickness behavior wanes. *Source of image: Modified from Dantzer et al. 2008.*

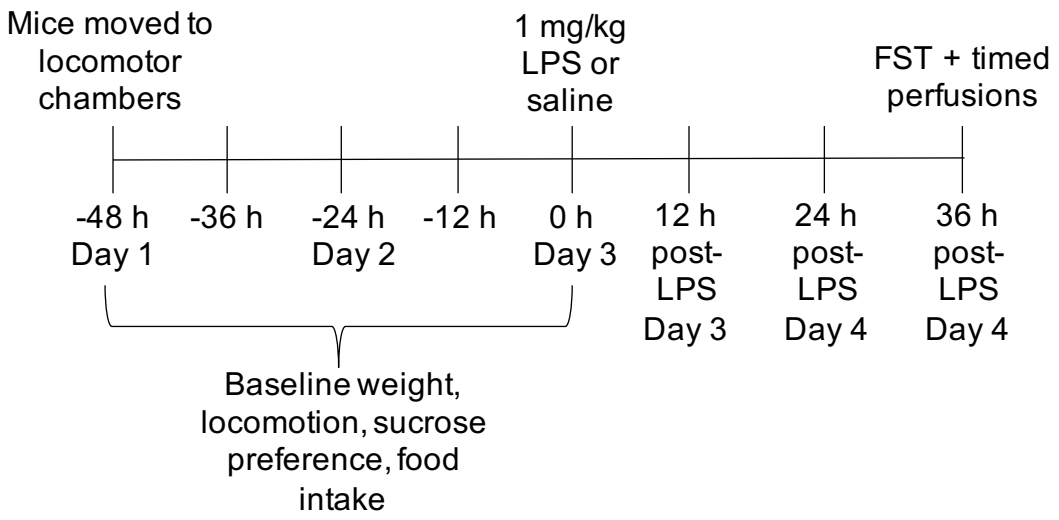

Figure A1.2 Experimental timeline. Mice were housed individually in locomotor recording chambers for the duration of the experiment. Baseline data was collected for 48 h prior to i.p injection of either 1 mg/kg LPS or saline and was then continued for 36 h post-injection. Data collection occurred every 12 h at 7 am and 7 pm. Mice were tested in the FST 36 h post-LPS and perfused 90 min later.

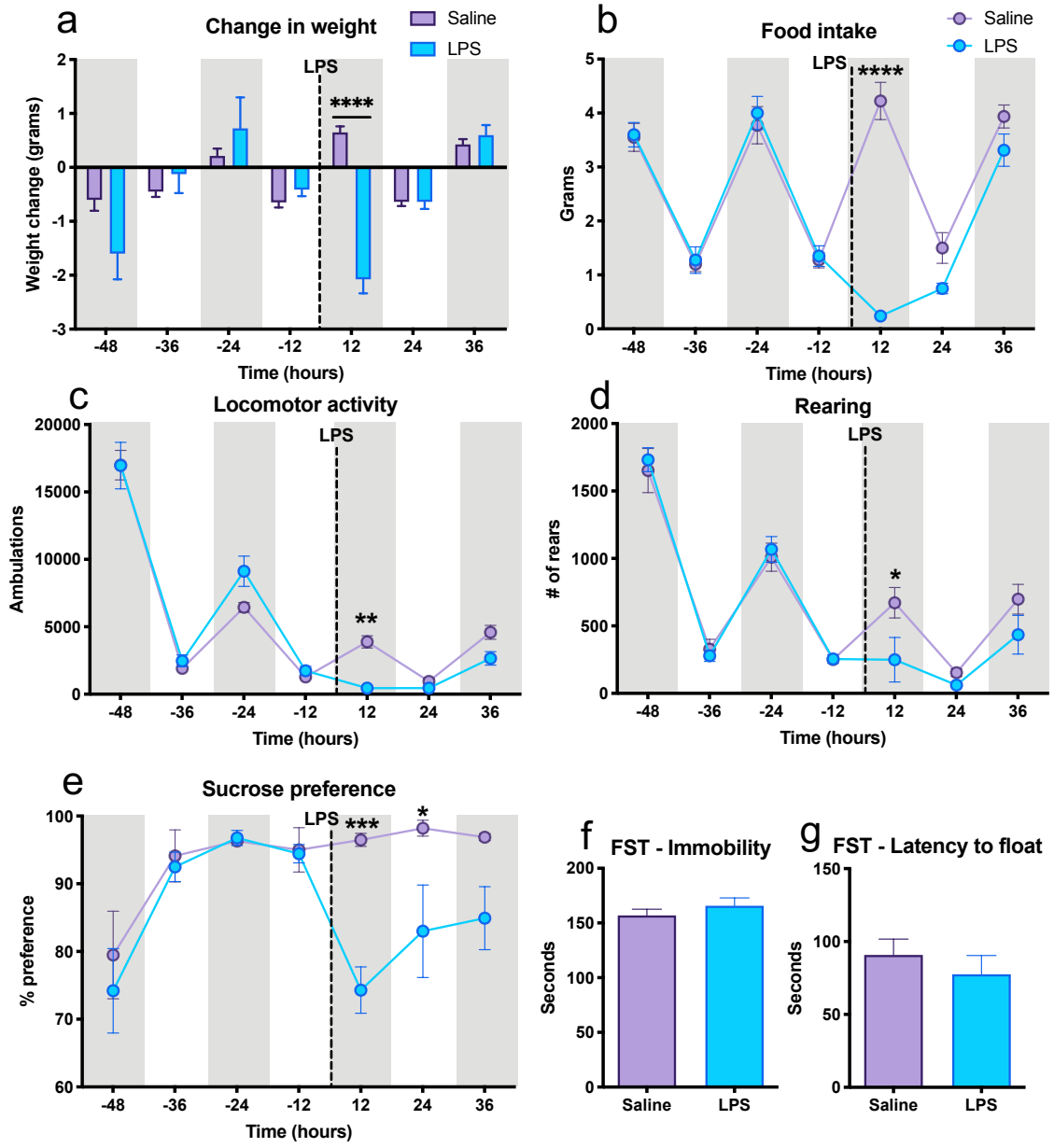

Figure A1.3. O26-B6 LPS with C57BL/6J mice. Mice treated with LPS showed a significant decrease in weight (a), food intake (b), locomotor activity (c), and rearing (d) 12 h post-injection, but not at 24 h or 36 h post-injection. LPS treated mice showed reduced sucrose preference both 12 h and 24 h post-injection (e). There were no differences between groups in the FST (f-g). LPS treatment timepoint is denoted by the vertical dashed line. Dark cycle (7 pm – 7 am) denoted by shaded regions. n = 8 mice per group, mixed males and females. Data were analyzed by two-way ANOVA or unpaired t-test. Error bars show SEM. *p<0.05, **p<0.01, ***p<0.001, ****p<0.0001.

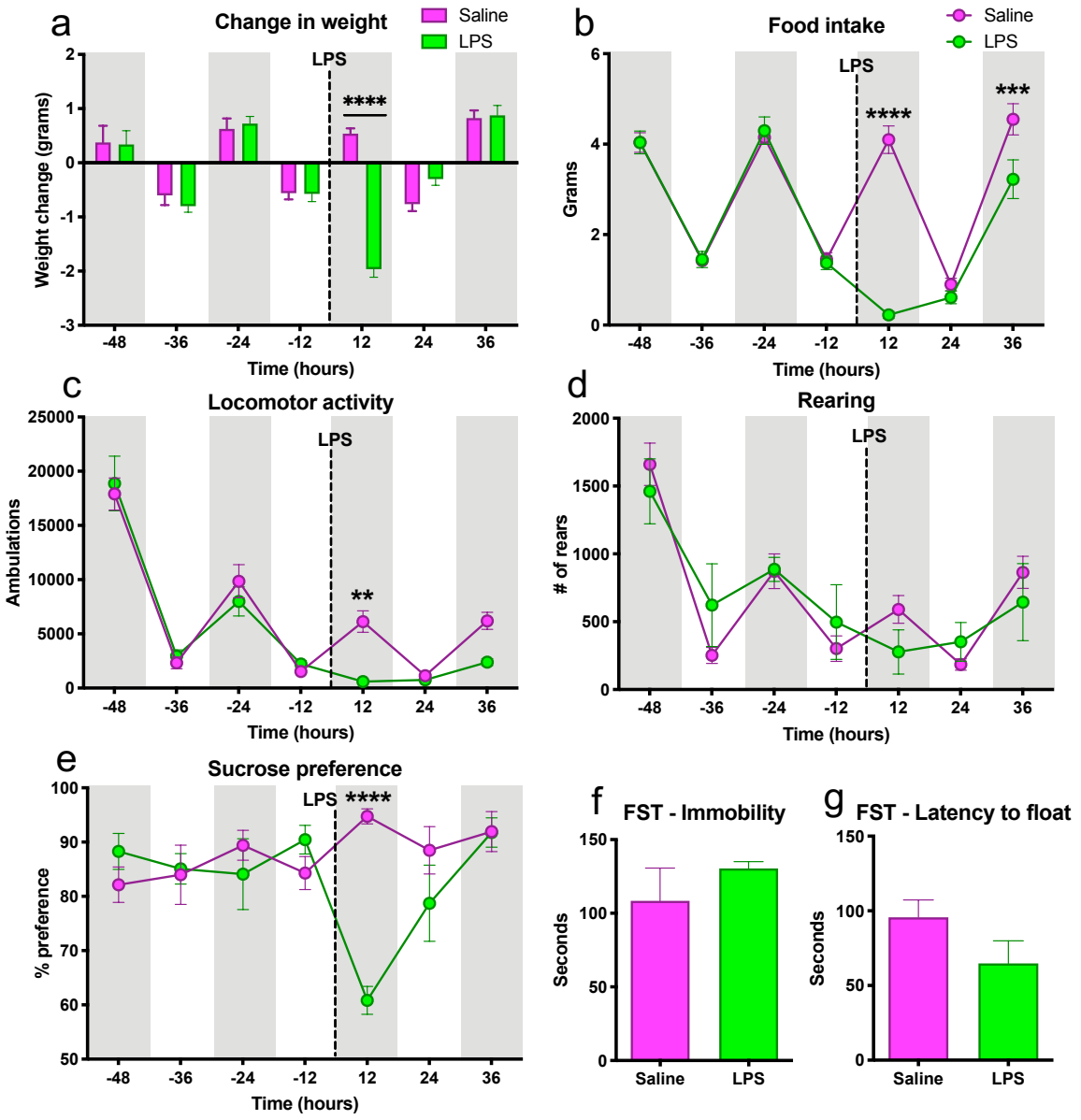

Figure A1.4. O127-B8 LPS with C57BL/6J mice. Mice treated with LPS showed a significant decrease in weight 12 h post-injection (a) and a decrease in food intake at both 12 h and 36 h post-injection (b). Locomotor activity was decreased 12 h post-injection for LPS mice (c). There were no differences in rearing behavior (d). Sucrose preference was decreased 12 h post-injection, but not at 24 h or 36 h post-injection (e). There were no differences between groups in the FST (f-g). LPS treatment timepoint is denoted by the vertical dashed line. Dark cycle (7 pm – 7 am) denoted by shaded regions. *n* = 8 mice per group, mixed males and females. Data were analyzed by two-way ANOVA or unpaired t-test. Error bars show SEM. ***p<0.001, ****p<0.0001.

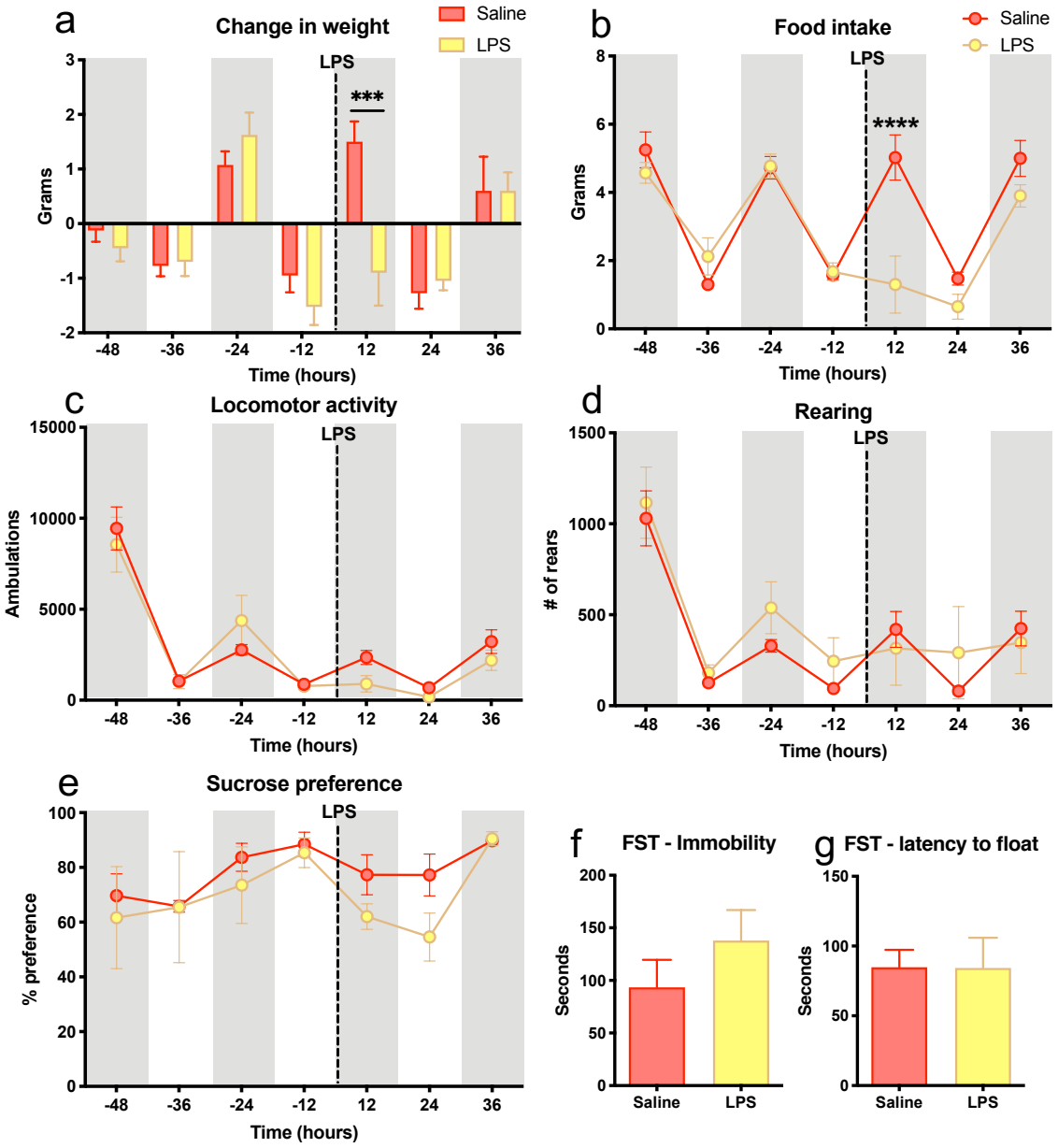

Figure A1.5. O127-B8 LPS with CD-1 mice. Mice treated with LPS showed a significant decrease in weight (a) and food intake (b) 12 h post-injection. There were no differences in locomotor activity (c), rearing (d), or sucrose preference (e). There were no differences between groups in the FST (f-g). LPS treatment timepoint is denoted by the vertical dashed line. Dark cycle (7 pm – 7 am) denoted by shaded regions. $n = 4$ mice per group, males. Data were analyzed by two-way ANOVA or unpaired t-test. Error bars show SEM. ***p<0.001, ****p<0.0001.

A1.6 References

Biesmans S, Meert TF, Bouwknecht JA, Acton PD, Davoodi N, De Haes P, Kuijlaars J, Langlois X, Matthews LJ, Ver Donck L, Hellings N, Nuydens R (2013) Systemic immune activation leads to neuroinflammation and sickness behavior in mice. Mediators Inflamm 2013:271359.

Borsody MK, Weiss JM (2002) Peripheral endotoxin causes long-lasting changes in locus coeruleus activity via IL-1 in the brain. Acta Neuropsych 14:303-321.

Borsody MK, Weiss JM (2004) The effects of endogenous interleukin-1 bioactivity on locus coeruleus neurons in response to bacterial and viral substances. Brain Res 1007:39-56.

Couch Y, Trofimov A, Markova N, Nikolenko V, Steinbusch HW, Chekhonin V, Schroeter C, Lesch KP, Anthony DC, Strekalova T (2016) Low-dose lipopolysaccharide (LPS) inhibits aggressive and augments depressive behaviours in a chronic mild stress model in mice. J Neuroinflammation 13:108.

Dantzer R, O'Connor JC, Freund GG, Johnson RW, Kelley KW (2008) From inflammation to sickness and depression: when the immune system subjugates the brain. Nat Rev Neurosci 9:46-56.

De La Garza R, 2nd (2005) Endotoxin- or pro-inflammatory cytokine-induced sickness behavior as an animal model of depression: focus on anhedonia. Neurosci Biobehav Rev 29:761-770.

Ehnvall A, Sjogren M, Zachrisson OCG, Agren H (2003) Lifetime burden of mood swings and activation of brain norepinephrine turnover in patients with treatment-refractory depressive illness. Journal of Affective Disorders 74:185-189.

Frenois F, Moreau M, O' Connor J, Lawson M, Micon C, Lestage J, Kelley KW, Dantzer R, Castanon N (2007) Lipopolysaccharide induces delayed FosB:DeltaFosB immunostaining within the mouse extended amygdala, hippocampus and hypothalamus, that parallel the expression of depressive-like behavior. Psychoneuroendocrinology 32:516-531.

Grant M, Weiss J (2001) Effects of chronic antidepressant drug administration and electroconvulsive shock on locus coeruleus electrophysiologic activity. Biological Psychiatry 49:117-129.

Kim Y, Perova Z, Mirrione MM, Pradhan K, Henn FA, Shea S, Osten P, Li B (2016) Whole-Brain Mapping of Neuronal Activity in the Learned Helplessness Model of Depression. Front Neural Circuits 10:3.

Kruijshaar MKB, J. Vos, T., de Graaf R, Spijker J, Andrews G (2005) Lifetime prevalence estimates of major depression- An indirect estimation method and a quantification of recall bias. Eur J of Epidemiology 20:103-111.

Kubera M, Curzytek K, Duda W, Leskiewicz M, Basta-Kaim A, Budziszewska B, Roman A, Zajicova A, Holan V, Szczesny E, Lason W, Maes M (2013) A new animal model of (chronic) depression induced by repeated and intermittent lipopolysaccharide administration for 4 months. Brain Behav Immun 31:96-104.

Kurosawa N, Shimizu K, Seki K (2016) The development of depression-like behavior is consolidated by IL-6-induced activation of locus coeruleus neurons and IL-1beta-induced elevated leptin levels in mice. Psychopharmacology (Berl) 233:1725-1737.

Maes M, Song C, Lin A, De Jongh R, Van Gastel A, Kenis G, Bosmans E, De Meester I, Benoy I, Neels H, Demedts P, Janca A, Scharpe S, Smith RS (1998) The Effects of

Psychological Stress on Humans: Increased Production of Pro-Inflammatory Cytokines and a Th1-like response in stress-induced anxiety. Cytokine 10:313-318.

Nestler EJ, Barrot M, DiLeone RJ, Eisch AJ, Gold SJ, Monteggia LM (2002) Neurobiology of Depression. Neuron 34:13-25.

Nikodemova M, Watters JJ (2011) Outbred ICR/CD1 mice display more severe neuroinflammation mediated by microglial TLR4/CD14 activation than inbred C57Bl/6 mice. Neuroscience 190:67-74.

O'Connor JC, Lawson MA, Andre C, Moreau M, Lestage J, Castanon N, Kelley KW, Dantzer R (2009) Lipopolysaccharide-induced depressive-like behavior is mediated by indoleamine 2,3-dioxygenase activation in mice. Mol Psychiatry 14:511-522.

Ordway G, Widdowson P, Smith K, A H (1994) Agonist Binding to a2-Adrenoceptors Is Elevated in the Locus Coeruleus from Victims of Suicide. Journal of Neurochemistry 63:617-624.

Painsipp E, Kofer MJ, Sinner F, Holzer P (2011) Prolonged depression-like behavior caused by immune challenge: influence of mouse strain and social environment. PLoS One 6:e20719.

Roy A, Pickar D, De Jong J, Karoum F, Linnoila M (1988) Norepinephrine and its metabolites in cerebrospinal fluid, plasma, and urine. Relationship to hypothalamic-pituitary-adrenal axis function in depression. Arch Gen Psychiatry 45:849-857.

Sekio M, Seki K (2014) Lipopolysaccharide-induced depressive-like behavior is associated with alpha(1)-adrenoceptor dependent downregulation of the membrane GluR1 subunit in the mouse medial prefrontal cortex and ventral tegmental area. Int J Neuropsychopharmacol 18.

Simson P, Weiss J (1988) Altered activity of the locus coeruleus in an animal model of depression. Neuropsychopharmacology 1:287-295.

Stone EA, Lehmann ML, Lin Y, Quartermain D (2006) Depressive behavior in mice due to immune stimulation is accompanied by reduced neural activity in brain regions involved in positively motivated behavior. Biol Psychiatry 60:803-811.

Stone EA, Lin Y, Sarfraz Y, Quartermain D (2009) Marked behavioral activation from inhibitory stimulation of locus coeruleus alpha1-adrenoceptors by a full agonist. Brain Res 1291:21-31.

Weiss J, Simson P, Hoffman L, Ambrose M, Cooper S, Webster A (1986) Infusion of adrenergic receptor agonists and antagonists into the locus coeruleus and ventricular system of the brain. Effects on swim-motivated and spontaneous motor activity. Neuropharmacology 25:367-384.

West CH, Ritchie JC, Boss-Williams KA, Weiss JM (2009) Antidepressant drugs with differing pharmacological actions decrease activity of locus coeruleus neurons. Int J Neuropsychopharmacol 12:627-641.

Wohleb ES, Franklin T, Iwata M, Duman RS (2016) Integrating neuroimmune systems in the neurobiology of depression. Nat Rev Neurosci 17:497-511.

Wong M, Kling M, Munsone P, Listwak S, Licinio J, Prolo P, Karp B, McCutcheon I, Geracioti T, DeBellis M, Rice K, Goldstein D, Veldhuis J, Chrousos G, Oldfield E, McCann S, Gold P (2000) Pronounced and sustained central hypernoradrenergic function in major depression with melancholic features- Relation to hypercortisolism and corticotropin-releasing hormone. PNAS 97:325-330.

Zhu M-Y, Klimek V, Dilley GE, Haycock JW, Stockmeier C, Overholser JC, Meltzer HY, Ordway GA (1999) Elevated Levels of Tyrosine Hydroxylase in the Locus Coeruleus in Major Depression. Biol Psychiatry 26:1275-1286.